Alma Mater Studiorum – Università di Bologna

DOTTORATO DI RICERCA IN

SCIENZE E TECNOLOGIE AGRARIE, AMBIENTALI E ALIMENTARI

Ciclo XXIX

Settore Concorsuale di afferenza: 07/E1

Settore Scientifico disciplinare: AGR/13

Water de-pollution: Different sorbents for different water pollutants

Presentata da: LOYISO LLOYD MZINI

Coordinatore: Prof. Giovanni Dinelli

Relatore: Prof.ssa Ilaria Braschi

Correlatore: Prof. Claudio Ciavatta

Esame finale anno 2017

Table of Contents

1. INTRODUCTION

1.1. Water crisis

About 70% of planet earth surface is covered by water and humans can only use 1% of that since 97% is saline water (sea sand oceans) and 2% is within the polar glacial ice caps (Gleick, 1993). The amount of water available for human use is either in underground sources or in surface water bodies such as river, lakes, and reservoirs. However, most of this water is not directly accessible. As a result, the available water for human use is categorised into three forms, rain water for food production, surface water and accessible ground water (Shiklomanov, 2000). Furthermore, in the regions where excesses fresh water available in surface water bodies, water is either lost through evaporation or reach the ocean without being utilized by humans. It was estimated that an average of 20% global runoff flows through Amazon River, without being used by indigenous population (Gleick, 1998). Therefore, whilst there are regions with excess water, in contrast, some regions such as Middle East, huge parts of Africa, and some portions of Europe and Southeast Asia suffer chronic water shortages, largely due to low rainfall distribution (Postel et al., 1996).

Presently, water demands are on the rise whilst the supply is approaching the depletion due to a growing global population, climate change, and the rising demand for water in industrial sectors. As a result half a billion people live in water-starved countries and this number is

expected to reach three billion by year 2025 (Hanjra and Qureshi, 2010). As we are approaching year 2025, physical and environmental constraints on the use of water resources are beginning to dwindle gradually. Aquifers are being recharged by precipitation and in many areas groundwater is also pumped up to replenish this huge water demand, but in the scourge of climate change, deviations from normal rainfall patterns and steady decline in annual average rainfall are encountered (Postel, 2000; Hendrix and Salehayn, 2012). This significant disruption in cyclical rainfall patterns, bring droughts and long dry spells which affects surface and underground water availability (Vetter, 2009; Green et al., 2011). The precipitation is erratic and not evenly distributed throughout years, there are wet and dry years. Water scarcity becomes the limiting factor in food production in many countries (Hanjra and Qureshi, 2010). And therefore, water-starved countries are not able to meet their food requirements when using the conventional and non-conventional resources within their borders (Qadir et al., 2007).

The largest consumer of water is the agricultural sector, which amounts up to 92% and the remaining part is shared between other industry and domestic water supply (Hoekstra et al., 2012). However, earlier predictions were indicating that 84.5% of total global freshwater available, was consumed by agricultural sector as illustrated in Table 1.1 (Shiklomanov, 1997). This rise in freshwater use is assumed to be driven by global population increase and a rise in increasing food demands. The second largest freshwater consumer is the reservoir losses through evaporation and leakages (Jury and Vaux 2007).

Table 1.1. Annual global water withdrawals of freshwater by water use category in 1995, data taken from Shiklomanov, 1997 (Source: Jury and Vaux, 2007).

Sector or use category	Annual withdrawal (km³/year)	Total withdrawal (%)	Annual consumption (km³/year)	Total consumption (%)
Agriculture	2504	66.1	1753	84.5
Municipal	344	9.1	50	2.4
Industry	752	19.9	83	4.0
Reservoir losses	188	4.0	188	9.1
Total	3788	100.0	2074	100.0

Water used in agricultural sector is not directly recycled back into the freshwater sources, and compounds contained in chemically synthesized fertilizers and pesticides, through leaching and surface runoffs, contaminate the freshwater sources. Henceforth, water becomes polluted through eutrophication, a process where surface water bodies are enriched with nutrients caused by fertilizer application on agricultural soils (Andreoli, 1993). Also, wastewater effluents from the industry and households amounts to 90-95% of wastewater regenerated by wastewater treatment plants (WWTP) are reticulated and treated to replenish the fresh water sources (Florke et al., 2013). Some of this water is treated and re-used, but the quality of effluents adjoining the receiving waters is under constant scrutiny, since there are resilient and persistent pollutants (e.g. antibiotics, heavy metals and pesticides etc) that are not well treated in WWTP. In developing countries, the situation is worsened by highly polluted wastewater returning to freshwater supplies, rendering fresh water from stream and rivers unusable (Jury and Vaux, 2007). Globally, pollutants contained in wastewater such as organic compounds, heavy metals, suspended solids and bacterial pathogens have been detected in receiving water sources in alarming concentrations (Schwarzenbach et al., 2010; Köck-Schulmeyer et al., 2013). To improve wastewater quality, treatments of various kinds are

employed to curb the pollution of fresh and underground water sources. Therefore, water scarcity is not only about physical availability, but other factors such as water quality, the efficiency of various uses, and the institutional capacity to meet rising demands.

1.2. Water pollution

The occurrences of regulated and emerging pollutants in the aquatic environments are caused by natural factors and human activities (Weiner, 2008). Major contributors to water pollution are agricultural practices, industrial and domestic wastes discharged into freshwater sources in different pathways (Schriever et al., 2007).

The extensive application of chemical fertilizers in cultivation of food crops gives rise to number of water pollutants. The major pollutants that are disseminated by this practise are nitrates, phosphates, sulphates, and toxic metals. The supplementary nutrients applied to the soil are not totally taken up by plant roots. The remaining quantities in the soil leach into underground water resulting in increased concentrations of nitrates, nitrites, ammonia, sulphates and phosphates into the water aquifers. These nutrients accelerate the growth of algae in surface water and cause eutrophication that poses direct and indirect threats to the environment. Some species of these algae such as *Cyanobacterium microcystis* produce toxins in water resources which are harmful to animals and humans (Jury and Vaux, 2007; Azizullah et al., 2011). Also, when the algae decompose, decomposing microbes use oxygen inducing biological oxygen demand (BOD), which consequently becomes detrimental to aquatic organisms. Early discoveries indicated that superphosphate fertilizers contain some heavy metals as cadmium as by-product (Schroeder and Ballassa, 1963). Even nowadays, a caution is given on extensive use of fertilizers containing toxic metals since it leads to the contamination of soil and water (Li and Wu, 2008).

Antibiotics are other emerging water pollutants that are brought through soil fertilization based on animal manure. Seemingly, the veterinary antibiotics after taken by animals, are not completely metabolised, and are discarded in animal excreta in portions of unchanged form (Martinez, 2009). Therefore, soils amended with antibiotic contaminated manure, disperse the antibiotics into the surface and underground water sources through surface runoffs and seepages, respectively. The release of antibiotics in the aquatic environments becomes ecological detrimental since it inhibits the growth of microorganisms, such as bacteria, fungi, or protozoa and it aggravates antibiotic resistance.

Likewise, pesticides are chemical compounds that are used extensively in agronomic practices to combat the effects of crop pests, weeds and nematodes in order to improve crops quality and yields. In the fields, pesticides are applied as seed coatings, dusts direct on the soil and by spraying on the leaves of the target crop. These methods of application create different pathways for pesticides to intrude the surrounding environment and eventually contaminate water sources. Surface runoffs become major pathway for spray drifts and spills from targeted crop, which can reach the atmosphere and the soil, respectively. For example, annual loss of herbicide metamitron through a surface run off in a sugarbeet field within 10 km^2 was estimated to be 2423 kg/year, ranging from 0.06 to 0.38% of the application (Huber et al., 1998). Alike, metamitron was applied on the rate of 700 g/ha with total application of 5.9 kg which through surface runoffs from the field, an average concentration of 1.23 µg/l was detected in the nearby stream (Schriever et al., 2007). In investigating the amount of pesticides in the river water, groundwater and in sediments of Danube River (Serbia), it was found that water samples contained about 1-5 ng/l, whereas sediments contained about 1-3 ng/g of total pesticides residues detected (Radovic et al., 2015). Amid the pesticides investigated, the most prevalent pesticides found in surface water, underground water and in sediments alike, were carbofuran, atrazine and propazine. Most pesticides are generic,

meaning they are not specifically targeting specific organisms. And therefore, they pose health risks to other untargeted organisms they come into contact with (Van der Werf, 1996; Arias-Estevez et al., 2008). Due to uncontrollable mobility of pesticide from the agricultural lands, extreme toxic substances had been banned to curb the scourge of environmental and diminish possible hazards towards living organisms.

Assessment of wastewater effluents from industries in India and Spain revealed that wastewater contained number of pollutants which were found to be the cause of water pollution in nearby water sources (Krishna et al., 2009; Lokhande et al., 2011, Neito et al., 2013). Among the pollutants that were found in surface water during these studies were: heavy metals, dyes, paints and pharmaceuticals from mining, textile and other industries. In developed countries the industrial wastewater is stringently prohibited to be discarded directly to freshwater streams without preceding proper treatment, however, in some of them the opposite is observed (Azizullah et al 2011). Wastewater from industries such as mining had proved to be paramount contributors to heavy metals pollution in aquatic environments (Owamah, 2014). Pharmaceutical manufacturing industries had been found to dispense huge amounts of antibiotics in the environment through their wastewater and additional presence of other organic solvents, catalysts, additives, reactants and raw materials contained in wastewater influent, make treatment of antibiotics in WWTP to be difficult (Sreekanth et al., 2009; Kummerer, 2009 b). Also, since hospital and municipal wastewater carried antibiotics resistant genes (Escher et al., 2011; Prayitno et al., 2013; Rodriguez-Mozaz et al., 2015), consequently pollution in surface water bodies was observed (Deng et al., 2016).

Domestic and urban wastewater was found to be the hub of bacterial pathogens. In developed world sewage spillages and pipe burst are well maintained, but in developing countries spillages are frequently experienced. Consequently, faecal coliform *Escherichia coli* is

detected in surface water sources and that serves as indicator of human waste contamination (Farooq et al., 2008). Since *E. coli* had developed resistance to sewage treatment methods, this makes them to pollute receiving water bodies (Costa et al., 2008). According to World Health Organisation (WHO) guidelines, neither *E. coli* nor thermo tolerant coliform organisms should be present in 100 ml of drinking water (WHO, 1993). However, in Africa most people are living in rural areas with lack of proper sanitation, and therefore found drinking water directly from the streams, wells and rivers. Reports of cholera and chronic diarrhoea had been indicated as the source of water-borne diseases from these bacterial pathogens. Also, landfills for domestic solid waste disposal are another source of polluting the underground water with various hazardous and toxic pollutants in the proximity of these domestic waste landfills (Guisti, 2009).

As mentioned previously, the existence of these pollutants in aquatic environments leads to serious public health hazards to humans, aquatic life and animals coming into contact with (Haddis and Devi 2008). Reports also indicated that directly drinking water polluted with impurities or indirectly ingested from food chain can cause serious health hazards to man, animals and the aquatic life (Webb et al., 2003; Watkinson et al., 2008). Recent studies investigated the effects of aquatic polychlorinated biphenyls and organochlorine pesticides on cancer mortality for elderly people, and it was found that the probability of mortality increased as the body fat increases (Kim et al., 2015). Hence, contamination of watersheds remains a big concern on accumulation of pollutants beyond acceptable levels. In addition, the abovementioned water polluting sources also exacerbate parameters such as BOD, chemical oxygen demand (COD), total dissolved solids (TDS), total suspended solids (TSS), and salinity and diminish the water quality to be unsafe for drinking and for other uses (Azizullah et al., 2011).

The main aquatic pollutants entailed in this thesis are antibiotics, heavy metals and pathogens because they are the major emerging and regulated water contaminants that the third world countries struggle to treat conventionally due to lack of technical and financial resources at their disposals.

1.2.1. Antibiotics

Antibiotics are used worldwide to cure bacterial infections in humans, pets, livestock, and fish farming (Lalumera *et al*., 2004). Antibiotic discovery was through screening and isolating soil-derived actinomycetes (Lewis, 2013). Since the early days of this discovery and their use, pathogenic microorganism shad ability to form resistant and persistent mutants, giving rise to vanity of antibiotics (Cohen et al., 2013; Mackay, 2014).With the development of antibiotic resistance genes, new antibiotic classes had been synthesised, namely sulfonamides, tetracyclines, β-lactams, aminoglycosides, chloramphenicols; macrolides, quinolones, diarylquinolines and many others. The mechanisms in which pathogenic organisms become resistance to antibiotic are displayed in Table 1.2.

Table 1.2. The resistance mechanism of pathogenic bacteria to antibiotics (Source: Acar and Rostel, 2001).

Mechanism	Antibiotic	Resistance level
Efflux	Tetracyclines, macrolides, quinolones	Low
Penetration	β-lactams, tetracyclines	Low
Target site alteration	β-lactams, aminoglucosids, macrolides, quinolones, glicopeptides	Variable
Bypass	Sulfonamides	High
Enzymatic inactivation	β-lactams, aminoglicosides, macrolids lincosamides	High

In general, antibiotics become efficient by destabilizing essential cellular functions of the target pathogenic organisms, however in defence of the target, organisms are able to trigger different resistance mechanisms such as increased efflux of the drug, destruction of the antibiotic, inactivation of enzymes, decreased penetration, develop bypass pathways and reproduce mutant genes modification (Lewis, 2013). The highest modes of resistance mechanism used by pathogenic organisms are bypass pathways and enzyme inactivation of the antibiotic. The rapid spread of antibiotic resistant bacteria in the environment had become a threat to public health since it results to problems of infection control. In addition, there are many pathways in which these antibiotic resistant bacteria are dispatched and transported due to existence of antibiotics in aquatic environment (Livermore, 2005; Manaia et al., 2016).

Firstly, animal manure had been found to contain portions of veterinary antibiotics and their metabolites, as previously mentioned. In China, samples of swine manure were investigated on the presence of sulfonamides, tetracyclines and macrolides (Pan et al., 2011). It was found that swine manure was containing all the antibiotic classes, with shocking maximum concentration of chlortetracycline (CTC) up to 764.4 mg/kg. Elsewhere, researchers detected recoveries of veterinary antibiotics in different animal manures and in soils (Martinez-Carballo et al., 2007; Karci and Balcioglu, 2009). The significance of these studies exhibit evidently that application of animal manure can lead to contamination of arable lands with veterinary antibiotics. Hence wastewater from livestock farming areas and surface water samples from the surroundings were investigated for the presence of veterinary antibiotics (Wei et al., 2011). It was found that wastewater from livestock farms contained about 10 types of antibiotics, and river samples contained 9 of them. The most frequently detected veterinary antibiotics from animal wastewater samples were sulfamethazine (SMZ), oxytetracycline (OTC), tetracycline (TC), sulfadiazine (SDZ) and sulfamethoxazole (SMX) with a maximum concentration of 211.0, 72.9, 10.3, 17.0 and 63.6 µg/l, respectively.

Consequently, lower concentrations were observed in river water samples, SMZ (4.7 µg/l), OTC (2.2 µg/l), TC (0.8 µg/l), SDZ (1.0 µg/l) and SMX (0.6 µg/l) than those found directly in animal wastewater.

Since antibiotics are used by humans and in livestock, fish productions, number of studies had reported that antibiotics had been found in animal wastewater (Wei et al., 2011), aquaculture (Sapkota et al., 2008), domestic solid waste landfills (from dumping expired antibiotics) (Wu et al., 2015), hospital, industrial and urban wastewater effluents (Escher et al., 2011; Prayitno et al., 2013; Rodriguez-Mozaz et al., 2015). The persistence of antibiotics in the environment had been closely associated to the spread of antibiotic resistant genes in the aquatic environment (Goa et al., 2012; Bouki et al., 2013; Rizzo et al., 2013). And also, since ponds and river water can be contaminated with antibiotics (Wei et al., 2011; Jiang et al., 2013), irrigating agricultural crops with contaminated wastewater from such water sources, resulted into antibiotic resistant strains accumulated on soils and possible underground water sources (Chefetz et al., 2008; Borgam and Chefetz, 2013). Due to mobile transportation of antibiotic resistant bacteria in the soil, plant roots uptake is encouraged, posing health risks to humans consuming those contaminated food crops (Rajapaksha et al., 2014; Williams et al., 2015). The fate of antibiotics in the aquatic environment became a major threat to fresh water systems, humans and animals as well as it affects largely available water quality. Various strategies had been sought to lessen the occurrence of antibiotics in aquatic environments as to reduce the emission of antibacterial resistant genes.

1.2.1.1. Strategies to remove antibiotics

In developed countries, all the domestic, industrial and animal farm wastewater containing antibiotics and antibiotic resistant bacteria end up reaching the WWTP. Conventional methods of eradicating antibiotics in the WWTP involve several steps such as flocculation,

sedimentation, filtration and chlorination; conversely, all these steps were unable to provide the barrier against pharmaceutical active compounds (Adams et al., 2002; Hebeer, 2002, Gobel et al., 2007). Due to poor adsorption of antibiotics in the active sludge of the WWTP, tertiary treated wastewater was found to contain antibiotics, giving a rise to accumulation of antibiotics in surface water bodies in the magnitude of 10-1000 ng/l (Le-Minh et al., 2010). Other retention methods used in WWTP such as chemical coagulation and sand filtration demonstrated an incompetent eradication of polar pharmaceuticals (Ternes et al., 2002; Nakada et al., 2008). Hence, literature revealed that tertiary treated municipal wastewater was found to contain antibiotics concentrations in the range of 0.26-2.8 µg/l and 0.65-1.1 µg/l for SMX and tetracycline, respectively (Batt et al., 2007; Gao et al., 2012).

Animal dung containing antibiotics when applied as organic fertilizers on soils has a potential to pollute underground water sources with antibiotics. However soils are considered as natural sorbents and through adsorption process, soils can prevent leaching down of antibiotics to the underground aquifers. Adsorption is a process whereby a dissolved contaminant adheres to the surface of a solid sorbent, due to host-guest hydrophobic and electrostatic interactions between the adsorbate and the adsorbent. Nevertheless, soils seem to have low affinity towards SMX antibiotic since it was found to be least retained among trimethoprim, clindamycin, clarithromycin antibiotics on 13 types of soils tested (Kodesova et al., 2015).The poor SMX sorption was due to the negative effects of soil pH, SMX existed mainly in anionic form at pH above its pK_a of 5.7. Besides, in soils with low content of soil organic matter (SOM), antibiotics become mobile and possible to contaminate ground water through leaching. Clay minerals and organic matter found in soils and sediments habitually occur in association with one another. Thus, in a model study that sought to adsorb sulfonamides using clay minerals, it was discovered that sorption was sensitive to pH and

laboratory results could not be used in real soils since clays in real soils could be coated with organic matter and metal oxides (Goa and Pedersen 2005).

The utilization of activated carbon in a post-filtration process of wastewater treatment was found to be most effective method for removing antibiotics (AWWA, 1990). Several studies had confirmed almost a complete removal of the most common types of antibiotics in deionised and surface water using powder activated carbon(PAC), and the adsorption increased with increased of PAC dosage with up to 4 h of time to reach the adsorption equilibrium (Adam et al., 2002; Nam et al., 2014; Zhang et al., 2016). Though, in the model study done by Nam and co-workers (2014), a decline in adsorption was observed due inhibiting competition of dissolved organic matter (DOM) contained in natural waters. Additionally, at low temperatures (5 ℃), a reduced antibiotic removal was observed; indicating that during cooler seasons the PAC would be less effective on field scale application. Moreover, the amount of dosage in a large scale operations and the regeneration of PAC render the use of activated carbon both uneconomical and environmentally unsafe (Babel and Kurniawan, 2003; Snyder et al., 2007).

Most recently, alternative cost effective adsorbent derived from wooden waste materials had been investigated to remove antibiotics from aqueous environments. Sawdust biomass was investigated for the adsorption of ciprofloxacin hydrochloride antibiotic from water (Bajpal et al., 2012). The adsorption of ciprofloxacin hydrochloride antibiotic on sawdust was optimum at pH 5.8 at a rate of 11.6 mg/g (64% of the initial concentration) and adsorption equilibrium reached within 1 h. In another study vine wood waste was separately activated by aqueous solution of NaOH, KOH, $ZnCl_2$, NaCl and HNO_3 at 600 ℃ for 2 h, in order to retain amoxicillin from water (Poureterdal and Sadegh, 2014). For a more accurate description of activation methods see Section 1.2.2.1.4. The activating agent NaOH (5% w/w) realised the best removal efficiency on amoxicillin (56%), cephalexin (76%), tetracycline (88%) and

penicillin G (74%) compared to other chemical agents. It is still early to rule out waste materials effectiveness on loading of antibiotics from water, since this phenomenon had been widely researched on heavy metal retention and valuable results had been obtained (Zhang et al, 2010).

Zeolites are natural minerals found in a volcanogenic sedimentary rock and zeolitic tuffs. Natural zeolites are hydrated alumino silicate minerals and due to their porous structure had been utilised largely in cation exchange, molecular sieving, catalysis and adsorption (Wang and Peng, 2010). Besides natural zeolites, it had been reported that zeolites can be synthesized from coal fly (Murayama et al, 2002, Li et al., 2011), carbon sources (Janssen et al., 2003), and colloidal silica (Li et al., 2007) just to mention a few. Synthesis of zeolite by hydrothermal treatment of coal fly ash in 2.0 M NaOH and modified using hexadecyltrimethylammonium (HDTMA) surfactant, increased the surface area from 1.02 to 91.50 m^2/g (Li et al., 2011). Also, impregnating carbon source with SiO_2 precursor and subjecting it to hydrothermal treatment at 150 ºC, it formed a zeolite crystal. In this method the carbon source is burned off to leave the mesopores in the crystallized zeolite with defined supercages of uniform pore size and shape, suitable to adsorb matching size molecules. Moreover, it was reported that hexagonal alumino silicate mesostructures can be modified by acidity and steam to promote AlO_4 and SiO_4 tetrahedral connectivity of crystalline zeolites with improved pore size and surface area (Liu et al., 2000). Modifying natural zeolites with iron oxides at 20 and 85 ºC increased the surface area from 27.5 m^2/g to 37.2 and 55.5 m^2/g, respectively (Mockovčiaková et al., 2006).

Natural zeolite had been found to be both cost-effective and efficient adsorbent for retaining both organic and inorganic contaminants found in water (Babel and Kurniawan, 2003; Polat et al., 2005). A clinoptilolite, a natural zeolite was investigated on removal of veterinary antibiotic enrofloxacin from water (Otker and Akmehmet-Balcıoglu, 2005). It was found that

enrofloxacin was almost completely removed at pH 5 after 1 h of contact time. For this reason, enormous model studies had been investing different antibiotic removal by different kinds of zeolites on aqueous environment (Braschi et al., 2010 a; Martucci et al., 2013; Liu et al., 2013). Some of these studies on removal of sulfonamides using zeolites will be discussed shortly.

In addition, efficient treatment method against particular antibiotics in WWTP does not necessary mean it also reduces the development of antibiotic resistance bacteria. For instance, β-lactams antibiotics since they are easy to hydrolyze have been found in the environment at very low concentrations (Helland et al., 2010). Contrary, resistant bacteria and genes encoding resistance against certain β-lactams have been detected in WWTP in alarming concentrations (Kummerer, 2009 b; Bouki et al, 2013). Therefore, antibiotic character and molecular structure should be considered for the effectiveness of removal strategy of individual antibiotic class and its encoded antibiotic resistant bacteria in the aquatic environment.

1.2.1.2. Sulfonamides

Sulfonamide antibiotic group is the first discovered antibiotics, which are broad spectrum antibiotics utilized to cure variety of ills in both humans and animals (Sarmah et al., 2006; Martinez, 2009). Sulfonamides (sulfa drugs) are mainly utilized to fight against urinary tract infections. Sulfa drugs restrain the multiplication of pathogenic bacteria by acting as competitive inhibitors of the enzyme dihydropteroate synthetase (DHPS), an enzyme involved in folic acid synthesis (Livermore 2005). Sulfonamides are amphoteric naturally; they generally function as weak acids in water due to their pK_a values ranging from 5.0 to 7.5. Also, most veterinary sulfonamides posses at least two nitrogen functions groups, and the

amide attached to the solfon group is referred to as N1 and deprotonates at pH > 5.5–7 (Sarmah et al., 2006). See the structure sketched below in Figure 1.1.

Figure 1.1. General chemical structure of selected sulfonamides

Sulfa drugs after administered, they are not completely metabolised and discarded as human or animal excreta in portions of unchanged form. For instance SMX found in sewage, consisted of 15% recoveries of parent compound (Hirsch et al., 1999), 60% of metabolites were transformed into N^4-acetyl-SMX (Göbel et al., 2007), 9% of SMX-N1-glucoronide conjugate and traces of N-hydroxyl-SMX, 4-nitroso-SMX and 4 nitro-SMX (Van der Ven et al., 1995, Bonvin et al., 2013). On photolysis degradation of 4–nitroso-SMX, it was observed that a back transformation to the original parental compound was possible (Kahle and Stamm, 2007; Bonvin et al., 2013). Other pathway in which sulfa drugs can reach the underground water sources is through leachates from animal excreta and soils ameliorated with antibiotic contaminated animal manure. It had been reported that when soil fertility is amended with pig manure containing sulfonamides, the development of resistance bacteria of *sul 1* and *sul 2* genes was evident (Heuer et al., 2011).

1.2.1.3. Strategies to remove sulfa drugs

A high silica zeolite Y was investigated on retention of sulfonamide antibiotics such as SDZ, SMZ, and sulfachloropyridazine (SC) in aqueous environment (Braschi et al., 2010 a). All these sulfonamide antibiotics were removed from water within 1min of contact time at room temperature. Also in another study, SMX was almost completely removed in water at pH 6 within a few minutes by zeolite Y (Blasioli et al., 2014). Several model studies indicated that organophylic high silica zeolites had ability to quickly remove sulfa drugs from aqueous environments: the host-guest interactions, adsorption capacity and sulfonamide arrangement into their porosities be explicated by *in situ* FTIR spectroscopy and confirmed by *ab initio* computational modelling (Fukahori et al., 2011; Braschi et al., 2010b; Martucci et al, 2013; Blasioli et al., 2014). A single molecule of sulfa drug was stabilized by either the vicinity of methyl or amino groups to the wall of the zeolite cage. In this way organic molecule was held tight by multiple weak H-bonds and van der Waals type interactions inside zeolite Y cage. The confinement of sulfonamides inside the cage is accountable for the irreversible extraction of adsorbed sulfa drugs from water. It was also demonstrated the adsorption mechanism of sulfa drugs on zeolite Y is irreversible with high adsorption rate and quick kinetics. In addition, adsorption of sulfonamides on zeolites was found to be pH dependant, it decreases as pH increases irrespective of sorbent dosage (Kahle and Stamm, 2007; Fukahori et al., 2011). The function of soil and water pH and the pK_a of the sulfonamides are very crucial for adsorption of sulfa drugs since at pH higher than the pK_a, sulfonamides exist primarily in disassociated anionic form and have higherwater solubility, thereby leading to lower sorption by zeolite (Fukahori et al., 2011). Therefore, since only neutral sulfa drug species could be adsorbed on zeolite supercages via hydrophobic interaction, removing of sulfa drugs at WWTP becomes problematic on the matrix of pH above 7.5.

The degradation of embedded sulfa drugs inside the adsorption sites of zeolite had been investigated by an *in situ* high-temperature synchrotron X-ray powder diffraction (XRPD) and thermal treatment of exhausted zeolite (Leardini et al., 2014). The imperative intention of this study was to remove the entrapped sulfa drugs and regenerate the zeolite. Authors observed no alteration of the zeolite crystal structure due to static heating in furnace at temperatures 575 ºC for 2 h, and the zeolite was able to re-adsorb equal amounts of sulfa drugs in their first cycle. Most recently, Braschi and co-workers (2016) had investigated the regeneration of exhausted zeolite preloaded with SC, SD, SM and SMX sulfa drugs employing physico-chemical treatments. Zeolite was loaded in both deionised and natural river water and the following physico-chemical treatments were examined, namely photolysis, Fenton-like reaction, thermal treatment and solvent extraction. Both photolysis and Fenton-like reaction resulted into insignificant abatement of sulfa drugs into the zeolite, whereas both thermal treatment and solvent extraction fully regenerated exhausted zeolite. The thermal treatment at 500 °C for 4 h, and mixture of equal amounts of acetonitrile, methanol and water for solvent extraction, achieved the best regeneration of loaded zeolite samples.

Most of all, the quick and irreversible sorption of sulfa drugs by zeolites, successful regeneration of exhausted zeolite by thermal and solvent extraction renders high silica zeolite Y an excellent sorbent in remedial of sulfonamides from aqueous environments.

1.2.2. Heavy metals

Heavy metals in aquatic environment are another environmental concern due to their toxicity to living organisms. Human activities such as industrialization and mining had proved to be paramount contributors to heavy metals (Owamah, 2014; Chand et al., 2015). At very low pH values, heavy metals become soluble in water leading to heavy metal contamination of

surface and underground water. Since heavy metals are not biodegradable, they can accumulate in food and potable water and become serious human health hazard and environmental pollution (Fu and Wang, 2011).

Nevertheless, some heavy metals such as cobalt (Co), copper (Cu), chromium (Cr), iron (Fe), magnesium (Mg), manganese (Mn), molybdenum (Mo), nickel (Ni), selenium (Se) and zinc (Zn) are considered essential trace elements for biochemical and physiological cellular functions in human bodies, their inadequate or excessive supply may lead into a variety of deficiencies and critical illnesses (WHO, 1996). The mechanism in which excessive heavy metal ions induces toxicity is through enzyme inhibition, oxidative stress and impaired antioxidant metabolism (Gumpu et al., 2015). Consequently, through free radical generation that leads to DNA damage, lipid peroxidation and depletion of protein sulfydryl leading to adverse health effects. Enhanced generation of reactive oxygen species (ROS) leads to oxidative stress which can overwhelm cell's intrinsic antioxidant defences resulting to cell damage or death (Ali et al., 2013). Other heavy metals such as arsenic (As), cadmium (Cd), chromium (Cr), lead (Pb) and mercury (Hg) had been reported as of significance public health concern due to their high degree of toxicity at very low concentrations (Tchounwou et al., 2014). Human exposure to drinking water or alimentary chain polluted with heavy metals, can lead to various sickness, brain damage and neurological disorders. For instance, human exposure to low concentrations of 2-3 µg Cd/g creatinine may result to kidney damage, bone effects and fractures (Järup, 2003).

Besides the public health risks associated with consuming crops containing high concentrations of heavy metals, concerns are also on effects on plant growth parameter. Plants require micronutrients such as Zn, Cu, Fe, Co and Mn for plant growth. However, excess of these trace elements may lead to plant growth inhibition and toxicity symptoms. Since Cu and Zn are constituents of various enzymes and plant proteins, they are considered

essential for plant growth and development (Hall, 2002). Excessive amounts of these trace elements can induce toxicity symptoms at due to their activeness at cellular levels, whereas inadequate supply can cause displacement by other essential elements resulting to deficiency symptoms. For instance Zn toxicity in vegetables showed young leaf chlorosis, browning of roots and reduction of plant growth parameters such as shoots and roots (ul Islam et al., 2007). In this study, plant growth reduction was observed to be 73% and 63% of shoot weight for fresh celery and Chinese cabbage, respectively. For this reason irrigation water quality had been regulated by FAO to contain Zn (200 µg/l), Cu (17 µg/l), Fe (500 µg/l) Co (50 µg/l) and Mn (500 µg/l) (Ayers and Westcott, 1994). Therefore contaminated water sources with heavy metals require adequate treatment before various utilizations.

1.2.2.1. Strategies of removing heavy metals from water: An overview

Since the pollution of water sources by heavy metals has been occurring, various remedial strategies had been investigated and employed. These heavy metal remedial techniques include but not limited to physico-chemical treatments and biosorption, and are well documented (Kurniawan et al., 2006; Mohan and Pittman, 2007; Barakat et al, 2011). Benefits and limitations of these heavy metal remedial strategies are tabulated in Table 1.3 below.

1.2.2.1.1. Physico-chemical strategies

Chemical precipitation and coagulation-floatation in treatment of heavy metal contaminated water can be summarised by addition of precipitant and coagulant agents to form insoluble precipitates of metal hydroxide and stabilisation of colloidal particles which are separated from the water by sedimentation at pH 9-11 conditions, respectively (Aziz et al., 2008;

Heredia and Martin, 2009). Ion-exchange process is a reversible interchange of ions between the solid and liquid phases; resin has the specific ability to exchange its cations with those of the metals in the solution (Khan and Paquiza, 2011). The membrane filtration processes successfully removed metals from the wastewater through ultrafiltration, reverse osmosis, nanofiltration and electrodialysis (Feini et al., 2008; Efligenir et al., 2014). Adsorption is a process of mass transfer of metal ions from the liquid phase to the solid phase surface, the solid retained heavy metal ions from the solution (Inyang et al., 2012). Since adsorption and ionic exchange strategies generate no toxic sludge, are emerging as the environmentally safe methods of redeeming heavy metals from aqueous environments.

1.2.2.1.2. Biosorbents

The efficiency of algae, bacteria and fungi to remove heavy metals from aqueous environment had been investigated (Veglio and Beolchini, 1997; Kadukova and Vircikova, 2005). The cell wall of microorganisms constitutes of functional groups such as polysaccharides, lipids and proteins, which have many binding sites for metals. The physico-chemical interactions between metal ions and functional groups of the cell wall are independent from cell metabolism; enabling a quick and active sorption. Another biological method of eliminating heavy metals from water is by phytofiltration (Tangau et al., 2011, Lone et al., 2008). Heavy metals from water are taken up by metal accumulating plant species through these processes, phytostabilization, rhizofiltration, phytoaccumulation and phytovolatilization. The mobilization of metal ions is assisted by microorganisms, bacteria and fungi, living at the rhizosphere closely associated with plants roots, which contribute to increase the bioavailable fraction of metal ions. As a result, heavy metals such as Cd, Zn, Co, Mn, Ni, and Pb are taken up to 100 or 1000 times more than those taken up by non-accumulator metal plants (Erdei et al., 2005). Also, live roots were more effective in heavy

metal biosorption than dried plant roots biomass (Dushenkov et al., 1995). However, live roots take time to grow, and using plant biomass is a destructive mechanism, for this reason agricultural waste biomass had been investigated as alternative biosorbents for heavy metal retention from water. Agro-waste material preparations and applications as either raw or modified biomass are discussed fully below.

1.2.2.1.3. Agro-waste raw materials

Biomass is a biosorbent that is prepared by drying of the plant material to reduce water content and to prevent mould and fungal development. Drying of the material is often done in ovens at low temperatures ranging from 60-120 °C (Hameed et al., 2009) or the material placed in the sun for few days (Mirsha et al., 2010). After the material is grounded and sieved to a desired particle diameter size ranging from 0.125 to 5 mm, it is ready to be used as adsorbent without any further treatment. The BET surface area of biomass from peel waste is very limited, ranging from 13 to 25 m^2/g (Annadurai et al., 2002; Memon et al., 2008; Memon et al., 2009; Hossain et al., 2012). Surface chemistry constitutes various functional groups responsible to enhance adsorption process; limited surface area and total pore volume reduce the adsorption capacity of such biomass materials (Prahas et al., 2008). However, raw biomass materials had been reported to had achieved excellent adsorption rates for various pollutants including heavy metals (Mishra et al., 2010), dyes (Arami et al., 2005), phenolic compounds (Achak et al., 2009) and cefradine pharmaceutical (Hu et al., 2012). Table 1.4 depicts the effect of particles size and treatment of waste materials on the surface area.

Table 1.3. Outlined heavy metal treatment techniques with their benefits and limitations.

Method of treatment			Benefits	Limitations
[1,2,3]Physico-chemical	Chemical precipitation		Simple process, convenient and safe operation	Large volume of sludge for disposal, slow metal precipitation, poor settling
	Coagulation-flocculation		Shorter time to settle out suspended solids, improved sludge settling	Large volume of sludge for disposal
	Floatation		Low cost, quick hydraulic retention	Subsequent treatments are compulsory
	Membrane filtration		Convenient operation, higher bonding selectivity, smaller space requirement	Inadequate selectivity, pre-treatment required, high residual metal concentration, prone to membrane fouling
	Ion exchange		Possible metal recovery, less time consuming, no sludge generation	Limited pH range for the ion-exchange resin
	Adsorption		Well established, higher removal efficiency and no sludge generations	High operational costs and very high selectivity
Biosorbents	[4]Living microorganisms		Biological sequesters of heavy metal through microbial precipitation.	High cost of growing pure cultures. Sorption can be reduced due to lower temperatures and lack of energy sources
	[5,6]Phytofiltration plants		Very effective remediation of heavy metals in very low concentrations in large volumes of water.	Requires pH adjustment, chelating agents addition may encourage leaching. Very slow process
	[7]Agro-wastes	Raw materials	Low cost sorbent, freely available and easy to prepare	Low adsorption efficiency
		Treated materials	Very effective adsorbent	Cost of thermal treatment and chemical agents become cost effective

[1]Kurniawan et al, 2006, [2]Fu and Wang, 2011, [3]Barakat, 2011, [4]Kadukova and Vircikova, 2005, [5]Tangau et al., 2011, [6]Lone et al., 2008, [7]Demirbas, 2008

In a study, an investigation on the adsorption capacity of sun dried pineapple peels, eucalyptus bark sawdust and mango bark sawdust towards retention of Zn(II) was established (Mishra et al., 2010). The results showed that eucalyptus sawdust obtained the highest adsorption percentage (84%) and pineapple peels showed the least (22.9%). In this investigation it was established that biosorption efficiency and metal ion interaction with adsorbent surface depended on the presence of hydroxylic or carboxylic functional groups involved in metal ion adsorption and surface porosity of these different base materials. In another study, banana peel biomass was investigated on adsorption of Pb(II) and Cd(II) (Anwar et al., 2010). The results showed that, 1g of banana peel biomass adsorbed 2.18 mg and 5.71 mg for Pb(II) and Cd(II), respectively. The optimal removal percentage on banana peels at pH 5 was 85.3% and at pH 3 was 89.2% for Pb(II) and Cd(II), respectively. Also, research done by Perez-Marin and co-workers (2007) on removal of Cd(II) from aqueous solution using biomass of orange peels revealed that adsorption was strongly influenced by pH. For instance, an increase of pH from 2 to 6 realised adsorption percentage of 8 to 98, respectively. A similar trend was observed for Cr(III) adsorption by orange peel biomass, where the removal of Cr(III) increased with the increase in pH (Perez-Marin et al., 2009). In the case of Cr(III), orange peel adsorption capacity increased from 0.57 to 1.44 mmol/g from pH 3 to 5. The lower adsorption of both heavy metals (i.e. Cd and Cr) at lower pH values was due to the competition with H^+ for adsorption sites, and by electrostatic repulsion of metal cations with the protonated biomass surface. Also the deprotonated carboxylic group ($-COO^-$) of orange biomass became responsible for uploading of heavy metals at pH values higher than 5.

1.2.2.1.4. Thermal treated agro-waste

The abovementioned method of biomass synthesis is subject to activation phase to become an activated carbon. There are two activation methods, namely physical and chemical. Physical activation is characterized by pyrolysis (carbonisation) of biomass material in the absence of O_2 or in the presence of CO_2 or steam in a muffle furnace at varying temperatures ranging from 200-1200ºC (Rajeshwarisivaraj et al., 2001; Rashidi et al., 2012). This is done to remove moisture, to eliminate non-carbon elements and open pores on the material (Sundaryanto et al., 2006). Increasing pyrolysis residence time and temperature, reduced the carbon yield percentage (Zhang et al., 2010). The reduction of carbon yield is due to increases of carbon burn-offs from the material and the formation of ash. The surface area of peel waste biochars prepared at 700 ºC ranged from 200 to 243 m^2/g (Chen and Chen, 2009; Foo and Hameed, 2012; Hashemain et al., 2014).

Potato peel waste biomass subjected to pyrolysis at 700 ºC, was investigated for adsorption of Cu(II) in aqueous solution of 150 mg/l (Aman et al., 2008). It was observed that optimum adsorption of 99.8 % was achieved at pH 6. Also, regeneration studies on exhausted potato peel biochar with deionised water and HCl, showed that up to 5 cycles, there was no significant difference between the adsorption and desorption. Therefore, potato peel biochars according to this study can be reused to adsorb Cu(II) repeatedly more than 5 times. Cu(II) removal by rice husk, olive pomace and orange waste biochars prepared at 300 and 600 ºC, was also studied (Pellera et al., 2012). In this study, it was discovered that the optimum adsorption percentage of 90.1, 88.7 and 77.8 % was achieved by biochars of rice husks, orange waste and olive pomace, respectively. Also, it was observed that adsorption of Cu(II) increased as pH increases from 2 to 7 and the optimum pH was 7, and precursors prepared at 300 ºC achieved better adsorption than when prepared at 600 ºC.

Table 1.4. Effects of agro-waste preparation method on BET surface area.

Precursor	Particle size (mm)	Condition	BET surface area (m^2/g)	References
Raw peels				
Orange and banana	5	Oven dried for 24 h at 100-120 °C	20.6-23.5	Annandurai et al., 2002
Banana peel	5	Oven dried for 24 h at 105 °C	22.59	Hossain et al., 2012
	0.125	Oven dried for 8 h at 100 °C	13	Memon et al., 2009
Orange peel	1-2	Oven dried for 72 h at 50 °C	128.7	Li et al., 2008
Thermal treated peels				
Pineapple	1-2	Pyrolyzed at 700 °C	233	Foo and Hameed, 2012
Cassava	0.15-0.25	Pyrolyzed at 700 °C for 1 h	270	Rajeshwarisivaraj et al., 2001
Banana	0.2	Pyrolyzed at 500 °C for 1 h	875.3	Mohammed and Chong, 2014
Orange	0.154	Pyrolyzed at 700 °C for 6 h	201	Chen and Chen, 2009
	1-5	Pyrolyzed at 700 °C for 1 h	243	Hashemain et al., 2014
Chemical treated peels				
Banana	0.2	Esterified by soaking in methanol and HCl	168.4	Mohammed and Chong, 2014
Jackfruit	-	Impregnated with HSO_4 and pyrolyzed at 550 °C for 45 min	1056- 1260	Prahas et al., 2008
Cassava	-	Impregnated with KOH and pyrolyzed at 650 °C for 1-3 h	1154-1183	Sudaryanto et al., 2006
	0.15-0.25	Impregnated with H_3PO_4 and pyrolyzed at 120 °C for 14 h	490	Rajeshwarisivaraj et al., 2001

1.2.2.1.5. Chemically treated agro-waste

Chemical activation is a one-step method where pryolysis and activation occurs simultaneously. Preparation combines the impregnation of carbon-based materials with chemicals such as H_3PO_4, KOH, HCl, NaOH, $ZnCl_2$, K_2CO_3 or H_2SO_4 and heating at temperatures in the range of 450–900 °C for 1 to 4 h (Ioannidou and Zabaniotou, 2007). Depending on chemicals used for activation, an increase of functional groups may be induced, and cation exchange capacity may also be improved (Li et al., 2008; Feng et al., 2010; Feng and Guo, 2012; Pouretedal and Sadegh, 2014). Also, combined effects of chemicals and temperature used in activation improved the pore development in the carbon structure. Increasing the activating temperature increases the pore development through realising of volatile species from the precursor but in this process the carbon yield percentage is reduced (Sudariyanto et al., 2006). However, pine wood activated with H_3PO_4 showed increase in porosity and BET surface area up to1400 m^2/g at 450 ºC due to increase of activating temperature, further increase of temperature beyond this point, reduced the surface area slightly (Hared et al., 2007).

Orange peels activated with NaOH and $CaCl_2$ were used as biosorbent for removal of Cu(II), Pb(II) and Zn(II) ions from simulated wastewater (Feng et al., 2010; Feng and Guo, 2012). The results indicated the maximum adsorption percentage reached at pH 5.5 with rapid kinetics of 10 min was observed in the order 99.4%, 93.7% and 86.6% for Pb(II), Cu(II) and Zn(II), respectively. Orange peel waste biomass was found to contain pectin, soluble sugars, cellulose, hemicelluloses (Rivas et al., 2009). These major constituents contain methyl ester which does not bind the metal ions significantly, however, treating the biomass with NaOH improve its metal-binding ability by hydrolysis of methoxyl groups. Additionally, activating orange peel with $CaCl_2$ makes the pectin contained in the orange peel to precipitate and reduces pectin solubility in solution. This combined effects of orange peel activated by NaOH

and NaOH-CaCl$_2$ significantly improved adsorption capacity of Cu(II) by 20% (Feng et al., 2010) and Pb(II) by 30% (Feng and Guo, 2012), respectively when compared to orange peel biomass.

Cassava peels activated with H$_3$PO$_4$ was found to remove effectively Cr(VI), Hg(II) and Fe(II), obtaining a removal percentage of 99.83%, 86.42 and 92.85 respectively (Rajeshwarisivaraj et al., 2001). In this study, the high efficiency of adsorption was promoted by formation of phosphate group since the agro-waste was initially activated by H$_3$PO$_4$. In a research done by Mamon and co-workers (2008) on adsorption of Cd(II) by banana peels biochar activated with HCl, optimal adsorption efficiency was 95% at pH 8. The main contributing factor attributed to these results was pH effect in a way that at lower pH, a cationic Cd(II) compete with H$^+$ ions for adsorption on a dried banana peels. Hence in this research, adsorption of Cd(II) on banana increased with increasing of pH up to pH 8, afterwards adsorption declined.

2. PART I: ZEOLITE ADSORPTION CAPACITY TOWARDS SMX IN THE PRESENCE OF HUMIC MONOMERS.

2.1. State of the art

It is widely known phenomenon that the existence of antibiotic compounds in aqueous environments provokes the spread of antibiotic resistant genes and antibiotic resistant bacteria (Goa et al., 2012; Bouki et al., 2013; Rizzo et al., 2013). The toxicity of antibiotic resistance genes bears both ecological and public health concerns. The antibiotic of interest for this thesis is SMX, belongs to the persistent sulfonamide antibiotic group. SMX is used as a model molecule to represent the other antibiotics in this group and particularly it is the most used drug after penicillin (Livermore et al., 2005). Sulfa drugs are used to inhibit the multiplication of pathogenic bacteria in both humans and animals. However, after SMX had been administered, it is not completely metabolised, and therefore discarded in portions of human and animal wastes. And so, SMX together with other antibiotic compounds had detected in surface water bodies, drinking water, animal, hospital, pharmaceutical and tertiary treated municipal wastewater (Kummerer, 2009 a; Wei et al., 2011; Goa et al., 2012). These traces of SMX had drawn the attention of researchers to come up with removal strategies to eradicate SMX from the aqueous environments, so as to eliminate the spread of antibiotic resistance genes (Gobel et al 2007; Nakada et al., 2008; Kodesova et al., 2015).

Proposed adsorption methods had been found to be an effective to be employed to remove antibiotics from aqueous environments (Liu et al., 2013; Nam et al., 2014; Zhang et al.,

2016). Although the use of adsorbents such as PAC is very effective on removal of antibiotics from natural waters, adsorption had been reduced drastically due pore clogging by DOM (Nam et al., 2014). Contrary, sulfa drug adsorption by high silica zeolite Y in water was not affected by the presence of DOM, instead marked with quick kinetics and irreversible adsorption (Braschi et al., 2010 a). The unclogging of high silica zeolite Y during adsorption of antibiotics was simply due to higher dimensions of DOM main components than those of zeolite micro pores (de Ridder et al., 2012). However, literature had not addressed the effect of organic components with molecular size similar with the pore diameter of high silica zeolites on adsorption of SMX whereby small molecular organic components and SMX can be adsorbed or pose competition for adsorption in the zeolite active sites.

Fresh-water DOM originates from terrestrial soil organic matter (SOM) by microbial and plant activity at the soil/water interface. However, SOM is mainly made up of three constituents depending on their solubility in acids and alkali conditions, namely fulvic acids, humic acids, and humin (Nebbioso and Piccolo, 2013). Humic acids are a branched macromolecular network built up by numerous organic components of relatively small molecular weight held together by weak non-covalent bonds. Along with other molecules, phenolic compounds like catechol, caffeic, ferrulic, and *p*-coumaric acids, *p*-hydroxybenzaldehyde, vanillin and many others are found to be building blocks of humic substances, hence are referred as humic monomers. For this thesis vanillin and caffeic acid were selected based on that they are both phenolic compounds with an aldehyde and carboxylic functional groups, respectively. Based on their molecular dimensions, both humic monomers are assumed to be diffusable into zeolite porosites. Therefore SMX adsorption into zeolite in the presence of these humic monomers was evaluated to check their adsorption

competition effects against SMX. In addition, to simulate natural, artificial and wastewater; the evaluation was conducted at different wide range of pH conditions.

2.2. Materials and methods

2.2.1. Chemicals

Sulfamethoxazole (4-amino-N-(5-methylisoxazol-3-yl)-benzenesulfonamide, SMX), was obtained from Dr. Ehrenstofer GmbH (Germany) as a white powder with a purity of 99%. Vanillin (4-hydroxy-3-methoxybenzaldehyde, VNL) and caffeic acid (3-(3,4-dihydroxyphenyl)-2-propenoic acid, CA) in powder form were supplied by Sigma Aldrich Co LLC (USA) with a purity of 95 % and 99 %, respectively.

Aqueous solutions of SMX, VNL and CA at 50 μM concentration were used for all the experiments except for adsorption isotherm determination in which solutions at the maximal solubility were prepared. The water solubility of SMX and humic monomers was determined by adding organic compounds to MilliQ water in amounts exceeding those required to saturate the solution. The obtained suspensions were sonicated for 15 min and, then, filtered through 0.45µm Durapore® membrane filters to eliminate undissolved solute from the solution. The solubility, measured by means of high performance liquid chromatography (HPLC-DAD), was 203 ± 2.7 μM for SMX, 9.5 ± 12.5 and 0.25 ± 3.4 mM for VNL and CA, respectively.

High silica Y type zeolite (SiO_2/Al_2O_3, 200 mol/mol) with a surface area of 750 m^2/g was purchased from Tosoh Corporation (Japan).

2.2.2. Persistence of VNL and CA

Aqueous solutions of humic monomers were prepared in polyallomer centrifuge tubes (Nalgene, NY, USA) dissolving 50 μM of each in buffered media at pH 5 and 6 (10 mM, CH$_3$COONa, Carlo Erba Reagents, Milano) and at pH 7 and 8 (10 mM Na$_2$HPO$_4$, Carlo Erba Reagents, Milano). The persistence was followed over 48 h at room temperature (RT) and the VNL and CA concentration was determined by HPLC. The experiment was conducted in triplicate.

2.2.3. Adsorption kinetics

To establish the time needed for SMX, VNL and CA to reach the adsorption equilibrium in zeolite Y, adsorption kinetics were followed over 2 h in non-buffered solutions (to eliminate buffering agent interference) at pH ranged between 5 to 8 (pH was regulated by using diluted solution of HCl and NaOH). Before the kinetics experiments, zeolite Y was pre-equilibrated to the desired pH value using water in a centrifuge tube. Then, the suspension was removed by centrifugation at 15000 rpm for 15 min and supernatant was replaced by solutions of SMX, VNL and CA (50 μM each) at controlled pH with a zeolite: solution ratio of 1 mg: 2 ml. Samples were shaken at RT and at different times, the supernatants were separated from the solid phase by centrifugation and directly analyzed by HPLC. To guarantee the pH stability, it was checked and eventually adjusted by adding few drops of HCl or NaOH diluted solutions for the entire experiment duration. The experiment was conducted in duplicate.

2.3.4. Adsorption screening

Solutions containing SMX, VNL, or CA alone, or combinations of them (binary, SMX/VNL and SMX/CA, and ternary, SMX/VNL/CA) at 50 µM initial concentration each, were

prepared at different pH value ranging from 5 to 8 by adding few drops of HCl and NaOH diluted solutions. Adsorption screening was performed on zeolite Y, subjected to the pH stabilization procedure described in the previous section, with a zeolite: solution ratio of 1mg: 2 ml. After contact, the suspensions were shaken for 1 hour, then centrifuged and the supernatants analyzed by HPLC. The pH of suspensions was checked and adjusted during the experiment. The amount of compounds adsorbed by zeolite Y, was calculated by the difference between initial and final concentration.

2.2.5. Adsorption isotherms

Adsorption isotherms of SMX and humic monomers on zeolite Y were carried out at RT and different pH values ranged between 5 and 8, with a zeolite: solution ratio of 1 mg: 2 ml. Adsorption isotherms were built at several initial concentrations in the range $0 - 200$ µM for SMX, and 0 - 9.5 mM for VNL.CA since we found marginal adsorption, so no adsorption isotherm was conducted. Suspensions of zeolite (at stable pH) and organic compound solutions were shaken for 1 h, then centrifuged and the supernatants analyzed by HPLC. The pH of suspensions was monitored and, eventually, adjusted for the entire experiment.

Owing to the excellent adsorption capacity of zeolite Y (Braschi et al., 2010 a; Blasioli et al., 2014) and the moderate solubility of SMX, additional points of the isotherm were obtained by exposing zeolite Y to subsequent adsorptions of the antibiotic solution at maximal solubility as follows: after 1 hour contact, suspensions of zeolite in SMX solution were centrifuged and the supernatant removed and analyzed by HPLC. Then it was replaced by fresh SMX solution. Subsequent adsorptions were performed until the zeolite reached its maximum adsorption capacity. Adsorption experiments were conducted in duplicate.

The concentration of antibiotic and humic monomers in aqueous phase at equilibrium was expressed as Ce (μM) whereas the amount adsorbed in zeolite (Cs, μmol /g of adsorbent) was calculated by the difference between the initial and final concentrations.

2.2.6. FT-IR spectroscopy

Harmonic vibrational frequencies were computed for SMX and VNL in their Density Functional Theory (DFT) optimized geometry (*vide infra*), and compared to experimental IR spectra.Experimental infrared spectra were collected on a Tensor27 spectrometer (Bruker, MA, USA) with 4 cm^{-1} resolution. Self-supporting pellets (10 mg each) of zeolite Y, singly loaded with SMX or VNL and with their mixture, were obtained with a mechanical press (SPECAC, UK) at ca. 7 tons cm^{-2} and placed into an IR cell equipped with KBr windows permanently attached to a vacuum line, allowing sample dehydration *in situ*. FTIR spectra of SMX or VNL in CH_2Cl_2 were performed in a NaCl cell for liquids. Spectrums of the bare zeolite were collected as a control.

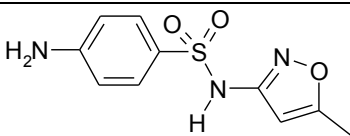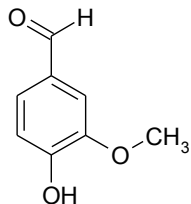## 2.2.7. Chromatographic analysis
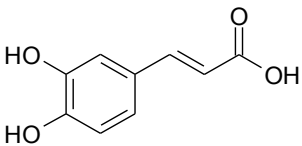
The concentration of SMX, VNL and CA was determined using HPLC-DAD. The system was assembled with Jasco 880-PU Intelligent pump, a Jasco AS-2055 plus Intelligent Sampler, a Jasco 875-UV Intelligent UV-vis diodarray detector at 271 nm, a Jasco ChromNAV1.14.01 chromatography data software, a Jones Chromatography model 7971 column heater and a 4.60 nm x 250 mm Waters Spherisorb® 5μm C8 analytical column (Waters, USA). The analytical column was kept at 35 ºC and eluted with acetonitrile: water (30:70 by volume, pH 2.7 for H_3PO_4) at a flow rate of 1ml/min. Under these conditions, the retention times were 6.8, 5.5 and 3.8 for SMX, VNL and CA respectively.

2.3. Results and discussions

2.3.1. Chemicals characteristics

The aim of this experiment was to investigate the adsorption of SMX on zeolite Y in the presence of humic monomers i.e. vanillin (VNL) and caffeic acid (CA) at different pH levels (5-8). These humic monomers were chosen based on their occurrence in waters and their size (containing one aromatic ring) which is smaller than the pore dimensions of zeolite Y. Since these molecules are smaller than SMX, they were assumed to pose competition during adsorption of SMX on zeolite Y. Both VNL and CA are phenols with aldehyde and carboxylic functional groups, respectively. The chemical structures and the pK_a values of investigated chemicals are reported in Table 2.1.

Table 2.1. Characteristics of molecules under investigation.

Chemical name	Acronym	Chemical structure	pK_a	Reference
Sulfamethoxazole	SMX		5.7	Koizumi et al., 1964
Vanillin	VNL		7.4; 11.4	The Chapman and Hall, 1995
Caffeic acid	CA		4.5; 8.6; 12.5	Kiss et al., 1989

2.3.2. Degradation of humic monomers in water

Humic monomers water persistence was conducted to test the stability of these molecules in water in order to exclude their degradation products during the adsorption process. The

degradation kinetics of CA and VNL in the pH range of 5-8 was followed for 48 h, as displayed in Figure 2.1.

Persistence of both humic monomers were stable at all pH investigated. A study done by Friedman and Jurgens (2000) confirms the stability of CA in acidic pH values 3-6 up to 24 h. Also, it was observed that CA degradation was evident at pH higher than 8 within 24 h contact time. Although in the present study two degradation products were observed, it was out the interest of this thesis to elaborate more on them. These results gave an indication of how long the adsorption experiments should be conducted to rule out the degradation effect. Hence the adsorption kinetics was conducted within 2 h.
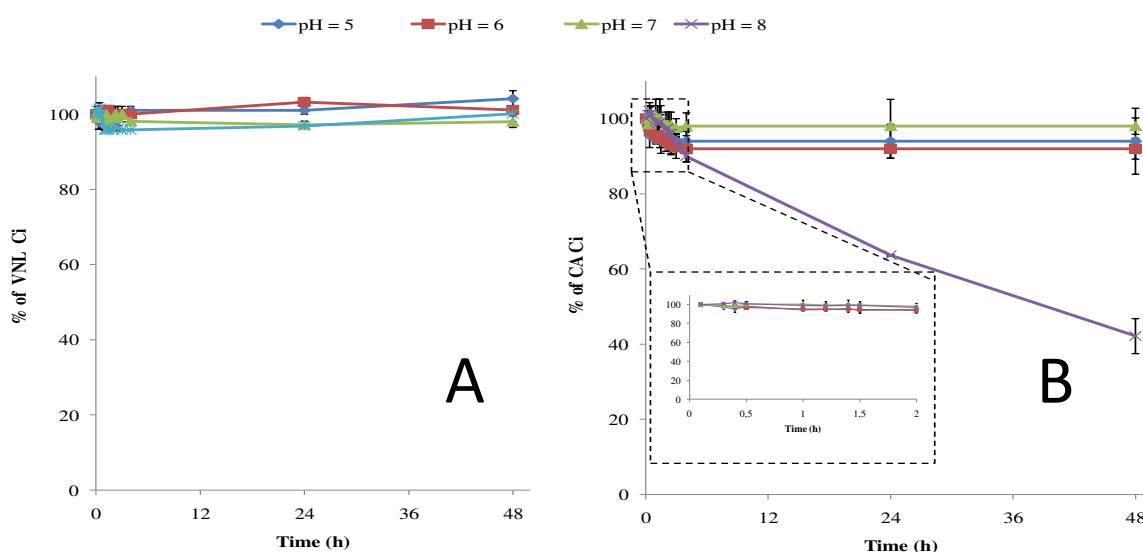

Figure 2.1. Degradation kinetics of vanillin (VNL) and caffeic acid (CA) (initial concentration, 50 µM) in buffered solution at pH 5 and 6 (CH$_3$COONa, 0.01M) and pH 7 and 8 (Na$_2$HPO$_4$, 0.01M). A detail of CA kinetics is reported in the inset B. Bars indicate an absolute error.

2.3.3. Adsorption trials

2.3.3.1. Adsorption kinetics

According to the observed humic monomers degradation, the adsorption kinetics of VNL, CA and SMX on zeolite Y was followed within 2 h contact time in the pH range of 5 to 8. Adsorption kinetics was conducted to investigate the time needed by each molecule to reach the adsorption equilibrium. Figure 2.2 depicts the adsorption kinetics of all the molecules in investigation.
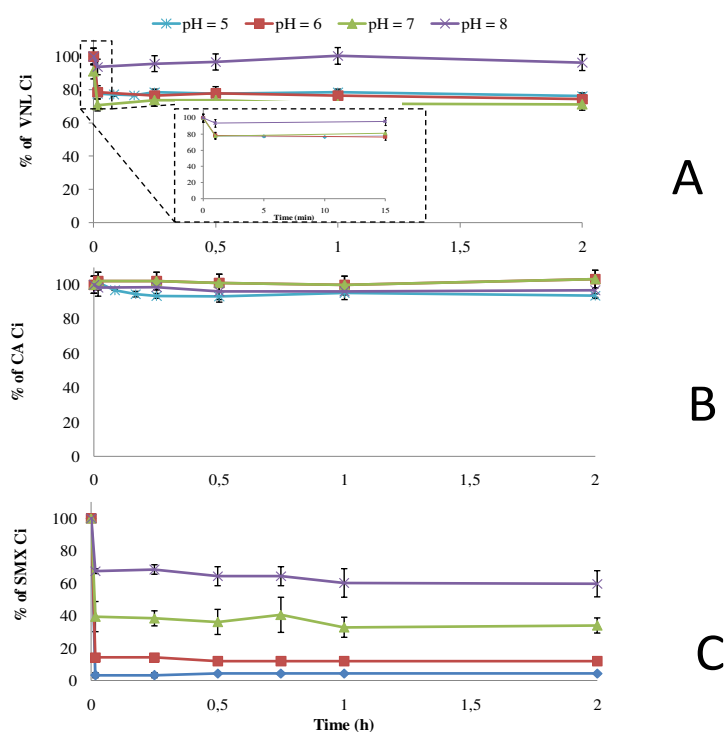
Figure 2.2. Adsorption kinetics of A) VNL B) CA and C) SMX on zeolite Y at different pH values (5-8) after 2 hours of contact time. A detail of VNL adsorption kinetics is reported. Bars indicate absolute error.

The adsorption equilibrium of CA at pH 5 was reached within 15 min, a time longer than that observed for VNL and SMX (ca. 1 min), whereas CA at the higher pH values (6-8) no significant decrease in its initial concentration was found. This behaviour can be explained by

the value of pK_a of 4.5 for CA (Table 4.1), when the pH is above the pK_a, more negative species are formed. At pH below the pK_a value, the molecule is in the neutral form so the affinity for the zeolite is higher. Likewise VNL's fast adsorption kinetics was inversely affected by pH, resulting in adsorption decreasing as the pH increasing. Furthermore, at pH 8 an inadequate amount of VNL (pK_a of 7.4) was retained by the zeolite Y due to the occurrence of species mainly in anionic form at pH 8.

The adsorption equilibrium of SMX was also very fast and was reached within 1 min at the entire pH range of 5-8. Several studies had confirmed this behaviour of SMX and other sulfa drugs on different kinds of zeolites (Braschi at al., 2010 a; Fukahori et al., 2011; Blasioli et al., 2014). On a slightly different zeolite HSZ-385, SMX adsorption was found to have quick kinetics reached within 1 min and the amount of SMX retained by the zeolite was inversely related to the pH value of water solution as in the present study (Fukahori et al., 2011). This adsorption behaviour can be explained in consideration of SMX pK_a value of 5.7 (Table 4.1), and the hydrophobic nature of the zeolite Y. For instance, at solution of pH 5, SMX is mainly in neutral associated form, thus allowing the highest amount to be retained due to the hydrophobic host-guest interactions into the zeolite pores (Fukahori et al., 2011). Furthermore, observations indicating that VNL and SMX were adsorbed at the same time by zeolite Y, it can be speculated that these molecules can compete for the zeolite adsorption active sites. Therefore, adsorption screening was deemed necessary to give an indication of the behaviour of these molecules in the mixture towards the zeolite adsorption porosities.

2.3.3.2. Adsorption screening

Adsorption screening was conducted to investigate the adsorption behaviour of molecules as a single component, as well as in binary mixture and in ternary mixture (Table 2.2). As single components, the adsorption of VNL and SMX decreased by increasing of pH value, confirming what had already been observed in the adsorption kinetics. Similarly to adsorption

kinetics, CA was not adsorbed significantly at any pH value investigated. In single component, the adsorption of SMX on zeolite Y was found to be significantly higher than that of VNL in the entire pH range. As far as the adsorption in the binary mixture of SMX and VNL is concerned, adsorption trends that were observed were similar to those as single components.

Table 2.2. Adsorption screening of VNL, SMX and CA [50μM each] on zeolite Y, alone and in the presence of equimolar concentration of each species at pH range between 5 to 8 within 1 h contact time. Numbers in parenthesis are absolute error.

pH	VNL, SMX and CA adsorbed on zeolite (% of initial concentration)									
	Single component			*Binary mixture*				*Ternary mixture*		
	VNL	SMX	CA	VNL	SMX	CA	SMX	VNL	SMX	CA
5	34.9 (1.3)	95.6 (0.0)	3.7 (1.1)	46.0 (0.0)	93.2 (1.0)	4.7 (0.6)	93.1 (0.6)	47.2 (0.4)	96.8 (0.5)	5.1 (0.3)
6	23.5 (1.6)	88.0 (1.5)	0.5 (0.0)	36.9 (3.5)	77.9 (4.9)	4.0 (1.5)	85.4 (4.2)	37.6 (0.9)	81.0 (2.0)	4.9 (0.5)
7	21.4 (0.8)	66.1 (4.6)	0.1 (0.0)	19.7 (6.3)	45.3 (4.9)	4.0 (1.0)	62.4 (11.8)	13.6 (0.3)	29.0 (0.4)	5.0 (2.0)
8	0.0 (2.4)	26.1 (8.5)	2.9 (1.5)	12.2 (2.9)	14.7 (6.5)	1.8 (0.3)	8.6 (1.9)	6.4 (1.5)	11.8 (0.4)	0.0 (0.3)

Since both SMX and VNL were co-adsorbed within 1 min, adsorption competition was induced, hence in the binary mixture SMX retention was reduced slightly reduced and VNL was enhanced compared to a single component. Similar trends of VNL and SMX adsorption

were also observed in the ternary mixture; due to ineffective adsorption of CA on zeolite Y. Since in the ternary mixture only VNL and SMX co-adsorption was observed, then CA non-interference did not lead to pore clogging. Therefore, it was interesting to evaluate zeolite loading capacity and the affinity for VNL and SMX, which can be observed by adsorption isotherm.

2.3.3.3. Adsorption isotherm

Adsorption isotherm was conducted at room temperature (RT) to assess the maximal amount of SMX and VNL adsorbed as single compounds in zeolite pores and the affinity of each compound on the zeolite active adsorption sites. The adsorption and desorption isotherm of SMX and VNL are reported in Figure 2.3. Adsorption isotherm gives an indication of maximal loading capacity of zeolite and the affinity of zeolite towards the each molecule. The affinity of zeolite can be observed by the slope of the curve and maximum loading capacity can be observed by the plateau value.
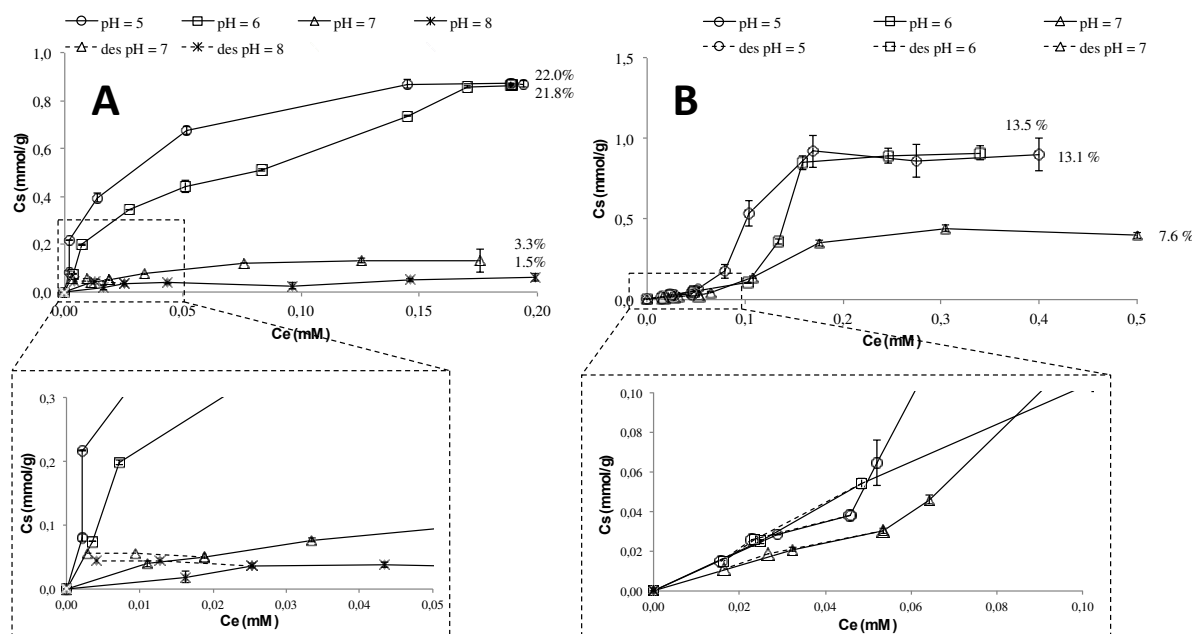
Figure 2.3. Adsorption and desorption isotherms of A) SMX and B) VNL by zeolite Y at different pH values 5-8 for 1 h contact time at RT. Bars indicate absolute error.

According to these findings, the amount adsorbed on zeolite Y at maximal concentration was about 22% (wt/wt) at pH 5 for SMX. In agreement with Blasioli and co-workers (2014), the isotherm curve of SMX exhibited two different adsorption regimes at pH 5.8-6. These adsorption regimes were due to different pores of zeolite. It was most probably that SMX was firstly adsorbed at higher affinity sites and when were completely filled, adsorption continued steadily at lower affinity sites. The maximal adsorption of SMX at pH 5 and 6 was almost equivalent to 22% of zeolite dry weight (dw), whereas at pH 7 and 8, it was only 3.3 and 1.5% zeolite dw, respectively. As clearly shown by the curve slope, at SMX low concentrations, the affinity for the sorbent is inversely related to the pH value. As already been explained in kinetics study, the antibiotic pK_a (5.7) can explain both the higher affinity for the zeolite at low concentrations and the higher antibiotic loading at the plateau at acidic pH values. Since adsorption at acidic pH already defined as irreversible (Blasioli et al., 2014), the SMX desorption experiments were investigated only at pH 7 and 8. As shown in caption of Figure 2.3 A, parallel lines to the x-axis indicates the irreversible adsorption of SMX from the zeolite Y cages also at pH 7 and 8. Several H-bonding, polar and van der Waals type host-guest interactions between single antibiotic molecules and the zeolite pore wall acted simultaneously to irreversibly extract sulfa drugs from water (Braschi et al., 2010 b; Braschi et al., 2013; Blasioli et al., 2014).

Since adsorption of VNL was negligible at pH 8, the adsorption and desorption isotherm for VNL by the zeolite Y was conducted in the pH range of 5-7. Zeolite affinity towards VNL and maximum loading capacity was inversely related to the water pH due to its pK_a value (7.4). The maximum adsorption of VNL as indicated by a plateau was achieved at ca. 13 and 8% zeolite dw at pH 5-6 and pH 7, respectively. At acidic pH, a full loading of the zeolite cages was found whereas 75% of cages were occupied at neutral pH. According to the desorption isotherm as detailed in Figure 2.3 B, the desorption curves overlapped the

adsorption ones at all investigated pH values, therefore indicating VNL adsorption as fully reversible.

2.3.4. Infrared analysis

Infrared analysis was conducted to check the host-guest interactions between each molecule and the zeolite adsorption sites. To observe the spectrum of single molecules of VNL, dichloromethane, a non polar solvent, was used (Figure 2.4 A).This allowed a better observation of the spectral features of the adduct that were eventually formed. Experimental FT-IR spectra of VNL in CH_2Cl_2 and singly embedded into the zeolite Y, along with the harmonic vibration spectrum calculated by the DFT level for the isolated molecule (in vacuum) are reported. In the spectrum of CH_2Cl_2, although strong solvent bands in the 3250-2750 and 1500-1400 /cm range are overlapped to those of VNL, as well as the occurrence of signals coming from water traces in the region above 3600 /cm, the most part of VNL vibrations were also observed.
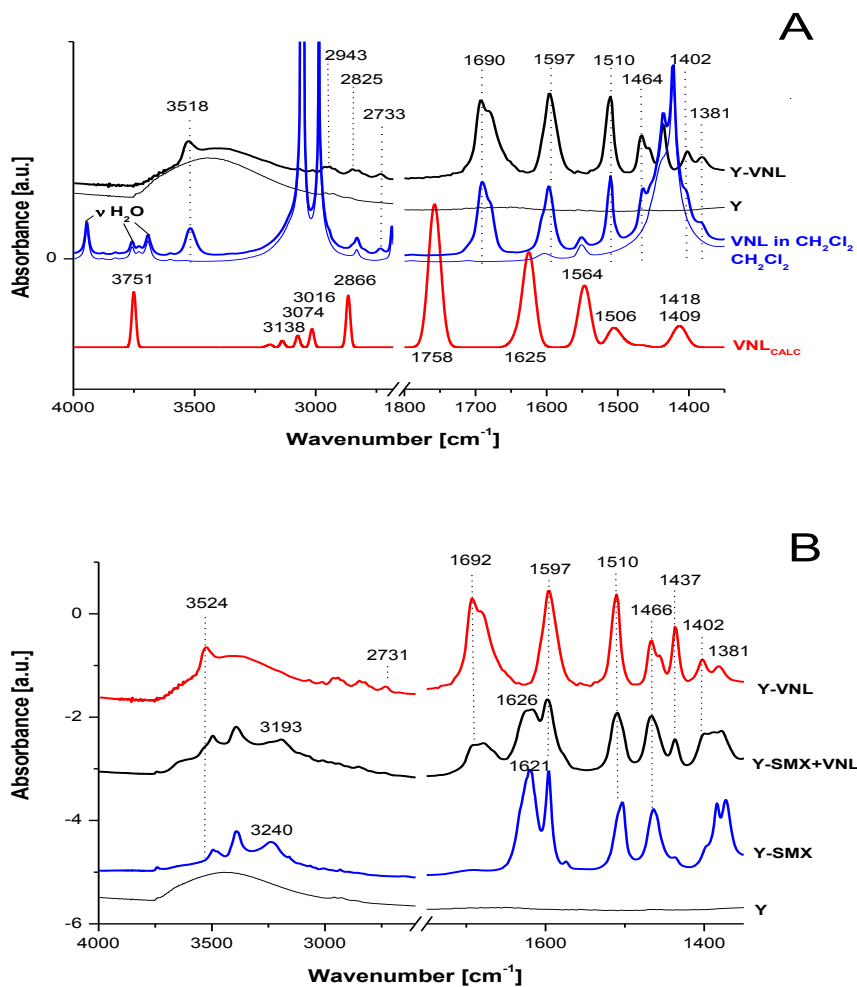
Figure 2.4. A) DFT calculated spectrum of VNL in vacuum (VNL$_{CALC}$) and experimental spectra of VNL in CH$_2$Cl$_2$ and adsorbed into zeolite Y (Y-VNL). Experimental spectra of CH$_2$Cl$_2$ and zeolite Y are reported for comparison. B) Experimental spectra of the zeolite singly loaded with VNL (13% zeolite dw) or SMX (21% zeolite dw) and with a SMX+VNL mixture (7 and 20 % of zeolite dw, respectively).

These features indicate that the interactions between VNL and the zeolite framework are due to weak dispersive forces whose contributions are strong enough to stabilize the intramolecular H-bonded VNL into the cage. Rietveld refinement performed on the VNL-

loaded zeolite revealed the presence of about 9.5 molecules per unit cell (corresponding to 11% zeolite dw and 1.18 molecules/cage), in good agreement with the loading data (13.3% zeolite dw) of the related adsorption isotherm.

A detailed description of the host-guest interactions developed by SMX embedded into the same zeolite in amide form has been clearly defined by Blasioli and co-workers (2014). To maximize the possible guest-guest interactions into the zeolite pores, a Y sample simultaneously loaded with SMX and VNL (6.9 and 20.1% zeolite dw, respectively) was investigated by infrared and Rietveld analysis. In the sample, 100% of pores contained at least one SMX molecule whereas ca. 50% embedded one VNL molecule on average. The experimental IR spectrum of the SMX+VNL loaded mixture is reported in Figure 3.3 B, at this point, spectra of singly loaded SMX or VNL are reported for comparison. In the spectrum of the loaded SMX-VNL mixture, resembled bands occurred at position similar to those of the singly embedded compounds. As far as the VNL contributions are concerned, a clear perturbation of the carbonyl stretching region could be observed between 1700 and 1650 cm^{-1}, thus indicating this group likely involved in the stabilization of a SMX-VNL cluster. Concerning the SMX signals, the bands of singly embedded SMX (ca. 50%) are found overlapped to contributions of those clusterised with VNL (remaining 50%) and a clear perturbation of the stretching and bending NH signals was observed. In clusterised SMX, the stretching of NH at 3193 cm^{-1} is downshifted (Δ = -47 cm^{-1}) with respect to its position when singly adsorbed (3240 cm^{-1}), whereas the NH bending at 1626 cm^{-1} is upshifted (Δ = +5 cm^{-1}) with respect to that as a single component (1621 cm^{-1}). These findings clearly indicates an H-bonding between the VNL carbonyl and the SMX NH (VNL-C=O···HN-SMX), with the latter group which can be originated from both (i) SMX in amide form (SO_2-NH-) and (ii) the heterocycle ring NH of SMX in imide form (SO_2-N=C).

2.4. Conclusions

By the experiments conducted to investigate the adsorption of SMX in the zeolite Y in the presence of humic monomers, the following can be concluded. VLN and CA was persistent in water at least for 1 h and VNL adsorption kinetics were as quickly as those of SMX on zeolite Y. CA adsorption on zeolite Y was marginal due to its acidity nature (pKa 4.7), as a result the CA did not show any effect on adsorption of SMX both in binary and ternary mixtures. Contrary, VNL doubled the amount adsorbed on zeolite Y in the presence of SMX both in binary and ternary mixture than as single component. Therefore neutral species of VNL that are formed due to pH lower than its pK_a (7.4), can compete with SMX for zeolite adsorption sites (i.e. pores). However, since the adsorption of SMX is irreversible whilst that of VNL is reversible, therefore SMX should be retained more firmly by the zeolite. Furthermore, zeolite Y showed a preferential adsorption towards SMX due to its molecular structure configuration of "V" shape. These findings are of utmost interest for scientists working with zeolite-based technologies to treat wastewaters where a variety of humic phenolic compounds always occur.

3. PART II: ADSORPTION CAPACITY OF PEEL WASTE ON HEAVY METALS

3.1. State of the art

Water pollution by heavy metals cause both environmental and health problems throughout the world, due to their toxicity and poor biodegradability (Fu and Wang, 2011). The eradication of these elements from water through conventional methods requires either highly technical skills or comes at very high cost in which developing countries find it difficult to afford (Kurniawan et al., 2006; Mohan and Pittman, 2007; Barakat et al, 2011).

Agro-waste by-products have been recently investigated as alternative cheap biosorbents for removing heavy metals from aqueous environment. These waste materials include residues of shells (walnuts, peanuts and hazelnuts), cereal waste (rice, wheat and maize), peels (banana, cassava, orange, and lemon) (Demirbas, 2008). Agro-waste materials are abundantly available and contain high organic carbon content, cellulose and lignin. Consequently, they have shown considerable potential for being used as sorbents for heavy metal removal.

The juice and starch extracting plants produce peels, pits and stems as waste material with no economical value. For instance, in developing countries it was estimated that the production of orange peel (OP) (among other fruit and vegetables peel waste) was more than 1 million tons per annum in Egypt (Nerm et al., 2009) and about 250000 tons in South Africa (Van

Heerden et al, 2001). Hence the peel wastes that have been considered in this thesis to be used as adsorbent for Zn(II) and Cu(II) removal from aqueous environments were banana, orange, pineapple and potato peel. Agro-waste peels are rich in cellulose, lignocellulose and pectin which are active components for metal ion binding sites (Sud et al., 2008; Rivas et al., 2009). These waste materials can be utilized as raw biomass sorbents or modified thermally or chemically. The main absorption mechanisms involved are: complexation, adsorption on the surface and in the pores, entrapment, ion exchange and chelation (Basso et al., 2002). Literature revealed high removal efficiency on Pb(II) and Cd(II) using banana peel biomass, obtaining 2.18 and 5.71 mg/g for Pb(II) and Cd(II), respectively (Anwar et al., 2010). Also, high removal efficiency above 95 % for Cd(II) and Cr(III) was achieved by using orange peel biomass (Perez-Marin et al. 2007; Perez-Marin et al., 2009). The abovementioned experiments were conducted on batch and the favourable pH for optimum condition was ranging between 4 and 6. However, amid precipitation of metal ions at pH values higher than 6, it had been reported that carboxylate functional group (R-COO$^-$) of banana peels probably was responsible of binding Cd(II) cations optimally at pH 8 (Memon et al., 2008). Therefore, without altering the pH of natural water which is expected to be in the range of 6-8, adsorption of metallic ions can be achieved.

However, batch experiments become disadvantageous on application in large scale continuous flow operations due to time taken to reach the adsorption equilibrium (Zulfadhly et al., 2001; Vinodhin and Das, 2010). Coupled with this practise, peel waste exposed to aqueous phase for long periods tends to degrade off and releases soluble organic components. Therefore, to simple avoid the abovementioned, fixed bed column experiments had been investigated for retention of heavy metals in simulated industrial wastewater using untreated peel waste (Chao et al., 2014; Chatterjee and Schiewer, 2014; Simate and Ndlovu, 2015). Hence in this thesis, column experiments were conducted using peel waste biomass for

sorption of Zn(II) and Cu(II) spiked in natural river water. Cu and Zn are essential trace elements for human and plant use; however, human activities such as mining become a major reason why these elements are found abundantly in surface and underground water.

This project is aiming to model the feasibility of using peel wastes materials in real applications on retention of Zn(II) and Cu(II) from polluted surface water sources. Furthermore, since river water is used for irrigation, the treated water samples using peels were evaluated on growth of romaine lettuce in hydroponic system.

3.2. Materials and methods

3.2.1. Peel wastes

Peel waste is abundant and freely accessible resource material with no significant value. To make the most of this invaluable resource, 4 different peel wastes were selected based on their abundantly availability, namely banana peel (BP), orange peel (OP), potato peel (PoP) and pineapple peel (PP). The peels were separately collected from a kindergarten school in Bologna (Italy).

The peels were oven dried at 120 ºC for 4 h. Dry peels were then crushed into a porcelain mortar and sieved at ≤ 0.5 mm particle diameter. Sieved peels underwent thermogravimetric analysis (TGA) using TG-DTA92 B (Setaram, France). Elemental analysis of the peels was conducted by a Spectro Arcos inductively coupled plasma spectrometer (ICP-OES) (Germany). Also, sieved peels were analyzed for their total organic carbon (TOC) and total nitrogen (TN) by a Thermo Fisher Scientific elemental analyzer (Mod. Flash 2000, USA).

3.2.2. Peel washing on column

A glass microfibre filter (4.7 cm diameter) (Whatman GF/D, USA) was placed at the bottom of a glass column (3.6 cm of internal diameter). Then the column was filled with 1 g of each peel and washed with distilled water until the eluate (peel washing) was clear (ca. 500 ml). Several aliquots of each peel washing were analyzed for Ca, K, Mg, Na, P, S, Zn and Cu by ICP-OES. Each peel washing was also characterized for pH using a portable pH meter (XS Instruments, Mod. 510, Italy) and electrical conductivity (EC) at 20 °C with a MeterLab EC analyzer (Mod. CDM210, France), respectively. TOC and TN were measured with a Shimadzu elemental analyzer (Mod. TOC-V CPN and TNM-1, Japan) according to ISO 8245:1999 and EN 1484:1997 methods, respectively. Briefly, ISO 8245:1999 involves oxidation of organic carbon in water to CO_2 by combustion whereas EN 1484:1997 involves releasing of CO_2 by using mineral acids to assist in N content analysis (Jensen et al., 2003). Peel washings were kept in dark and stored at 4°C.

3.2.3. River water spiked with Zn and Cu

Natural water samples were collected from river Reno in Bologna (44°31'00.4"N 11°17'54.2"E) (Italy) and immediately filtered through 0.22 μm Whatman filter paper (USA) to remove microorganisms and suspended solids. The filtered water was characterized for chemical and physical characteristics as already described above for peel washings. River water was kept in dark and stored at 4 °C before use.

A solution of Cu(II), Zn(II) or a mixture of both were prepared by adding 10 mg of $CuCl_2$ Sigma-Aldrich (Germany) or/and 10 mg of $ZnCl_2$ (Sigma-Aldrich, Germany), to 1 l of 0.22 μm-filtered river water. The Cu, Zn, and Cu+Zn solutions were then sonicated using an Elma sonicator (Germany) for 10 min and filtered again at 0.22 μm with Whatman filter paper (USA). The last filtration step was necessary to eliminate the suspended soluble solids from

the metal solution. After filtration, the concentrations of Cu (10 l), Zn (5 l), and Cu+Zn (2 l) in river water obtained by ICP-OES were 1.8 (±0.2), 4.8 (±0.7), 6.4 (±0.6) and 1.8 (±0.1) + 6.4 (±0.6) ppm, respectively. The solutions were used as eluants in peel columns.

3.2.4. Water treatment on peel column

About 10 l, 5 l and 2 l of river water spiked with Cu (II), Zn (II) and their mixture, respectively, were passed through 1 g of each peel (BP, OP, PoP or PP) in column. Each eluate was collected in 100 ml aliquots up to 1 l and thereafter, aliquots of 1 l were collected in to make a total of 2, 5 and l0 l of different experiments. All experiments were conducted in duplicate. The retention of Zn and Cu by peel column was calculated as the difference between their concentrations before and after the treatment by ICP-OES (Spectro Arcos, SPECTRO Analytical Instruments GmbH, Germany) and was expressed as a percentage of peel dry weight (dw). After the adsorption experiment, treated water samples were kept in the dark at 4°C before used in other experiments.

Adsorption isotherms of Cu and Zn on peel waste were carried out at RT. Adsorption isotherms were built at initial concentrations at 1.8 and 4.8 mg/l for Cu and Zn, respectively. A column with 1 g of peel waste was established and Zn and Cu solution were repeatedly percolated up to saturation of the adsorption sites of each peel. The metal amounts retained by the peel were calculated as the difference between the initial Cu and Zn concentrations (eluant solutions) and their concentrations after peel adsorption (eluate solutions) and related to the peel dry mass. All the total metal content measures were done by ICP-OES.

Peel X and Gamma Ray mapping: BP, before and after adsorption of Zn was analyzed to detect the elements in the peel using motorized XRF for X Ray Fluorescence mapping analyzer (XG Lab, Italy). Besides Zn detection, Ca, Ti, Fe, Mo and Ni were also analyzed within 1 min at 50 kV tube voltage.

3.2.5. Lettuce growth experiment

The effect of treated water samples collected from each peel column on the growth of romaine lettuce was investigated by a floating system in a glasshouse. The adopted floating system comprised of a hydroponic system equipped with a styrofoam sheet drilled to fit plants roots and a 34 cm x 24 cm x 10 cm polypropylene plastic bowl containing nutrient solution. Once the styrofoam sheet was cut to fit the size of plant roots, and put over the bowl with 4 l of nutrient solution, the roots became submerged to the nutrient solution and leaves were kept afloat by the styrofoam sheet.

The following nutrient solutions were tested: the river water spiked with Cu (RWCu), Zn (RWZn) and their mixture (RWCu+Zn), as a positive control, waters treated by peels (i.e. Peel Cu, Peel Zn and Peel Cu+Zn), river water (RW) and tap water (TW) as a negative controls. Each water sample was corrected to fit the desired value of the standard nutrient solution (SNS) for macro elements: 0.6 mM of KH_2PO_4 and 5 mM of KNO_3. All nutrient solutions were adjusted to pH 6 (±0.9) using diluted H_2SO_4 (AppliChem, Germany) and EC was found to be ≤ 2 mS/cm. Each trial (three plants-floating system container) was replicated three times.

The chemical and physical analysis of water samples were conducted as previously mentioned for river water.

The plant growth was followed for 28 days (4 weeks). Samples of nutrient solutions from each trail were taken to evaluate the nutrient plant uptake. At the end of 28 days, the lettuce was harvested and the fresh and dry weight for leaves and roots were recorded separately. The harvested lettuce leaves and roots were dried at 60°C for 72 h.

The concentration of Cu and Zn contained in the edible and non-edible parts of dried lettuce was determined by ICP-EOS after acid digestion. Briefly, an amount of 0.250 g of dry lettuce parts was weighed into PTFE recipients, added with 6 ml of 15.8 M of HNO_3 (Sigma-Aldrich, Germany) and 1.5 ml of 9.79 M of H_2O_2 (VWR Chemicals, Italy) and digested in a Mileston microwave oven (Shelton, CT, USA). The digested suspension was filtered at 0.45 μm through Whatman no.42 paper filters, brought to 20 ml with de-ionised water, and analysed through ICP-OES spectrophotometer.

3.3. Results and discussions

3.3.1 Characterisation of peels and water samples

The TGA was executed to evaluate thermal degradation of carbonaceous materials in terms of moisture content, volatile matter, fixed carbon and ash. TG-DTG of the starting material (before washing) is displayed in Figure 3.1. In the derivative of thermograms (DTG curve), five major mass loss peaks can be observed for all peels in the following temperature ranges: below 150 °C, from 150 up to 280 °C, from 280 up to 360°C, from 360 up to 550 °C and above 550°C. According to the literature, the first loss at < 150 °C is due to the moisture content while the following losses are due to the decomposition of pectins, hemicelluloses and cellulose, respectively (Chen and Chen 2009). In Chen and Chen (2009) study, it was observed that lignin degraded in a wider temperature range above 300 ºC.
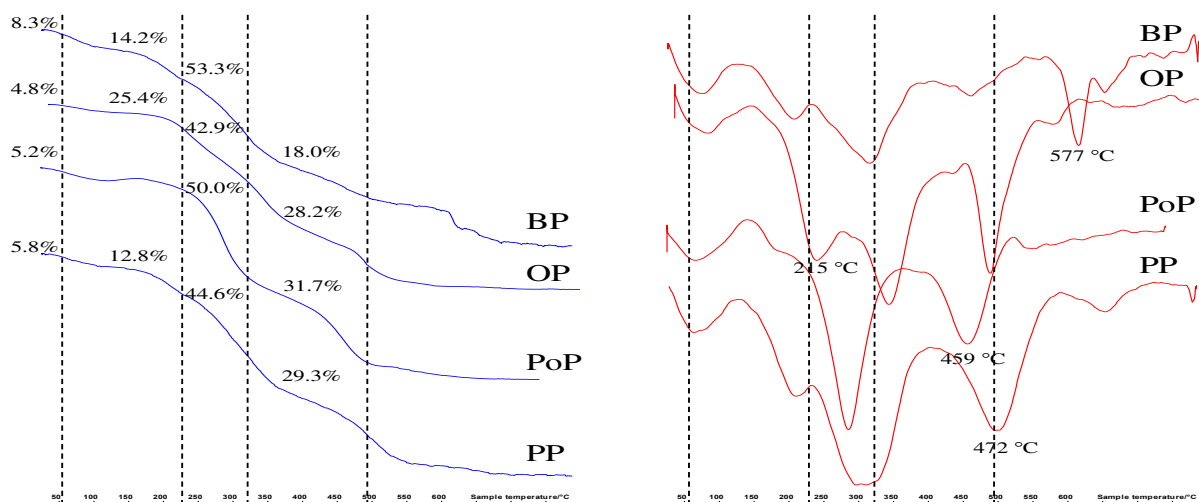
Figure 3.1. TGA-DTG analysis of different peels before washing. Change in mass of peel as a function of temperature (left) and the derivative curves (right).

Therefore, it can be deduced that the major weight loss occurred at the temperature ranged between 280 and 360 °C, was attributed to cellulose decomposition up to 53.3, 50.0, 44.6 and 42.9 wt % for BP, PoP, PP and OP, respectively. However, recent studies indicated average weight loss of 21 wt % at 312 ºC for cellulose decomposition of BP, OP and PP (Sanchez et al., 2014; Selvarajoo and Hanson, 2014). Nonetheless, what was observed in the raw material of peels was altered slightly due to washing of peels (washing process is described below) as presented in Figure 3.2. Alterations are observed at the temperature where decomposition peaks are occurring. For instance, due to washing of peels, decomposition peak for hemicellulose seemed to be absent (temperature range, 150 – 280 °C). This was due to partial decomposition of pectins and hemicellulose between 150 and 360 °C as a result a major weight loss was observed at this temperature range up to 87.3 and 59.8 wt % for PP and PoP, respectively.
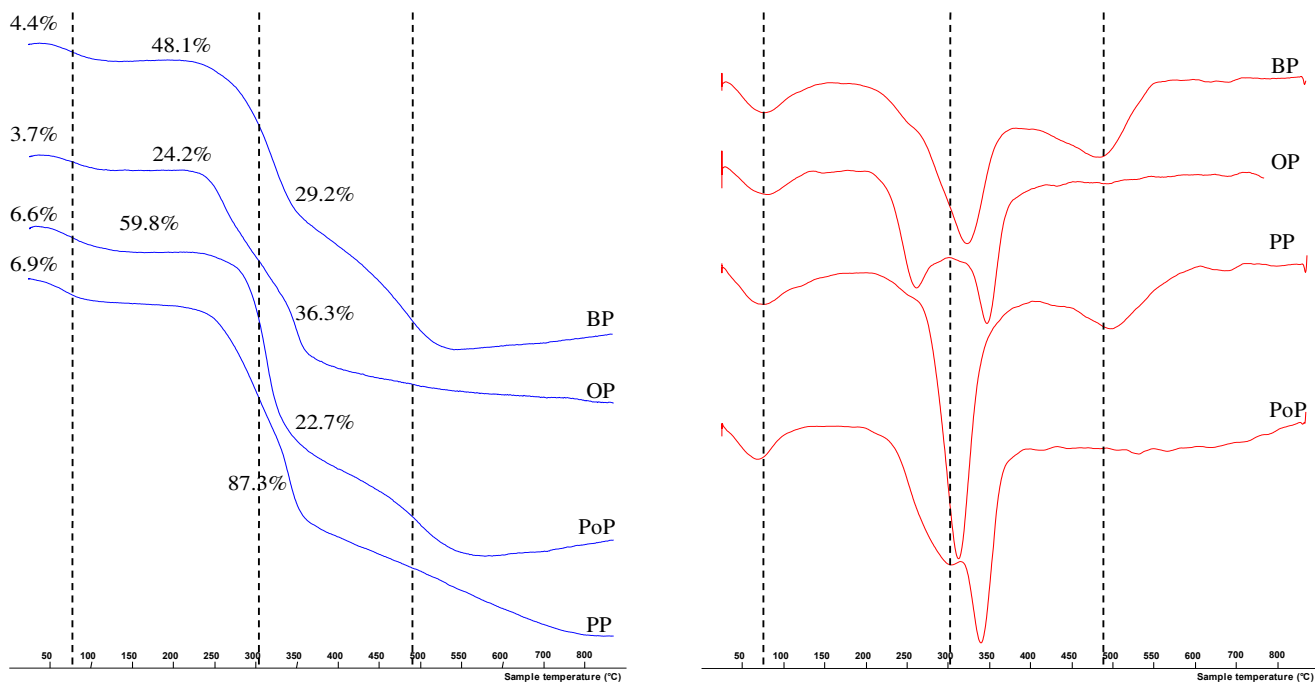
Figure 3.2. Curves of thermogravimetric analysis (TGA-DTG) of different peels after washing. Change in mass of peel as a function of time (left) and the derivative curves (right).

Above 400 °C, it was observed that a further loss in weight which affected all the peels, due to the total decomposition of the cellulose and the decomposition of lignin. BP, OP and PP decomposition peaks demonstrated another weight loss temperature above 550 °C relative to the complete decomposition of the residual carbonaceous material (Chen & Chen, 2009). Variations in temperature for the various decompositions recorded in the peels can be attributed to several side branches of the macromolecules and the different compositions of individual peels.

Chemical content analysis of all peels was done to verify how much of heavy metals were contained in it before their use as sorbents. Peel wastes analysis performed on raw material (rm) revealed that all selected peels were free of Cu but contain traces of Zn and other chemical elements as displayed in Figure 3.3. Contrary to the finding of Rivas and co-

workers (2008) who also found traces of other heavy metals such as Mn, Fe, Al, Ni, Cu, Cr on chemical content of OP biomass.

The total organic carbon (TOC) was found to be more than 35 mg/g for BP, OP and PP with the exception of PoP where TOC was slightly lower (33 mg/g). However, PoP indicated higher levels of TN (1.92 mg/g) compared to 0.79, 090 and 1.22 mg/g for OP, PP and BP, respectively.

Pulverized peel waste still contained pigments, which are responsible for the colour formation in fruit and vegetables, particularly flavedo of the orange peel (Mzini, 2002). To eliminate soluble components like organic acids or pigments contained in raw peels, before the adsorption experiments, it was necessary to wash the crushed peel waste with deionised water until the eluate was colourless. Washing out 1 g of peel wastes with 500/600 ml of deionised water drastically reduced the chemical composition of the raw materials. Apparently, K was the most significantly reduced chemical component of the peels by up to 11, 9 and 4 mg/g for BP/PoP, PP and OP, receptively. Also an equal amount (1.5 mg/g) of removed P in BP, PP and PoP was observed.
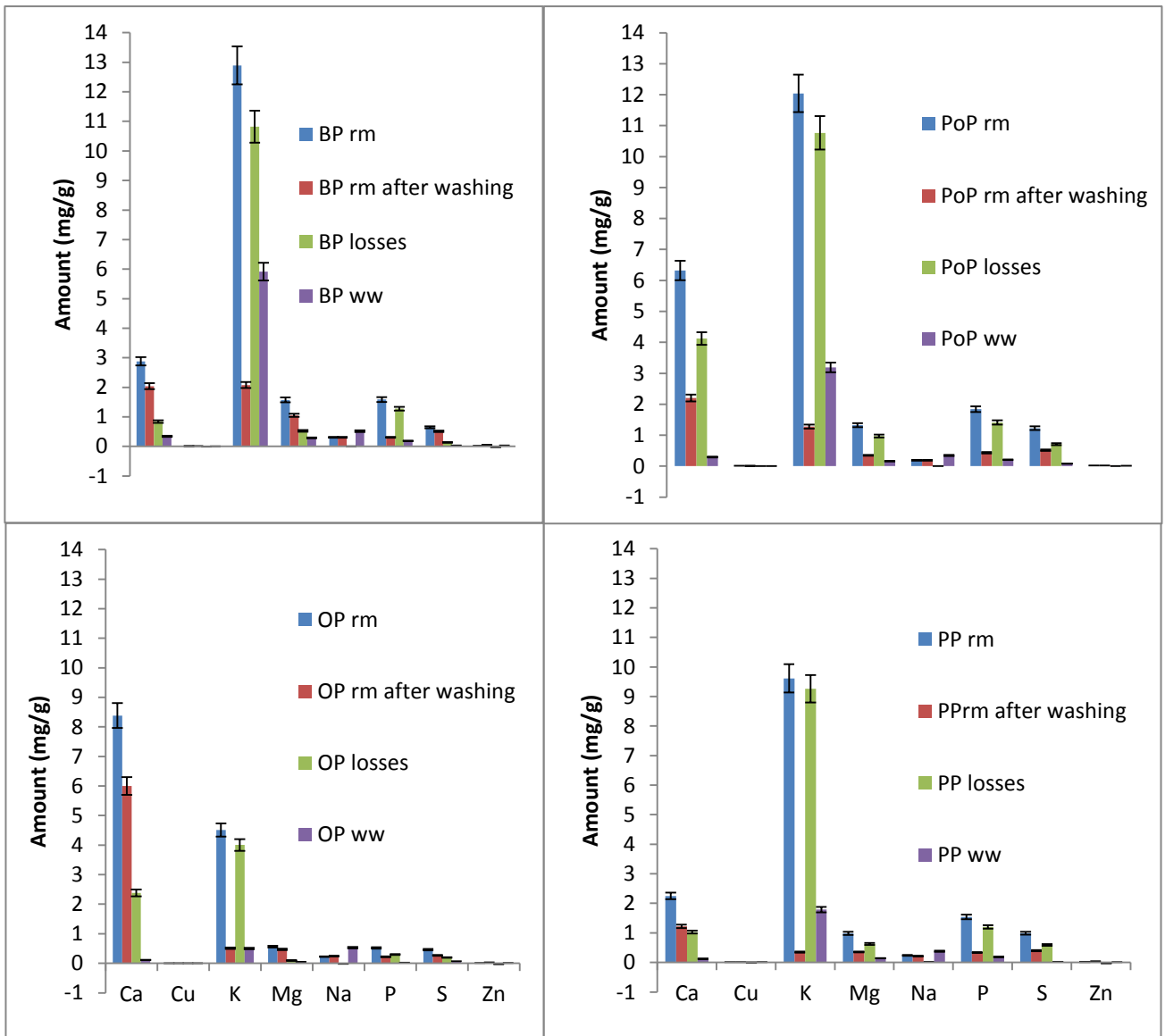
Figure3.3.Elemental analysis of peel raw materials (rm), washed raw material, chemical losses and chemical content contained in washing water (ww). BP: (banana peel); OP: (orange peel); PoP: (potato peel) and PP: (pineapple peel).

Also, washing water removed substantial amount of TOC and TN content in peels as reported in Table 3.1. TOC was removed up to more than 50% for OP and PP. Likewise TN removal percentage by washing water was more than 50% for PoP and PP.

Table 3.1.Chemical characteristics of peel washings (ca. 500 ml).

Peels	Raw material (mg/100 g)		Water washings (mg/100 ml)		Removal percentage (%)	
	TOC	TN	TOC	TN	TOC	TN
BP	37.11	1.22	15.7	0.3	42.3	24.6
OP	38.02	0.79	20.5	0.3	53.9	38.0
PoP	33.13	1.92	9.0	1.0	27.2	52.1
PP	36.80	0.90	20.8	0.5	56.5	55.6

BP: (banana peel); OP: (orange peel); PoP: (potato peel) and PP: (pineapple peel)

Natural water (river water) was selected to model a depollution strategy of natural waters contaminated with heavy metals The river water samples spiked with heavy metals were filtered using a 0.22 micron filter papers to consider the soluble forms of heavy metals and to eliminate those adsorbed on suspended solids. The general physico-chemical properties of river water are presented in Table 3.2.

It was evident that the water was free of toxic heavy metals besides Zn which was found in very minute traces. According to WHO regulations on inorganic content of drinking water is 2 and 3 mg/l for Cu and Zn, respectively. However, these regulations differ from country to country, for instance accepted limits for Cu and Zn in drinking water in South Africa is 1 and 5 mg/l whereas in Netherlands is 2 and 3 mg/l, respectively (Mamba et al., 2008).

Table 3.2. The average of chemical and physical characteristics of river water samples filtered at 0.22 micron.

Ca	Fe	K	Mg	Na	P	S	Zn	TOC	TN	EC	PH
				(mg l^{-1})						(μS/cm)	
54.36	0.08	3.78	14.28	39.78	0.07	15.12	0.03	1.60	0.79	3.26	8.60

The average pH of all river water samples was 8.6, where metals can be solubilised by dissolved organic matter that contains many negative charges, helping cationic metals to increase their apparent solubility. River water samples spiked with the heavy metals resulted with the following concentrations: Cu(II), Zn(II), and Cu+Zn were 1.8 ($\pm$0.2), 4.8 ($\pm$0.7) and 1.8 ($\pm$0.1) + 6.4 ($\pm$0.6) mg/l, respectively.

3.3.2. Adsorption screening of heavy metals

River water spiked with Cu, Zn and their mixture was percolated in glass columns containing the washed peels. The results of metal retention by the peels are shown in Table 3.3 below. Cu retention by BP was up to 17.8 mg/g and OP was least retaining 6.9 mg/g. According to the knowledge of the author, column experiments for adsorption of Cu and Zn utilizing peel waste are scanty. Therefore the present study cannot be compared to other similar studies. However, in some batch experiments a maximum adsorption capacity for BP biomass was found to be 20.37 mg/g Cu (Hossain et al., 2012). In the present study, BP retained about 23.5 mg/g of Zn as a single component, whereas PP obtained a third of that amount when PP retained 6.9 mg/g. In another batch experiment, Cu and Zn were absorbed using BP and OP (Annadurai et al., 2002). With initial concentration of 15 mg/l of each metal at pH 6-8, BP

realised adsorption equilibrium of 4.75 (Cu), 5.80 (Zn) and OP obtained 3.65(Cu), 5.25 mg/g (Zn). From these results it can be comprehended that Zn had preferential adsorption than Cu and BP performed better than OP. A remarkable difference was observed when Cu and Zn was in binary mixture, all biosorbents had a preferential adsorption of Zn than Cu. Also, the adsorption of Zn remained slightly unchanged in single component and in binary with a total volume of 2 l, except for PP. As far as this study is concerned, Cu adsorption in singular component was in this order: BP>PP>PoP>OP but for Zn adsorption on peel waste was in this order: BP>OP>PoP >PP for both single and in binary mixture.

Table 3.3. Adsorption screening of heavy metals in river water by peel wastes. Initial concentration was 1.8, 4.8, 6.4 and 1.8+6.4 mg/l for Cu (10 l), Zn* (5 l), Zn** (2 l) and Cu+Zn (2 l), respectively. Numbers in parenthesis are absolute error.

| Peel | Retained metal | | | | |
| | Single metal | | | Binary mixture | |
	Cu (mg/g)	Zn* (mg/g)	Zn** (mg/g)	Cu (mg/g)	Zn (mg/g)
BP	17.8 (0.6)	23.5 (0.6)	12.4 (3.1)	2.2 (0.1)	12.8 (0.7)
OP	6.9 (0.3)	12.2 (1.3)	9.4 (6.6)	2.1 (0.1)	8.0 (0.6)
PoP	8.2 (0.3)	9.1 (4.2)	4.5 (1.7)	1.6 (0.3)	5.4 (0.1)
PP	10.5 (0.9)	6.9 (2.4)	6.8 (2.5)	2.5 (0.2)	2.5 (0.0)

The adsorption results obtained by peel columns were reported as adsorption isotherms. The adsorption isotherms of Cu and Zn on peels at RT are presented in Figure 3.4. Each adsorption isotherm was conducted to assess the maximal amount of Cu and Zn adsorbed in peel waste biomass. The affinity of peel waste biomass can be observed by the slope of the curve and maximum loading capacity can be observed by the plateau value.
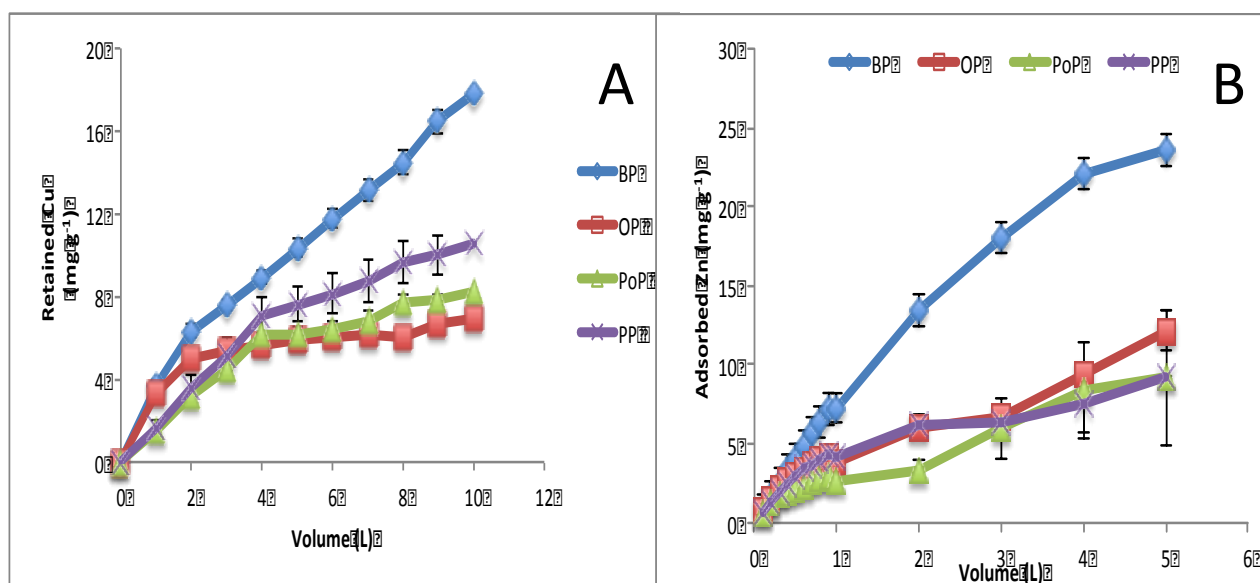
Figure 3.4. Metal retention capacity of 1 g peel waste on glass column. a) Cu retention [1.8 mg/l]. b) Zn retention, [4.8 mg/l].

Although the adsorption increased as the volume of the metal solution increased, no maximal adsorption was reached by any peel sample was observed. BP showed the highest affinity towards Cu and Zn compared to the other peel waste biomass investigated.

Various studies had demonstrated that maximum adsorption capacity of unmodified peel wastes as ones used in this study were having higher affinity towards Cu and Zn. For example, OP biomass obtained a maximal adsorption capacity of 44.28 and 21.25 mg/g at pH 5.5 for Cu and Zn, respectively (Feng and Guo, 2012).

Zn, K and Ca mapping of BP, before and after adsorption of Zn in the column experiment (Figure 3.5 A and B), was recorded using a portable XRF spectrometer ELIO produced by XGLAB SRL (Milano, Italy). The spectrum indicated that Zn and Ca concentrations clearly increased in the peel after water percolation whereas K content clearly decreased, in full agreement with the analysis of total metal content on treated water.
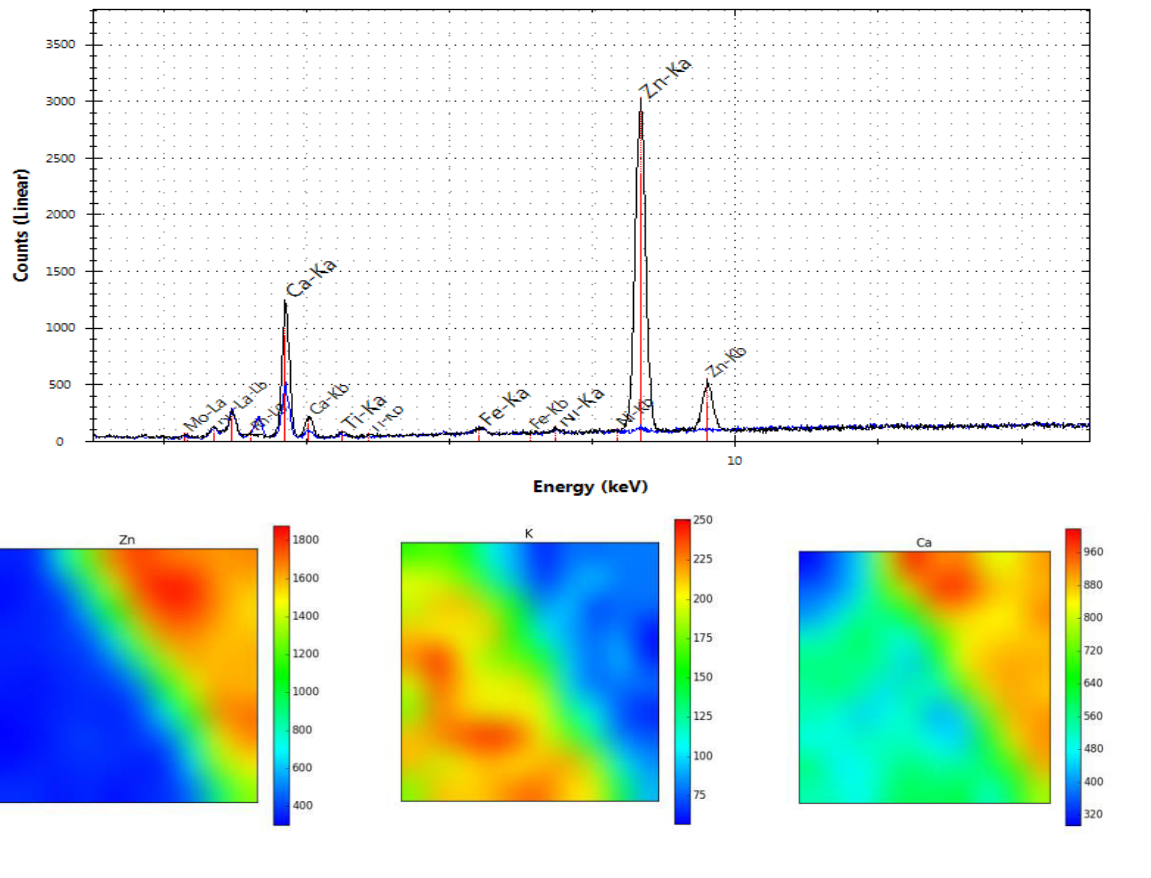
Figure 3.5. In the upper part, XRF spectra of BP before (blue curves) and after (black curves) percolation of river water spiked with Zn. In the lower part, single Zn, K and Ca mapping of peels before and after percolation of river water spiked with Zn.

3.3.3. Effects of eluates on lettuce growth

Hydroponics system was established to test the effects of treated water eluted from the peel column on growth of romaine lettuce (*Lactuca sativa* L. var. *longifolia*). The initial concentration of chemical content of all water samples were analyzed and stipulated in Table 3.4, below. Thereafter, each water sample of 4 l was adjusted to fit the desired value of the standard nutrient solution of essential macro nutrients (SNS) and pH. The water samples were

tap water (TW), river water (RW), and eluates (BPCu, OPCu, PoPCu, PPCu; BPZn, OPZn, PoPZn, PPZn; BPCu+Zn, OPCu+Zn, PoPCu+Zn and PPCu+Zn).

Table 3.4. Physical and chemical characteristics of water samples before used for hydroponics production of *Lactuca sativa* L. var. *longifolia*. (*lod: limit of detection).

Treatment	pH	Electrical conductivity mS/cm	TOC	N	K	P	Cu	Zn
					mg/l			
TW	7.3	21	0.8	5.5	4.0	<*lod	0.014	0.054
RW	7.4	21	0.5	4.0	3.0	<lod	0.002	<lod
BPCu	7.2	18	15.1	0.6	16.2	<lod	0.166	0.090
OPCu	7.1	18	24.9	0.7	5.0	<lod	0.597	0.122
PoPCu	7.4	18	14.4	1.4	10.5	<lod	0.157	0.100
PPCu	7.3	18	16.8	0.6	10.0	<lod	0.430	0.064
RWCu	7.4	18	1.3	0.6	0.5	<lod	0.639	0.008
BPZn	6.7	22	7.4	3.3	18.2	0.3	0.005	0.447
OPZn	6.2	24	102.1	6.1	16.2	0.3	0.011	0.796
PoPZn	6.9	22	82.8	7.0	16.8	0.3	0.011	0.835
PPZn	6.7	21	148.6	4.9	9.0	0.6	0.010	0.945
RWZn	6.9	24	0.5	3.0	2.9	<lod	0.003	3.103
BPCu+Zn	6.7	8	109.0	4.1	29.2	0.4	0.021	0.477
OPCu+Zn	6.5	19	56.9	7.4	6.7	<lod	0.028	0.326
PoPCu+Zn	6.9	22	56.9	4.9	17.6	0.3	0.043	0.628
PPCu+Zn	6.8	17	109.5	8.1	9.9	0.5	0.074	0.757
RWCu+Zn	7.0	24	0.5	4.4	2.9	<lod	0.312	3.179

The fresh weight of lettuce leaves and roots were measured at the end of the 28 day experiment as displayed in Table 3.5. There were no significant differences observed on lettuce leaves fresh weight due to all Cu percolated water samples. However, the root biomass of lettuce was significantly reduced by RWCu when compared to OPCu and TW. Cu is known to be essential in CO_2 assimilation and photosynthetic systems, hence plant excessive exposure to Cu leads to reduced plant growth (Yadav 2010). It is worth noting that the heavy metal effects on plant growth differ with different type of vegetables.

In Zn experiment, significant differences were observed in both leaves and roots biomasses. BPZn obtained significantly higher fresh weight of leaves compared to other treatments except for OPZn and RWZn. Similarly trend was also observed in the roots biomass, whereby BPZn, was significantly obtained higher yields than the other treatments, with the exception of RWZn and TWZn. Apparently, in Cu+Zn experiment, BPCu+Zn obtained better yields on leaves and root biomass. These results indicate that the higher adsorption of Cu, Zn and Cu+Zn by BP, as previously mentioned, result to reduced metal ions and consequently higher lettuce growth.

Table 3.5.Effects of water samples on fresh weight of romaine lettuce grown for 28 days in a floating system.

Water sample Treatment	Cu		Zn		Cu+Zn	
	Leaves	Roots	Leaves	Roots	Leaves	Roots
			(g)			
BP	20.13 a	4.933 ab	25.53a	3.04 a	25.00a	3.52 a
OP	20.17 a	5.200 a	17.16 ab	1.70 b	20.61ab	2.23 b
PoP	19.77 a	4.933 ab	17.00 bc	1.74 b	10.68 c	2.83 ab
PP	19.43 a	4.867 ab	13.40 c	2.27 b	18.47 ab	2.01 bc
RW	18.70 a	4.800 ab	24.82 ab	2.57 ab	18.52 ab	2.26 b
RWMetal	20.57 a	3.233 b	14.65 bc	1.93 bc	14.65 bc	1.93 bc
TW	22.53 a	5.167 a	15.27 bc	2.94 ab	15.27 bc	2.94 ab
LSD (≤0.05)	Ns	1.888	7.789	0.898	7.789	0.898

Values in a column followed by different letters are significantly different ($P \leq 0.05$, LSD). ns, Non-significant

The Zn and Cu content of leaves and roots in all treatments were also measured. The distribution of these metals on leaves and roots is shown in Figure 3.5, below. It is indicated that Cu is more predominately on roots than on leaves, whereas Zn shows a vice versa. Cu is more concentrated on the non-edible part of lettuce, on the roots, and therefore leading to not much of concern. On the other hand Zn content on lettuce leaves was up to 1.6 µg/g, is far less than the accepted limit. A maximum Zn tolerance of 20 mg/kg for edible parts of vegetable crops has been suggested (Long et al., 2003). However, since Zn has nutritional value to humans, vegetable crops containing at least 5 mg/kg of Zn are considered to have a better nutritional quality than those with less (Worthington, 2001). Therefore, lettuce grown in hydroponics systems using eluates and river water spiked with heavy metals are edible, since they contained limited concentration of heavy metal content in their edible portions.
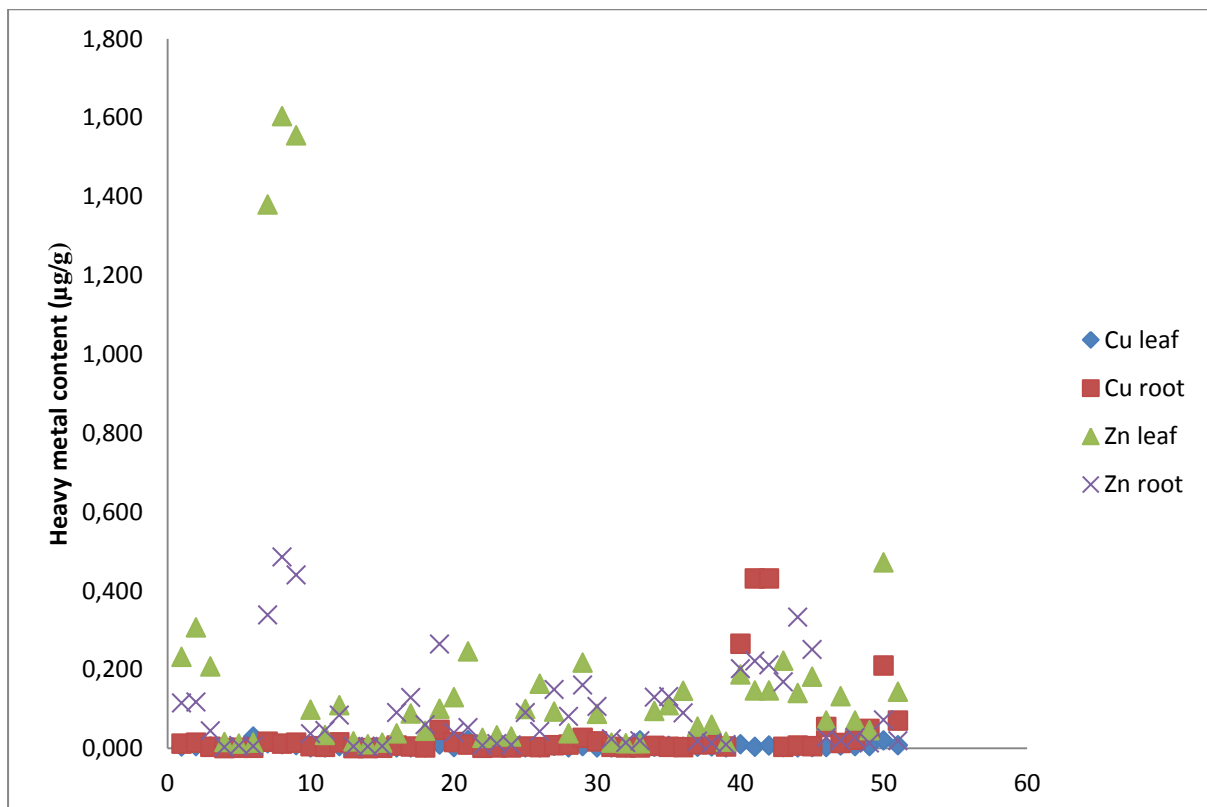
Figure 3.4. The heavy metal distribution on a lettuce grown in hydroponics system.

3.4. Conclusions

3.4.1. Adsorption capacity of peel waste on Cu and Zn

The metal (Cu, Zn and Cu+Zn mixture) retention capacity of BP, OP, PoP and PP on column experiment was established. It was observed that river water with initial pH of 8.6, when in solution with $CuSO_4$, $ZnSO_4$ and the Cu-+Zn mixture, the pH is altered to be 7.3, 6.7 and 6.8 respectively. BP was found to be the most effective biosorbent to adsorb Cu, Zn and Zn in the mixture up to 17.8, 23.5 and 12.8 mg/g, respectively. The reputable order was BP>PP>PoP>OP for Cu in singular component but for Zn was BP>OP>PoP>PP in single and in binary mixture. Therefore, peel waste proved to be the best alternative sorbents for decontaminating river streams contaminated with Cu(II), Zn(II) or the mixture.

3.4.2. Lettuce grown in hydroponic system

Lettuce was grown in a hydroponic system for 28 day in the standard nutrient solution of eluates from previous column studies and river water and tap water. RWCu reduced the root fresh weight significantly. BPZn and BPZn+Cu, showed significantly higher biomass yield of lettuce leaves and roots compared to negative controls. The leaves of lettuce accumulated more Zn than in the roots, and vice versa for the Cu. Therefore it can be concluded that treating Zn or Cu contaminated river water with peel waste is the alternatively suited best for lettuce production in the hydroponics system.

Since the adsorption process depends entirely on a charge of the adsorbent's surface and the pH of the solution, therefore, adsorbent surface modification for organic pollutants becomes highly recommended. So, an investigation to adsorb organic pollutants using heavy metal exhausted peels that went through pyrolysis modification to form biochars, can be suggested.

64

As biochar retention capacity on organic pollutants is assessed, it can be regenerated and reused repeatedly for inorganic pollutants found in aquatic environments.

4. REFERENCES

Acar, J., & Rostel, B. (2001). Antimicrobial resistance: an overview. *Revue Scientifique et Technique-Office International des Epizooties*, *20*(3), 797–807.

Achak, M., Hafidi, A., Ouazzani, N., Sayadi, S., & Mandi, L. (2009). Low cost biosorbent "banana peel" for the removal of phenolic compounds from olive mill wastewater: Kinetic and equilibrium studies. *Journal of Hazardous Materials*, 166, 117–125.

Adams, C., Wang, Y., Loftin, K., &Meyer, M. (2002). Removal of antibiotics from surface and distilled water in conventional water treatment processes. *J. Environ. Eng.*, 10.1061.

Ali, H., Khan, E., & Sajad, M. A. (2013). Phytoremediation of heavy metals—concepts and applications. *Chemosphere*, *91*(7), 869-881.

Aman, T., Kazi, A.A., Sabri, M.U.,& Bano Q. (2008). Potato peels as solid waste for the removal of heavy metal copper (II) from waste water/industrial effluent. *Colloids and Surfaces B: Biointerfaces*, *63*, 116–121.

American Water Works Association, (AWWA) (1990). Water treatment plant design, 3rd Ed., McGraw-Hill, New York.

Andreoli, C. V. (1993). The influence of agriculture on water quality. In ''Prevention of water pollution by Agriculture and related activities.'' Proceedings of the FAO Expert Consultation, Santiago, Chile, 20–23 Oct. 1992. pp. 53–65. Water Report 1. FAO, Rome.

Annadurai, G., Juang, R., & Lee, D. (2002). Use of cellulose-based wastes for adsorption of dyes from aqueous solutions. *Journal of Hazardous Materials B.*, *92*, 263–274.

Anwar, J., Shafique, U., Zaman, W., Salman, M., Dar, A., & Anwar, S. (2010). Removal of Pb(II) and Cd(II) from water by adsorption on peels of banana. *Bioresource Technology*, *101*, 1752–1755.

Arami, M., Limaee, N.Y., Mahmoodi, N.M., & Tabrizi, N.S. (2005). Removal of dyes from colored textile wastewater by orange peel adsorbent: Equilibrium and kinetic studies. *Journal of Colloid and Interface Science*, *288*, 371–376.

Arias-Estevez, M., Lopez-Periago, E., Martınez-Carballo, E., Simal-Gandara, J., Mejuto, J., & Garcıa-Rıo, L. (2008). The mobility and degradation of pesticides in soils and the pollution of groundwater resources: Review. *Agriculture, Ecosystems and Environment*, *123*, 247–260.

Ayers, R.S., & Westcot, D.W. (1994). Water quality for agriculture.FAO Irrigation Drainage Papers-29.

Aziz, H. A., Adlan, M.N., & Ariffin, K.S. (2008). Heavy metals (Cd, Pb, Zn, Ni, Cu and Cr (III)) removal from water in Malaysia: Post treatment by high quality limestone. *Bioresource Technology*, *99*(6), 1578–1583.

Azizullah, A., Khattak, M. N. K., Richter, P., & Häder, D. P. (2011).Water pollution in Pakistan and its impact on public health—a review. *Environment International*, *37*(2), 479-497.

Babel, S., & Kurniawan, T. A. (2003). Low-cost adsorbents for heavy metals uptake from contaminated water: A review. *Journal of Hazardous Materials*, *97*(1), 219–243.

Bajpai, S.K., Bajpai, M., & Rai, N. (2012). Sorptive removal of ciprofloxacin hydrochloride from simulated wastewater using sawdust: Kinetic study and effect of pH. *Water SA,* *38*(5), 673–682.

Barakat, M. A. (2011). New trends in removing heavy metals from industrial wastewater. *Arabian Journal of Chemistry*, *4*(4), 361–377.

Basso, M. C., Cerrella, E. G., & Cukierman, A. L. (2002). Lignocellulosic materials as potential biosorbents of trace toxic metals from wastewater. *Industrial & Engineering Chemistry Research*, *41*, 3580–3585.

Batt, A. L., Kim, S., & Aga, D. S. (2007). Comparison of the occurrence of antibiotics in four full-scale wastewater treatment plants with varying designs and operations. *Chemosphere*, *68*(3), 428–435.

Blasioli, S., Martucci, A., Paul, G., Gigli, L., Cossi, M., Johnston, C. T., & Braschi, I. (2014). Removal of sulfamethoxazole sulfonamide antibiotic from water by high silica zeolites: A study of the involved host–guest interactions by a combined structural, spectroscopic, and computational approach. *Journal of Colloid and Interface Science*, *419*, 148–159.

Bonvin, F., Omlin, J., Rutler, R., Schweizer, W. B., Alaimo, P. J., Strathmann, T. J., & Kohn, T. (2012). Direct photolysis of human metabolites of the antibiotic sulfamethoxazole: evidence for abiotic back-transformation. *Environmental Science & Technology*, *47*(13), 6746–6755.

Borgman, O., & Chefetz, B. (2013). Combined effects of biosolids application and irrigation with reclaimed wastewater on transport of pharmaceutical compounds in arable soils. *Water Research*, *47*(10), 3431–3443.

Bouki, C., Venieri, D., & Diamadopoulos, E. (2013). Detection and fate of antibiotic resistant bacteria in wastewater treatment plants: a review. *Ecotoxicology and Environmental Safety*, *91*, 1-9.

Braschi, I., Blasioli, S., Buscaroli, E., Montecchio, D., & Martucci, A. (2016). Physicochemical regeneration of high silica zeolite Y used to clean-up water polluted with sulfonamide antibiotics. *Journal of Environmental Sciences*, *43*, 302-312.

Braschi, I., Blasioli, S., Gigli, L., Gessa, C. E., Alberti, A., & Martucci, A. (2010 a). Removal of sulfonamide antibiotics from water: Evidence of adsorption into an organophilic zeolite Y by its structural modifications. *Journal of Hazardous Materials*, *178*(1), 218–225.

Braschi, I., Gatti, G., Paul, G., Gessa, C.E., Cossi, M., & Marchese, L (2010 b). Sulfonamide antibiotics embedded in high silica zeolite Y: A combined experimental and theoretical study of host-guest and guest-guest interactions. *Langmuir*, *26*(12), 9524–9532.

Brown, K. D., Kulis, J., Thomson, B., Chapman, T. H., & Mawhinney, D. B. (2006). Occurrence of antibiotics in hospital, residential, and dairy effluent, municipal wastewater, and the Rio Grande in New Mexico. *Science of the Total Environment*, *366*(2), 772–783.

Chand, P., Bafana, A., & Pakade, Y. B. (2015). Xanthate modified apple pomace as an adsorbent for removal of Cd(II), Ni(II) and Pb(II), and its application to real industrial wastewater. *International Biodeterioration & Biodegradation*, *97*, 60–66.

Chao, H. P., Chang, C. C., & Nieva, A. (2014). Biosorption of heavy metals on Citrus maxima peel, passion fruit shell, and sugarcane bagasse in a fixed-bed column. *Journal of Industrial and Engineering Chemistry*, *20*(5), 3408-3414.

Chatterjee, A., & Schiewer, S. (2014). Effect of competing cations (Pb, Cd, Zn, and Ca) in fixed-bed column biosorption and desorption from citrus peels. *Water, Air, & Soil Pollution*, *225*(2), 1-13.

Chefetz, B., Mualem, T., & Ben-Ari, J. (2008). Sorption and mobility of pharmaceutical compounds in soil irrigated with reclaimed wastewater. *Chemosphere*, *73*(8), 1335–1343.

Chen, B., & Chen, Z. (2009). Sorption of naphthalene and 1-naphthol by biochars of orange peels with different pyrolytic temperatures. *Chemosphere*, *76*(1), 127–133.

Cohen, N. R., Lobritz, M. A., & Collins, J. J. (2013). Microbial persistence and the road to drug resistance. *Cell Host & Microbe*, *13*(6), 632–642.

Costa, P. M.; Vaz-Pires, P., & Bernardo, F. (2008). Antimicrobial resistance in *Escherichia coli* isolated in wastewater and sludge from poultry slaughterhouse wastewater plants. *J. Environ. Health,70*(7), 40–45.

Demirbas, A. (2008). Heavy metal adsorption onto agro-based waste materials: A review. *Journal of Hazardous Materials*, *157*(2-3), 220–229.

Deng, W., Li, N., Zheng, H., & Lin, H. (2016). Occurrence and risk assessment of antibiotics in river water in Hong Kong. *Ecotoxicology and Environmental Safety*, *125*, 121-127.

de Ridder,D.J, Verberk, J.Q.J.C., Heijman, S.G.J., Amy, G.L., & van Dijk J.C.(2012). Zeolites for nitrosamine and pharmaceutical removal from demineralised and surface water: Mechanisms and efficacy. *Separation and Purification Technology*, *89*, 71-77.

Dushenkov, V., Kumar, P. N., Motto, H., & Raskin, I. (1995). Rhizofiltration: the use of plants to remove heavy metals from aqueous streams. *Environmental Science & Technology*, *29*(5), 1239–1245.

Efligenir, A., Déon, S., Fievet, P., Druart, C., Morin-Crini, N., & Crini, G. (2014). Decontamination of polluted discharge waters from surface treatment industries by pressure-driven membranes: removal performances and environmental impact. *Chemical Engineering Journal*, *258*, 309–319.

EN 1484: (1997). Water analysis – Guidelines for the determination of total organic carbon (TOC) and dissolved organic carbon (DOC).

Erdei, L., Mezˆosi, G., Mécs, I., Vass, I., Fˆoglein, F., & Bulik, L. (2005). Phytoremediation as a program for decontamination of heavy-metal polluted environment. *Acta Biologica Szegediensis*, *49*(1-2), 75–76.

Escher, B. I., Baumgartner, R., Koller, M., Treyer, K., Lienert, J., & Mc Ardell, C. S. (2011). Environmental toxicology and risk assessment of pharmaceuticals from hospital wastewater. *Water Research*, *45*(1), 75–92.

Farooq, S., Hashmi, I., Qazi, I.A., Qaiser, S., & Rasheed, S. (2008). Monitoring of coliforms and chlorine residual in water distribution network of Rawalpindi, Pakistan. *Environ. Monit. Assess, 140*, 339–47.

Feini, L., Zhang, G., Qin, M., &Zhang , H. (2008). Performance of nanofiltration and reverse osmosis membranes in metal effluent treatment. *Chinese Journal of Chemical Engineering*, *16*(3), 441–445.

Feng, N., & Guo, X. (2012). Characterization of adsorptive capacity and mechanisms on adsorption of copper, lead and zinc by modified orange peel. *Trans. Nonferrous Met. Soc. China*, *22*, 1224–1231.

Feng, N., Guo, X., & Liang, S. (2010). Enhanced Cu (II) adsorption by orange peel modified with sodium hydroxide. *Trans. Nonferrous Met. Soc. China*, *20*, 146–152.

Flörke, M., Kynast, E., Bärlund, I., Eisner, S., Wimmer, F., & Alcamo, J. (2013). Domestic and industrial water uses of the past 60 years as a mirror of socio-economic development: A global simulation study. *Global Environmental Change*, *23*(1), 144-156.

Foo, K.Y., & Hameed, B.H. (2012). Porous structure and adsorptive properties of pineapple peel based activated carbons prepared via microwave assisted KOH and K_2CO_3 activation. *Microporous and Mesoporous Materials*, *148*, 191–195.

Friedman, M., & Jürgens, H. S. (2000). Effect of pH on the stability of plant phenolic compounds. *Journal of Agricultural and Food Chemistry*, *48*(6), 2101-2110.

Fu, F., & Wang, Q. (2011). Removal of heavy metal ions from wastewaters: a review. *Journal of Environmental Management*, *92*(3), 407–418.

Fukahori, S., Fujiwara, T., Ito, R., & Funamizu, N. (2011). pH-Dependent adsorption of sulfa drugs on high silica zeolite: Modelling and kinetic study. *Desalination*, *275*(1), 237–242.

Gao, J., & Pedersen, J. A. (2005). Adsorption of sulfonamide antimicrobial agents to clay minerals. .*Environmental Science & Technology*, *39*(24), 9509–9516.

Gao, P., Munir, M., & Xagoraraki, I. (2012). Correlation of tetracycline and sulfonamide antibiotics with corresponding resistance genes and resistant bacteria in a conventional municipal wastewater treatment plant. *Science of the Total Environment*, *421*, 173–183.

Giusti, L. (2009). A review of waste management practices and their impact on human health. *Waste Manag.*,*29*, 2227–39.

Gleick, P.H. (1993). Water in crisis: a guide to the world's fresh water resources. In Igor Shiklomanov's chapter "World fresh water resources" in Peter H. Gleick (editor), Oxford University Press, New York.

Gleick, P.H. (1998). An introduction to global fresh water issues. In ''Water in Crisis: A Guide to the World's Fresh Water Resources'' (P. Gleick, Ed.). Oxford University Press, New York.

Göbel, A., McArdell, C. S., Joss, A., Siegrist, H., & Giger, W. (2007). Fate of sulfonamides, macrolides, and trimethoprim in different wastewater treatment technologies. *Science of the Total Environment*, *372*(2), 361–371.

Green, T. R., Taniguchi, M., Kooi, H., Gurdak, J. J., Allen, D. M., Hiscock, K. M., & Aureli, A. (2011). Beneath the surface of global change: Impacts of climate change on groundwater. *Journal of Hydrology*, *405*(3), 532–560.

Gumpu, M. B., Sethuraman, S., Krishnan, U. M., & Rayappan, J. B. B. (2015). A review on detection of heavy metal ions in water−An electrochemical approach. *Sensors and Actuators B: Chemical*, *213*, 515-533.

Haddis, A., & Devi, R. (2008). Effect of effluent generated from coffee processing plant on the water bodies and human health in its vicinity. *Journal of Hazardous Materials*, *152*(1), 259–262.

Hall, J. L. (2002). Cellular mechanisms for heavy metal detoxification and tolerance. *Journal of Experimental Botany*, *53*(366), 1-11.

Hameed, B.H., Krishni, R.R., & Sata, S.A. (2009). A novel agricultural waste adsorbent for the removal of cationic dye from aqueous solutions. *Journal of Hazardous Materials*, *162*, 305–311.

Hanjra, M. A., & Qureshi, M. E. (2010). Global water crisis and future food security in an era of climate change. *Food Policy*, *35*(5), 365–377.

Hared, I.A., Dirion, J., Salvador, S., Lacroix, M., & Rio, S. (2007). Pyrolysis of wood impregnated with phosphoric acid for the production of activated carbon: Kinetics and porosity development studies. *J. Anal. Appl. Pyrolysis*, *79*, 101–105.

Hashemian, S., Salari, K., & Yazdi, Z.A. (2014). Preparation of activated carbon from agricultural wastes (almond shell and orange peel) for adsorption of 2-pic from aqueous solution. *Journal of Industrial and Engineering Chemistry*, *20*, 1892–1900.

Heberer, T. (2002). Occurrence, fate, and removal of pharmaceutical residues in the aquatic environment: a review of recent research data. *Toxicology Letters*, *131*(1), 5–17.

Helland, T., Bergheim, M., Langin, A., Kallenborn, R., & Kummerer, K. (2010). Temperature dependent degradation of benzylpenicillin (Penicillin-G) under controlled laboratory conditions. *Chemosphere, 81*, 1477–1485.

Hendrix, C. S., & Salehyan, I. (2012). Climate change, rainfall, and social conflict in Africa. *Journal of Peace Research*, *49*(1), 35–50.

Heredia, J. B., & Martín, J. S. (2009). Removing heavy metals from polluted surface water with a tannin-based flocculant agent. *Journal of Hazardous Materials*, *165*(1), 1215–1218.

Heuer, H., Schmitt, H., & Smalla, K. (2011). Antibiotic resistance gene spread due to manure application on agricultural fields. *Current Opinion in Microbiology*, *14*(3), 236–243.

Hoekstra, A. Y., Mekonnen, M. M., Chapagain, A. K., Mathews, R. E., & Richter, B. D. (2012). Global monthly water scarcity: blue water footprints versus blue water availability. *PLoS One*, *7*(2), e32688.

Hossain, M.A., Ngo, H.H., Guo, W.S., Nguyen, T.V. (2012). Biosorption of Cu (II) from water by banana peel based biosorbent. *Experiments and Models of Adsorption and Desorption*, *2* (1), 87–104.

Hu, Z., Wanga, N., Tan, J., Chen, J., & Zhong, W. (2012). Kinetic and equilibrium of cefradine adsorption onto peanut husk. *Desalination and Water Treatment*, *37*, 160–168.

Huber, A., Bach, M., & Frede, H.G. (1998). Modelling pesticide losses with surface runoff in Germany. *Science of the Total Environment, 223,* 177-191.

Inyang, M., Gao, B., Yao, Y., Xue, Y., Zimmerman, A. R., Pullammanappallil, P., & Cao, X. (2012). Removal of heavy metals from aqueous solution by biochars derived from anaerobically digested biomass. *Bioresource Technology*, *110*, 50–56.

Ioannidou, O., & Zabaniotou A. (2007): Agricultural residues as precursors for activated carbon production - A review. *Renewable and Sustainable Energy Reviews*, *11*, 1966–2005.

ISO 8245: (1999). Water quality − Guidelines for the determination of total organic carbon (TOC) and dissolved organic carbon (DOC).

Janssen, A. H., Schmidt, I., Jacobsen, C. J. H., Koster, A. J., & De Jong, K. P. (2003). Exploratory study of mesopore templating with carbon during zeolite synthesis. *Microporous and Mesoporous Materials*, *65*(1), 59–75.

Järup, L. (2003). Hazards of heavy metal contamination. *British Medical Bulletin*, *68*(1), 167–182.

Jiang, L., Hu, X., Yin, D., Zhang, H., & Yu, Z. (2011). Occurrence, distribution and seasonal variation of antibiotics in the Huangpu River, Shanghai, China. *Chemosphere*, *82*(6), 822-828.

Kadukova, J., & Vircikova, E. (2005). Comparison of differences between copper bioaccumulation and biosorption. *Environ. Int.*, *31*(2), 227–232.

Kahle, M., & Stamm, C. (2007). Sorption of the veterinary antimicrobial sulfathiazole to organic materials of different origin. *Environmental Science & Technology*, *41*(1), 132–138.

Karcı, A., & Balcıoğlu, I. A. (2009). Investigation of the tetracycline, sulfonamide, and fluoroquinolone antimicrobial compounds in animal manure and agricultural soils in Turkey. *Science of the Total Environment*, *407*(16), 4652-4664.

Karthikeyan, K. G., & Meyer, M. T. (2006). Occurrence of antibiotics in wastewater treatment facilities in Wisconsin, USA. *Science of the Total Environment*, *361*(1), 196–207.

Khan, A. A., & Paquiza, L. (2011). Characterization and ion-exchange behaviour of thermally stable nano-composite polyaniline zirconium titanium phosphate: Its analytical application in separation of toxic metals. *Desalination*, *265*(1), 242–254.

Kim, S., Kim, K., Lee, Y., Jacobs, D.R., & Lee, D. (2015). Associations of organochlorine pesticides and polychlorinated biphenyls with total, cardiovascular, and cancer mortality in elders with differing fat mass. *Environmental Research*, *138*,1–7.

Kiss, T., Nagy, G., Pécsi, M., Kozlowski, H., Micera, G., & Erre, L.S. (1989). Complexes of 3,4-dihydroxyphenyl derivatives—X. Copper(II) complexes of chlorogenic acid and related compounds. *Polyhedron*, *8*, 2345–2349.

Köck-Schulmeyer, M., Villagrasa, M., de Alda, M. L., Céspedes-Sánchez, R., Ventura, F., & Barceló, D. (2013). Occurrence and behavior of pesticides in wastewater treatment plants and their environmental impact. *Science of the Total Environment*, *458*, 466-476.

Kodešová, R., Grabic, R., Kočárek, M., Klement, A., Golovko, O., Fér, M., & Jakšík, O. (2015). Pharmaceuticals' sorptions relative to properties of thirteen different soils. *Science of the Total Environment*, *511*, 435–443.

Koizumi, T., Arita, T.,& Kakemi, K.(1964). Absorption and excretion of drugs. XIX: some pharmacokinetic aspects of absorption and excretion of sulfonamides (1): absorption from rat stomach. *Chem. Pharm. Bul*. *12*, 413–420.

Krishna, A.K., Satyanarayanan, M., & Govil, P. K. (2009). Assessment of heavy metal pollution in water using multivariate statistical techniques in an industrial area: a case study from Patancheru, Medak District, Andhra Pradesh, India. *Journal of Hazardous Materials*, *167*(1), 366-373.

Kümmerer, K., (2009 a). Antibiotics in the aquatic environment–a review–Part I. *Chemosphere*, *75*(4), 417–434.

Kummerer, K., (2009 b). Antibiotics in the aquatic environment—a review—Part II. *Chemosphere, 75*(4), 435–441.

Kurniawan, T. A., Chan, G. Y., Lo, W. H., & Babel, S. (2006). Physico–chemical treatment techniques for wastewater laden with heavy metals. *Chemical Engineering Journal*, *118*(1), 83–98.

Lalumera, G. M., Calamari, D., Galli, P., Castiglioni, S., Crosa, G., & Fanelli, R. (2004). Preliminary investigation on the environmental occurrence and effects of antibiotics used in aquaculture in Italy. *Chemosphere*, *54*(5), 661–668.

Leardini, L., Martucci, A., Braschi, I., Blasioli, S., & Quartieri, S. (2014). Regeneration of high-silica zeolites after sulfamethoxazole antibiotic adsorption: a combined in situ high-

temperature synchrotron X-ray powder diffraction and thermal degradation study. *Mineralogical Magazine*, *78*(5), 1141-1160.

Le-Minh, N., Khan, S. J., Drewes, J. E., & Stuetz, R.M. (2010). Fate of antibiotics during municipal water recycling treatment processes. *Water Research*, *44*(15), 4295–4323.

Lewis, K. (2013). Platforms for antibiotic discovery. *Nature reviews Drug discovery*, *12*(5), 371-387.

Li, C., Dong, Y., Wu, D., Peng, L., & Kong, H. (2011). Surfactant modified zeolite as adsorbent for removal of humic acid from water. *Applied Clay Science*, *52*(4), 353–357.

Li, D.P., & Wu, Z.J. (2008). Impact of chemical fertilizers application on soil ecological environment. *Ying Yong Sheng Tai Xue Bao*, *19*,1158–1165.

Li, H., Sakamoto, Y., Liu, Z., Ohsuna, T., Terasaki, O., Thommes, M., & Che, S. (2007). Mesoporous silicalite-1 zeolite crystals with unique pore shapes analogous to the morphology. *Microporous and Mesoporous Materials*, *106*(1), 174–179.

Li, X., Tang, Y., Cao, X., Lu, D., Luo, F., & Shao, W. (2008). Preparation and evaluation of orange peel cellulose adsorbents for effective removal of cadmium, zinc, cobalt and nickel. *Colloids and Surfaces A: Physicochem. Eng. Aspects*, *317*, 512–521.

Liu, M., Hou, L. A., Yu, S., Xi, B., Zhao, Y., & Xia, X. (2013). MCM-41 impregnated with A zeolite precursor: synthesis, characterization and tetracycline antibiotics removal from aqueous solution. *Chemical Engineering Journal*, *223*, 678-687.

Liu, Y., Zhang, W., & Pinnavaia, T. J. (2000). Steam-stable aluminosilicate mesostructures assembled from zeolite type Y seeds. *Journal of the American Chemical Society*, *122*(36), 8791–8792.

Livermore, D. M. (2005).Minimising antibiotic resistance.*The Lancet Infectious Diseases*, *5*(7), 450-459.

Lokhande, R. S., Singare, P. U., & Pimple, D. S. (2011). Toxicity study of heavy metals pollutants in waste water effluent samples collected from Taloja Industrial Estate of Mumbai, India. *Resources and Environment*, *1*(1), 13-19.

Lone, M. I., He, Z. L., Stoffella, P. J., & Yang, X. E. (2008). Phytoremediation of heavy metal polluted soils and water: progresses and perspectives. *Journal of Zhejiang University Science B*, *9*(3), 210–220.

Long, X.X., Yang, X.E., He, Z.L., Calvert, D.V. & Soffella, J.P.(2003). Assessing zinc threshold for phytotoxicity and potential dietary toxicity in selected vegetable crops. *Communication of Soil Science & Plant Analysis, 34* (9-10):1421-1434.

Mackay, T. F. (2014). Epistasis and quantitative traits: using model organisms to study gene-gene interactions. *Nature Reviews Genetics*, *15*(1), 22–33.

Mamba, B.B., Rietveld, L.C., & Verberk, J.Q.J.C. (2008). SA drinking water standards under the microscope. *The Water Wheel*(January/February), 25-27.

Manaia, C. M., Macedo, G., Fatta-Kassinos, D., & Nunes, O. C. (2016). Antibiotic resistance in urban aquatic environments: can it be controlled? *Applied Microbiology and Biotechnology*, *100*(4), 1543–1557.

Martinez, J.L. (2009). Environmental pollution by antibiotics and by antibiotic resistance determinants. *Environmental Pollution*, *157*(11), 2893–2902.

Martínez-Carballo, E., González-Barreiro, C., Scharf, S., & Gans, O. (2007). Environmental monitoring study of selected veterinary antibiotics in animal manure and soils in Austria. *Environmental Pollution*, *148*(2), 570-579.

Memon, J.R., Memon ,S.Q., Bhanger ,M.I., Hallam, K.R, Allen, G.C., & El-Turki, A. (2009). Banana peel: A green and economical sorbent for the selective removal of Cr(VI) from industrial wastewater. *Colloids and Surfaces B: Biointerfaces*, *70*, 232–237.

Memon, J.R., Memon, S.Q., Bhanger, M.I., Memon, G.Z., El-Turki, A., & Allen, G.C. (2008) Characterization of banana peel by scanning electron microscopy and FT-IR spectroscopy and its use for cadmium removal. *Colloids and Surfaces B: Biointerfaces*, *66*, 260–265.

Mishra, V., Balomajumder, C., & Agarwal, V. K. (2010). Biosorption of Zn (II) onto the surface of non-living biomasses: a comparative study of adsorbent particle size and removal capacity of three different biomasses. *Water, Air, & Soil Pollution*, *211*(1-4), 489-500.

Mockovčiaková, A., Orolínová, Z., Matik, M., Hudec, P., & Kmecová, E. (2006). Iron oxide contribution to the modification of natural zeolite. *Acta Montan. Slovaca*, *11*, 353–357.

Mohammed, R. R., & Chong, M. F. (2014). Treatment and decolorization of biologically treated Palm Oil Mill Effluent (POME) using banana peel as novel biosorbent. *Journal of Environmental Management*, *132*, 237–249.

Mohan, D., & Pittman, C. U. (2007). Arsenic removal from water/wastewater using adsorbents—a critical review. *Journal of Hazardous Materials*, *142*(1), 1–53.

Murayama, N., Yamamoto, H., & Shibata, J. (2002). Mechanism of zeolite synthesis from coal fly ash by alkali hydrothermal reaction. *International Journal of Mineral Processing*, *64*(1), 1–17.

Mzini, L.L. (2002). Aspects of fruit size and quality in citrus. MSc Thesis, University of Stellenbosch, Stellenbosch, South Africa, pp 35-36.

Nakada, N., Yamashita, N., Miyajima, K., Suzuki, Y., Tanaka, H., Shinohara, H., Takada, H., Sato, N., Suzuki, M., & Ito, M. (2008).Multiple evaluation of soil aquifer treatment for water reclamation using instrumental analysis and bioassay.*Southeast Asian Water Environment,* 2, 303–310.

Nam, S.W., Choi, D.J., Kim, S.K., Her, N., & Zoh, K.D. (2014). Adsorption characteristics of selected hydrophilic and hydrophobic micropollutants in water using activated carbon. *Journal of Hazardous Materials*, *270*, 144–152.

Nebbioso, A., & Piccolo, A. (2013). Molecular characterization of dissolved organic matter (DOM): a critical review. *Analytical and Bioanalytical Chemistry*, *405*(1), 109-124.

Nemr, A. E., Abdelwahab, O., El-Sikaily, A., & Khaled, A. (2009). Removal of direct blue-86 from aqueous solution by new activated carbon developed from orange peel. *Journal of Hazardous Materials*, *161*, 102–110.

Nieto, J.M., Sarmiento, A.M., Canovas, C.R., Olias, M., & Ayora, C. (2013). Acid mine drainage in the Iberian Pyrite Belt: 1. Hydrochemical characteristics and pollutant load of the Tinto and Odiel rivers. *Environmental Science and Pollution Research*, *20*(11), 7509-7519.

Ötker, H. M., & Akmehmet-Balcıoğlu, I. (2005). Adsorption and degradation of enrofloxacin, a veterinary antibiotic on natural zeolite. *Journal of Hazardous Materials*, *122*(3), 251–258.

Owamah, H. I. (2014). Biosorptive removal of Pb(II) and Cu(II) from wastewater using activated carbon from cassava peels. *Journal of Material Cycles and Waste Management*, *16*(2), 347–358.

Pan, X., Qiang, Z., Ben, W., & Chen, M. (2011). Residual veterinary antibiotics in swine manure from concentrated animal feeding operations in Shandong Province, China. *Chemosphere*, *84*(5), 695-700.

Pellera, F., Giannis, A., Kalderis, D., Anastasiadou, K., Stegmann, R., Wang, J., & Gidarakos, E. (2012). Adsorption of Cu(II) ions from aqueous solutions on biochars prepared from agricultural by-products. *Journal of Environmental Management*, *96*, 35–42.

Pérez-Marín, A.B., Aguilar, M.I., Meseguer, V.F., Ortuno, J.F., Sáez, J., & Lloréns, M. (2009). Biosorption of chromium (III) by orange (*Citrus cinensis*) waste: batch and continuous studies. *Chemical Engineering Journal*, *155*(1), 199–206.

Pérez-Marín, A.B., Zapata, V.M., Ortuno, J.F., Aguilar, M., Sáez, J., & Lloréns, M. (2007). Removal of cadmium from aqueous solutions by adsorption onto orange waste. *Journal of Hazardous Materials*, *139*(1), 122–131.

Polat, E., Karaca, M., Demir, H., & Naci-Onus, A. (2004). Use of natural zeolite (clinoptilolite) in agriculture. *Journal of Fruit and Ornamental Plant Research*, *12*(1), 183–189.

Postel, S., Daily, G.C., & Ehrlich, P.R. (1996). Human appropriation of renewable fresh water. *Science, 271*, 785–788.

Postel, S.L. (2000). Entering an era of water scarcity: the challenges ahead. *Ecological Applications*, *10*(4), 941–948.

Pouretedal, H.R., & Sadegh, N. (2014). Effective removal of amoxicillin, cephalexin, tetracycline and *Penicillin G* from aqueous solutions using activated carbon nano particles prepared from vine wood. *Journal of Water Process Engineering,1*, 64–73.

Prahas, D., Kartika, Y., Indraswati, N., & Ismadji, S. (2008). Activated carbon from jackfruit peel waste by H_3PO_4chemical activation: Pore structure and surface chemistry characterization. *Chemical Engineering Journal*, *140*, 32–42.

Prayitno, Z., Kusuma, Z., Yanuwiadi, B. & Laksmono, R.W. (2013). Study of hospital wastewater characteristic in Malang City. *International Journal of Engineering and Science*, *2*, 13–16.

Qadir, M., Sharma, B. R., Bruggeman, A., Choukr-Allah, R., & Karajeh, F. (2007). Non-conventional water resources and opportunities for water augmentation to achieve food security in water scarce countries. *Agricultural Water Management*, *87*(1), 2–22.

Radović, T., Grujić, S., Petković, A., Dimkić, M., & Laušević, M. (2015). Determination of pharmaceuticals and pesticides in river sediments and corresponding surface and ground water in the Danube River and tributaries in Serbia. *Environ Monit. Assess, 187,* 1–17.

Rajapaksha, A. U., Vithanage, M., Lim, J. E., Ahmed, M. B. M., Zhang, M., Lee, S. S., & Ok, Y. S. (2014). Invasive plant-derived biochar inhibits sulfamethazine uptake by lettuce in soil. *Chemosphere*, *111*, 500–504.

Rajeshwarisivaray, S., Sivakumar, S., Senthilkumar, P., & Subburam, V. (2001). Carbon from cassava peel, an agricultural waste, as a adsorbent in removal of dyes and metal ions from aqueous solution. *Bioresource Technology*, *80*, 233–235.

Rashidi, N.A., Yusup, S., Ahmad, M.M., Mohamed, N.M., & Hameed, B.H. (2012). Activated carbon from the renewable agricultural residues using single step physical the activation: A preliminary analysis. *APCBEE Procedia*, *3*, 84–92.

Rivas, B., Torrado, A., Torre, P., Converti, A., & Domínguez, J.M. (2008). Submerged citric acid fermentation on orange peel autohydrolysate. *J. Agric. Food Chem.*,*56*(7), 2380–2387.

Rizzo, L., Manaia, C., Merlin, C., Schwartz, T., Dagot, C., Ploy, M. C., & Fatta-Kassinos, D. (2013). Urban wastewater treatment plants as hotspots for antibiotic resistant bacteria and genes spread into the environment: a review. *Science of the Total Environment*, *447*, 345-360.

Rodriguez-Mozaz, S., Ricart, M., Köck-Schulmeyer, M., Guasch, H., Bonnineau, C., Proia, L., & Barceló, D. (2015). Pharmaceuticals and pesticides in reclaimed water: efficiency assessment of a microfiltration–reverse osmosis (MF–RO) pilot plant. *Journal of Hazardous Materials*, *282*, 165–173.

Sapkota, A., Sapkota, A. R., Kucharski, M., Burke, J., McKenzie, S., Walker, P., & Lawrence, R. (2008). Aquaculture practices and potential human health risks: current knowledge and future priorities. *Environment International*, *34*(8), 1215-1226.

Sarmah, A. K., Meyer, M. T., & Boxall, A. B. (2006). A global perspective on the use, sales, exposure pathways, occurrence, fate and effects of veterinary antibiotics (VAs) in the environment. *Chemosphere*, *65*(5), 725-759.

Schoerder, H., & Balassa, J.J. (1963). Cadmium: Uptake by vegetables from superphosphate in soil. *Science, 140*(3568), 819–820.

Schriever, C. A., Peter, C., & Liess, M. (2007). Estimating pesticide runoff in small streams. *Chemosphere*, *68*(11), 2161–2171.

Schwarzenbach, R. P., Egli, T., Hofstetter, T. B., Von Gunten, U., & Wehrli, B. (2010). Global water pollution and human health. *Annual Review of Environment and Resources*, *35*, 109-136.

Shiklomanov, I. A. (1997).''Comprehensive Assessment of the Fresh water Resources of the World.''World Meteorological Organization and Stockholm Environment Institute, Stockholm, Sweden.

Shiklomanov, I. A. (2000). Appraisal and assessment of world water resources. *Water Int.,* 25, 11–32.

Simate, G. S., & Ndlovu, S. (2015). The removal of heavy metals in a packed bed column using immobilized cassava peel waste biomass. *Journal of Industrial and Engineering Chemistry*, *21*, 635-643.

Snyder, S.A., Adham, S., Redding, A.M., Cannon, F.S., De Carolis, J., Oppenheimer, J., & Yoon, Y. (2007). Role of membranes and activated carbon in the removal of endocrine disruptors and pharmaceuticals. *Desalination*, *202*(1), 156–181.

Sreekanth, D.; Sivaramakrishna, D.; Himabindu, V., & Anjaneyulu,Y. (2009). Thermophilic treatment of bulk drug pharmaceutical industrial wastewaters by using hybrid up flow anaerobic sludge blanket reactor. *Bioresour.Tech*., *100*(9), 2534–2539.

Sudaryanto, Y., Hartono, S.B., Irawaty, W., Hindarso, H., Ismadji, S. (2006). High surface area activated carbon prepared from cassava peels by chemical activation. *Bioresource Technology*, *97*, 734–739.

Tangahu, B. V., Sheikh Abdullah, S. R., Basri, H., Idris, M., Anuar, N., & Mukhlisin, M. (2011). A review on heavy metals (As, Pb, and Hg) uptake by plants through phytoremediation. *International Journal of Chemical Engineering*, *2011*, 1–32.

Tchounwou, P. B., Yedjou, C. G., Patlolla, A. K., & Sutton, D. J. (2014). Heavy metal toxicity and the environment. *Molecular, Clinical and Environmental Toxicology*,133-164.

Ternes, T.A., Meisenheimer, M., Mc Dowell, D., Sacher, F., Brauch, H.J., Haist-Gulde, B., Preuss, G., Wilme,U., & Zulei-Seibert, N. (2002). Removal of pharmaceuticals during drinking water treatment. *Environ. Sci. Technol*., *36*, 3855–3863.

The Chapman & Hall (1995). Chemical database. Chapman & Hall/CRC, UK.

ul Islam, E., Yang, X. E., He, Z. L., & Mahmood, Q. (2007). Assessing potential dietary toxicity of heavy metals in selected vegetables and food crops. *Journal of Zhejiang University Science B*, *8*(1), 1–13.

Van der Ven, A. J., Vree, T. B., Ewijk-Beneken Kolmer, E. W., Koopmans, P. P., & Meer, J. W. (1995).Urinary recovery and kinetics of sulphamethoxazole and its metabolites in HIV-seropositive patients and healthy volunteers after a single oral dose of sulphamethoxazole. *British Journal of Clinical Pharmacology*, *39*(6), 621-625.

Van der Werf, H.M.G. (1996). Assessing the impact of pesticides on the environment. *Agriculture, Ecosystems and Environment*, *60*, 81–96.

Van Heerden, I., Cronje, C., Swart, S.H., & Kotze, J.M. (2002). Microbial, chemical and physical aspects of citrus waste composting. *Bioresource Technology*, *81*, 71-76.

Veglio, F., & Beolchini, F. (1997). Removal of metals by biosorption: A review. *Hydrometallurgy*, *44*, 301–316.

Vetter, S. (2009). Drought, change and resilience in South Africa's arid and semi-arid rangelands. *South African Journal of Science*, *105*(1-2), 29–33.

Vinodhini, V., & Das, N. (2010). Packed bed column studies on Cr (VI) removal from tannery wastewater by neem sawdust. *Desalination*, *264*(1), 9-14.

Wang, S., & Peng, Y. (2010). Natural zeolites as effective adsorbents in water and wastewater treatment. *Chemical Engineering Journal*, *156*(1), 11–24.

Watkinson, A. J., Murby, E. J., Kolpin, D. W., & Costanzo, S. D. (2009). The occurrence of antibiotics in an urban watershed: from wastewater to drinking water. *Science of the Total Environment*, *407*(8), 2711–2723.

Webb, S., Ternes, T., Gibert, M., & Olejniczak, K. (2003).Indirect human exposure to pharmaceuticals via drinking water.*Toxicology Letters*, *142*(3), 157–167.

Wei, R., Ge, F., Huang, S., Chen, M., & Wang, R. (2011). Occurrence of veterinary antibiotics in animal wastewater and surface water around farms in Jiangsu Province, China. *Chemosphere*, *82*(10), 1408-1414.

Weirner, E.R. (2008). Application of Environmental aquatic chemistry: A practical guide. 2nd ed. pp 9. CRC Press, Florida, USA.

Williams, M., Martin, S., & Kookana, R. S. (2015). Sorption and plant uptake of pharmaceuticals from an artificially contaminated soil amended with biochars. *Plant and Soil*, *395*(1-2), 75–86.

World Health Organization (1993). Guidelines for drinking water quality. (2nd edn), Vol. 1, Recommendations, Geneva.

Worthington, V., (2001). Nutritional quality of organic versus conventional fruits, vegetables and grains. *The Journal of Alternative & Complementary Medicine, 7*(2):161-173.

Wu, D., Huang, Z., Yang, K., Graham, D., & Xie, B. (2015). Relationships between antibiotics and antibiotic resistance gene levels in municipal solid waste leachates in Shanghai, China. *Environmental Science & Technology*, *49*(7), 4122–4128.

Zhang, H., Yan, Y., & Yang, L. (2010). Preparation of activated carbon from sawdust by zinc chloride activation. *Adsorption*, *16*(3), 161–166.

Zulfadhly Z., Mashitah, M.D., Bhatia, M. (2001). Heavy metals removal in fixed-bed column by the macro fungus *Pycnoporus sanguineus*. *Environ. Pollut*,*112*, 463–470.

Effect of humic monomers on the adsorption of sulfamethoxazole sulfonamide antibiotic into a high silica zeolite Y: An interdisciplinary study

Ilaria Braschi [a, *], Annalisa Martucci [b], Sonia Blasioli [a], Loyiso L. Mzini [a], Claudio Ciavatta [a], Maurizio Cossi [c]

[a] Department of Agricultural Sciences, University of Bologna, 40127 Bologna, Italy
[b] Department of Physics and Earth Sciences, University of Ferrara, 44100 Ferrara, Italy
[c] Department of Sciences and Technological Innovation, University of Eastern Piedmont A. Avogadro, 51121 Alessandria, Italy

HIGHLIGHTS

- Reversible and pH-dependent adsorption of vanillin by HS zeolite Y.
- Negligible adsorption of caffeic acid by HS zeolite Y at any pH.
- Irreversible and pH-dependent adsorption of sulfamethoxazole by HS zeolite Y.
- Evidence of a vanillin-sulfamethoxazole adduct into the zeolite pores.
- Guest-guest interactions into zeolite pores and computation of stabilization energy.

GRAPHICAL ABSTRACT
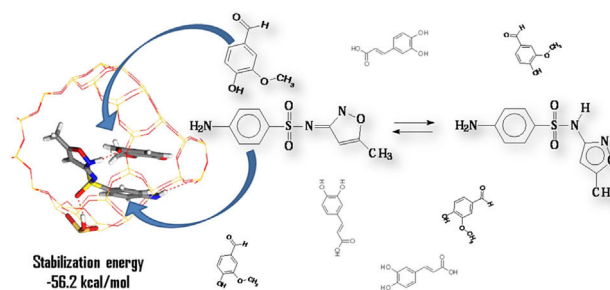
ARTICLE INFO

ABSTRACT

The adsorption efficiency of a high silica zeolite Y towards sulfamethoxazole, a sulfonamide antibiotic, was evaluated in the presence of two humic monomers, vanillin and caffeic acid, representative of phenolic compounds usually occurring in water bodies, owing their dimension comparable to those of the zeolite microporosity. In the entire range of investigated pH (5–8), adsorption of vanillin, as a single component, was reversible whereas it was irreversible for sulfamethoxazole. In equimolar ternary mixtures, vanillin coadsorbed with sulfamethoxazole, conversely to what observed for caffeic acid, accordingly to their adsorption kinetics and pKa values. Lower and higher adsorptions were observed for sulfamethoxazole and vanillin, respectively, than what it was observed as single components, clearly revealing guest-guest interactions. An adduct formed through H-bonding between the carbonyl oxygen of vanillin and the heterocycle NH of sulfamethoxazole in amide form was observed in the zeolite pore by combined FTIR and Rietveld analysis, in agreement with Density Functional Theory calculations of the adduct stabilization energies. The formation of similar adducts, able to stabilize other naturally occurring phenolic compounds in the microporosities of hydrophobic sorbents, was proposed.

© 2016 Elsevier Ltd. All rights reserved.

1. Introduction

The release of antibiotics in the environment has been

associated to chronic toxicity and the onset of the antibiotic resistance phenomena in bacteria (Gao et al., 2012). For these reasons, the removal of antibiotics from water bodies has become a public health issue which should be urgently addressed. Sulfonamides (sulfa drugs) were the first group of synthetic antimicrobials systematically used to treat/prevent bacterial infections. (Sweetman, 2011). Due to the beneficial effect on production efficiency in poultry and swine, sulfonamides are usually administrated as growth promoters in livestocks (Dibner and Richards, 2005; Neu and Gootz, 1996). Owing to their pH-dependent anionic nature, sulfonamides accumulate in water bodies, being neither completely retained by soils (Pan and Chu, 2016) nor by activated sludge in biological treatment plants (Manaia et al., 2016). Sulfamethoxazole (SMX) is one of the top-selling sulfonamide antibiotic used in human and veterinary therapy. Several studies report about its occurrence in aquatic ecosystems such as surface and drinking water, as well as wastewater treatment plants and hospital effluents (Kummerer, 2001; Brown et al., 2006; Tamtam et al., 2008; Watkinson et al., 2009). Above all, hospital and breeding farm outputs represent point source pollution which requests special consideration.

High silica (HS) zeolites have been recently tested to remove pharmaceutical from waters (de Ridder et al., 2012; Martucci et al., 2012; Grieco and Ramarao, 2013). In this contest, several model studies have indicated HS zeolites to quickly remove high amount of sulfonamide antibiotics from water (Braschi et al., 2010, 2013; Fukahori et al., 2011; Blasioli et al., 2014; Martucci et al., 2014) and to be easily regenerated (Leardini et al., 2014). Possible effect of dissolved organic matter (DOM), naturally present in water bodies, on sulfonamide adsorption into these zeolites has been ruled out, owing to the dimensions of its main components which are higher than those of the zeolite microporosities (Braschi et al., 2010), but no investigation on the effect of organic components of molecular size comparable with their pore window diameter has been addressed. This aspect is of utmost importance in order to exploit the zeolite microporosities to reduce the sulfonamide point source pollution as breeding farm effluents.

Natural and wastewaters contain plenty of low molecular weight organic molecules (Hem, 1987; Kordel et al., 1997). Among them, the phenolic component, which is formed by compounds like catechol, caffeic, ferulic, and *p*-coumaric acids, as well as *p*-hydroxybenzaldehyde, vanillin, and other more, can be simultaneously found. The tendency of these compounds to aggregate through biotic and abiotic oxidative coupling in soils to form humic substances, where their chemical structures can be resembled, is the reason for calling them humic monomers (Nyanhongo et al., 2006; Tossel, 2009; Nuzzo and Piccolo, 2013). Due to the different structure of phenolic compounds and their coexistence in natural water compartments (Muscolo et al., 2013), two of them were identified as a model to evaluate their effect on the adsorption of sulfonamide antibiotics into a HS zeolite Y and, of more general knowledge, their ability to clog eventually the microporosities of siliceous hydrophobic sorbents. Vanilin and caffeic acid were selected as representative of humic monomers because of their different chemical nature (an aldehyde the former and an hydroxycinnamic acid the latter) and reactivity in water. Their adsorption competition against SMX, as a sulfonamide antibiotic model, was tested into a large pH range to embrace that of natural, artificial and wastewaters.

2. Materials and methods

2.1. Chemicals

Sulfamethoxazole (4-amino-*N*-(5-methylisoxazol-3-yl)-benzenesulfonamide, SMX), was obtained from Dr. Ehrenstofer GmbH (Germany) with 99% purity. Vanillin (4-hydroxy-3-methoxybenzaldehyde, VNL) and caffeic acid (3-(3,4-dihydroxyphenyl)-2-propenoic acid, CA) were supplied by Sigma Aldrich Co LLC (USA) with 95 and 99% purity, respectively. Their chemical structures and *pKa* values are reported in Table 1.

The water solubility of SMX and the two phenols at room temperature (RT) was determined by adding each compound to MilliQ water in amount exceeding that required to saturate the solution. The suspensions were sonicated (15 min) and filtered at 0.45 μm (Durapore® membrane filters) to eliminate undissolved particles. The solubility measured by HPLC was 203 ± 2.7 μM for SMX, 9.46 ± 1.03 and 2.53 ± 0.31 mM for VNL and CA, respectively.

HS zeolite Y with SiO_2/Al_2O_3 = 200 and surface area of 750 m^2 g^{-1} was purchased from Tosoh Corporation (Japan).

In the experiments conducted in the presence of zeolite, the desidered pH values were achieved and kept constant by addition of 0.1 N HCl/NaOH to avoid any possible coadsorption of buffering components. The pH was controlled for the entire duration of the trial.

2.2. Persistence of humic monomers in water

Aqueous solutions of VNL or CA (50 μM each) were prepared in polyallomer centrifuge tubes (Nalgene, NY, USA) dissolving the compounds in media buffered at pH 5 and 6 (10 mM CH_3COONa, Carlo Erba Reagents, Milano, Italy) and at pH 7 and 8 (10 mM Na_2HPO_4, Carlo Erba Reagents, Milano, Italy). The persistence of the two phenols was followed over 48 h at RT by HPLC. Each experiment was conducted in triplicate.

2.3. Adsorption kinetics

Several aliquots of zeolite Y (1 mg) pre-equilibrated at the desired pH in the 5–8 range were placed into polyallomer centrifuge tubes where 2 mL of SMX, VNL or CA solutions (50 μM each) at the same pH were added. The suspensions were then placed on a horizontal shaker at RT and, at different times, the supernatants were separated from the pellet by centrifugation and analyzed by HPLC. To guarantee the pH stability, the pH of each suspension was checked and eventually adjusted by a few drops of 10 mM HCl/NaOH solution for the entire experiment duration. The experiment was conducted in duplicate.
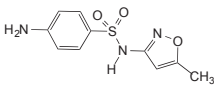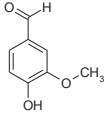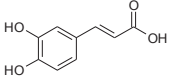
2.4. Adsorption-desorption isotherms

Adsorption isotherms of SMX or VNL on zeolite Y were performed at RT in the 5–8 pH range (zeolite:solution = 1 mg:2 ml). Each suspension was shaken for 1 h, then centrifuged and the supernatants analyzed by HPLC. The pH of the suspensions was monitored and adjusted during the entire experiment.

Owing to the high SMX adsorption capacity of zeolite Y and the low SMX solubility at RT (203 ± 2.7 μM), the isotherm data points at high concentrations were obtained as described in Blasioli et al. (2014). The desorption trials were conducted with the dilution method as reported in Blasioli et al. (2014). All adsorption-desorption experiments were conducted in duplicate.

The concentration of antibiotic and humic monomers in aqueous phase at equilibrium was expressed as Ce (μM) whereas the amount adsorbed by the zeolite, expressed as Cs (μmol g zeolite^{-1}), was calculated by the difference between the initial and final concentrations.

Table 1
Characteristics of chemicals under investigation.

Chemical name (Acronym)	Chemical structure	MW (mol g^{-1})	pK_a
Sulfamethoxazole (SMX)		253.3	5.7[a]
Vanillin (VNL)		152.15	7.4; 11.4[b]
Caffeic acid (CA)		180.16	4.5; 8.6; 12.5[c]

[a] Koizumi et al., 1964.
[b] The Chapman and Hall Chemical Database, 1995.
[c] Kiss et al., 1989.

2.5. Adsorption screening

Solutions containing SMX, VNL or CA (50 μM each), and their possible combinations (binary solutions − SMX + VNL or SMX + CA − and ternary solution − SMX + VNL + CA) were prepared at different unbuffered pH values in the range 5−8. The adsorption screening was performed at RT (zeolite:solution = 1 mg:2 ml). The suspensions were shaken for 1 h then centrifuged and the supernatants analyzed by HPLC. The adsorbed amount of each compound was calculated by the difference between initial and final concentration.

2.6. FT-IR spectroscopy

Harmonic vibrational frequencies were computed for SMX and VNL in their Density Functional Theory (DFT) optimized geometry (*vide infra*), and compared to experimental IR spectra.

Experimental infrared spectra were collected on a Tensor27 spectrometer (Bruker, MA, USA) with 4 cm^{-1} resolution. Self-supporting pellets (10 mg each) of zeolite Y, singly loaded with SMX or VNL and with their mixture, were obtained with a mechanical press (SPECAC, UK) at ca. 7 tons cm^{-2} and placed into an IR cell equipped with KBr windows permanently attached to a vacuum line, allowing sample dehydration *in situ*. FTIR spectra of SMX or VNL in CH$_2$Cl$_2$ were performed in a NaCl cell for liquids. Spectrum of the bare zeolite were collected as a control.

2.7. X-ray powder diffraction

X-ray powder diffraction (XRPD) data were collected on a Bruker D8 Advance Diffractometer equipped with a Sol-X detector, using Cu K$_{\alpha1,\alpha2}$ radiation. The spectra were measured in the 3°−110° 2θ range with a counting time of 12 s step^{-1}. All the structure refinements were performed by using the Rietveld method (EXPGUI version of GSAS (Toby, 2001)) in the *Fd-3* space groups. The crystal data and refinement details are summarized in the Supplementary Materials (see Table 1S).

The structures in Fig. 4 were generated using the VESTA software package (Momma and Izumi, 2011).

2.8. Chromatographic analysis

Concentrations of SMX, VNL, and CA were determined by HPLC-Diodarray analysis (Jasco, Japan) set at 267, 231, and 324 nm, respectively, equipped with a 4.60 nm × 250 mm Waters Spherisorb® 5μm C8 analytical column (Waters, USA) kept at 35 °C into a column oven (Jones Chromatography model 7971) and eluted with acetonitrile:water (30:70 by volume, pH 2.7 for H$_3$PO$_4$, flow rate 1 ml min^{-1}). Under these conditions, the retention times were 6.8, 5.5, and 3.8 min for SMX, VNL, and CA, respectively.

2.9. DFT calculations

All the calculations were performed at the DFT level with B3LYP density functional (Becke, 1988, 1993), the most popular hybrid density functional for molecular structure optimization and vibrational spectra simulation: the B3LYP performances for this kind of applications have been recently reviewed (Kovacs et al., 2015). Different basis sets, both double- and triple-ζ (cc-pVDZ and cc-PVTZ) were used for geometry optimizations, and energy and frequency calculations; in the zeolite cage model, Si atoms were assigned Hay and Wadt (LANL2) effective core potential and basis set (Hay and Wadt, 1985a,b; Wadt and Hay, 1985). Dispersion energy corrections were included through the semiempirical approach proposed by Grimme and implemented in Gaussian09 (GD3 procedure) (Grimme et al., 2010). The Y zeolite cage was modeled by extracting a suitable cluster from the database periodic structure as described e.g. in Braschi et al. (2012).

3. Results and discussion

Freshwater lakes, ponds and streams usually have a pH of 6−8 depending on the surrounding soil and bedrock (http://geology.com/rocks). For this reason, all the adsorption experiments were conducted in the 6−8 pH range in order to evaluate the effect of water pH on possible adsorption of SMX, VNL, and CA by the zeolite. For sake of completeness, pH 5 was considered as well, due to the acidic nature of the investigated compounds which are likely to be better retained by the sorbent under acidic conditions.

To rule out the degradation of the humic monomers within the time duration of adsorption trials, their persistence in buffered water was firstly evaluated. The degradation kinetics of VNL and CA in the 5−8 pH range is reported in the Supplementary Materials (see Fig. 1S).

The concentration of VNL remained constant within 24 h in the entire range of the investigated pHs whereas CA concentration unchanged in the 5−7 pH range. At pH 8, CA was transformed with a half-life time of 48 h into two degradation products. Since the

effect of basic pHs on the abiotic oxidation mechanism of CA is well-known (Cilliers and Singleton, 1989), the identification of the byproducts was considered beyond the scope of this study. As shown in the inset of Fig. 1S(b), CA concentration could be considered constant up to 1 h (~2% was transformed), thus safely allowing the investigation of its adsorption for short contact times (adsorption equilibrium of sulfonamides into this zeolite within a few minutes (Braschi et al., 2010; Blasioli et al., 2014)).

3.1. Adsorption trials

In the light of the observations described above, the adsorption kinetics of SMX, VNL, and CA on zeolite Y were followed within 1 h contact as shown in Fig. 2S. The SMX adsorption equilibrium was favourable in the entire range of pH investigated: the equilibrium was reached within 1 min and the amount retained by the zeolite was inversely related to the pH of water solutions. These findings can be explained considering the hydrophobic nature of the sorbent and pH-dependent nature of SMX.

The hydrophobicity of zeolites is inversely related to the content of extraframework cations counterbalancing the isomorphic substitution of Al^{3+} for Si^{4+} in the framework and to the content of defects (silanol groups) in the framework (Kawai and Tsutsumi, 1992). The high SiO_2/Al_2O_3 ratio (200) and the low content of H-bonded silanols (24 SiOH per Y unitary cell, Braschi et al., 2010) make the selected zeolite Y a hydrophobic material as proved by its low water content when air dried (ca. 1% dw).

As far as the affinity of SMX for the hydrophobic zeolite is concerned, the adsorption is favoured when the antibiotic molecule is in associated form (pKa 5.7, Table 1). Therefore, the SMX affinity was in the order: pH 5 (SMX mainly in neutral form) > pH 6 (both neutral and anionic forms) > pH 7 (mainly anionic form) > pH 8 (anionic form).

The adsorption equilibrium of CA at pH 5 was reached within 15 min, whereas at higher pH values no visible adsorption was found within 1 h. The CA pKa of 4.5 could explain its scarce affinity for the zeolite in that in the entire pH investigate, the negative form of CA predominate. For VNL, the adsorption equilibrium was reached in 1 min over the entire range of pH, making thus its adsorption competitive with SMX for the zeolite adsorption sites, although the retained amount was significant only in the 5–7 pH range. At pH 8, only a limited amount of VNL was retained by the zeolite as expected by its pKa value (7.4) due to the occurrence of species mainly in anionic form.

In the following, only the adsorption-desorption isotherms of SMX and VNL are reported owing to the negligible adsorption of CA in the investigated pH range.

As shown in Fig. 1A, the maximal adsorption of SMX at pH 5–6 was similar and attested at ca. 22% of zeolite dry weight (dw) whereas at pH 7 and 8, the plateau was reached at 3.3 and 1.5% zeolite dw, respectively.

As clearly shown by the curves slope at low concentrations, the affinity for the zeolite is inversely related to the pH of the solution. As already detailed, the antibiotic pK_a value (5.7, Table 1) can explain both the higher affinity and loading at acidic pH values. Considering the number of cages contained in 1 g zeolite (4.2×10^{20}, Braschi et al., 2010) and the antibiotic molecules adsorbed at pH 5–6 (5.3×10^{20} on average), the presence of at least one molecule per cage could be calculated, whereas a partial loading was achieved at pH 7 and 8 (20 and 9% of cages embeds one SMX molecule, respectively). The SMX adsorption reversibility was investigated only at pH 7 and 8, being the adsorption at acidic pH already defined irreversible (Blasioli et al., 2014). As shown in the detail, both the SMX desorption isotherms at pH 7–8 run parallel to the x-axis, thus indicating an irreversible adsorption at neutral-

basic pH values as well.

Fig. 1B shows the adsorption isotherms of VNL on the zeolite in the pH range of 5–7 owing to its negligible adsorption at pH 8. The VNL adsorption curves resemble an "S" type (Giles et al., 1960), also known as a "cooperative" adsorption. According to the model, the affinity of the adsorbate for the sorbent increases by increasing the retained amount due to an extrastabilization among guest species by interactions with those previously adsorbed, as well as with the sorbent. The plateau concentration was inversely related to the water pH and attested at ca. 13 and 8% zeolite dw at acidic and neutral pH, respectively. At acidic pHs, a full occupancy of the zeolite cages was found whereas 75% of cages were occupied at pH 7. As the desorption curves (see detail in Fig. 1B) overlapped to the adsorption ones at any investigated pH, the VNL adsorption was defined fully reversible, in accordance to its solubility (9.46 mM at RT and pH 6).

As far as the possible effect of the humic monomers on SMX retention by the zeolite is concerned, Table 2 reports an adsorption screening conducted in aqueous solutions containing different combinations of the investigated compounds at equimolar concentrations.

The adsorption of SMX and VNL, as single components, decreased at increasing pH in accordance to their pKa. For SMX, a similar adsorption profile as a function of pH has been already reported for a zeolite Y with a $SiO_2/Al_2O_3 = 100$ (Fukahori et al., 2011), thus highlighting a similar affinity for the antibiotic in the 100–200 range of SiO_2/Al_2O_3 ratio. In our study, the adsorption of SMX was ca. threefold that of VNL in the entire pH range, with the exception of pH 8, where only SMX was retained by the zeolite. As a single component, CA adsorbed in low amount at pH 5 whereas it was not retained at higher pH values.

When binary mixtures of SMX + VNL were contacted with the zeolite, a coadsorption of both compounds was observed in agreement with their comparable and fast kinetics (<1 min, Fig. 2S). In the entire range of pH, the SMX amount retained in the presence of VNL was found reduced with respect to what it was observed as a single component. On the contrary, VNL adsorption was found higher in the presence of SMX than as a single component, thus highlightening possible interactions with SMX into the zeolite pores (vide infra). Interestingly, at pH 8 which is a pH common to most part of natural surface waters, the embedded amount of VNL and SMX was comparable (14.7 and 12.2% of initial concentration, respectively). According to the pKa value of VNL with respect to SMX (7.4 and 5.7, respectively), VNL adsorption should be favoured at all the pH values. Likely, the lower SMX solubility, besides its bulky structure that maximizes the van der Waals interactions with the pore wall (Blasioli et al., 2014), favours its adsorption with respect to VNL.

When binary mixtures of CA and SMX were exposed to the zeolite, no significant amount of CA was retained in the entire range of investigated pHs, whereas SMX showed an adsorption profile resembling that observed as a single component. These findings can be explained by the lower pKa of CA with respect to SMX (4.5 and 5.7, respectively), besides its higher solubility (2.53 mM and 203 μM respectively).

The adsorption trend observed for the binary mixtures (VNL + SMX and CA + SMX) was confirmed when ternary mixtures of SMX + VNL + CA were contacted with the zeolite: only a simultaneous adsorption of SMX and VNL was observed.

3.2. Host-guest interactions between VNL and HS zeolite Y

To maximize the host-guest interactions, a zeolite sample loaded with VNL at 13.2% zeolite DW was investigated by IR analysis combined to Rietveld structure refinement of XRPD data. This
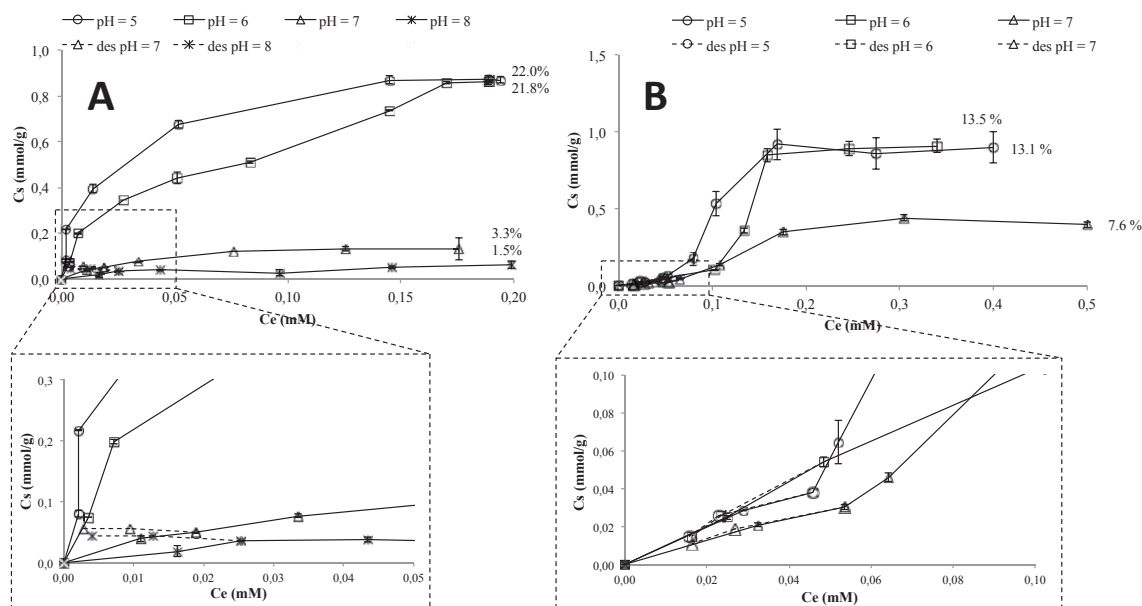
Fig. 1. Adsorption and desorption isotherms (solid and dashed lines) of (A) sulfamethoxazole and (B) vanillin by HS zeolite Y at different pH (1 h contact time at RT). A detail of isotherms is reported. Bars indicate the absolute error.

Table 2
Adsorption on HS zeolite Y of equimolar concentration of VNL, CA, and SMX as single components, binary and ternary mixtures at different pH (1 h contact time at RT). In parenthesis the absolute error.

pH	Amount adsorbed by the HS zeolite Y as a percentage of initial concentration (50 μM)									
	Single component			Binary mixture				Ternary mixture		
	VNL	SMX	CA	VNL	SMX	CA	SMX	VNL	SMX	CA
5	34.9 (1.3)	95.6 (0.0)	3.7 (1.1)	46.0 (0.0)	93.2 (1.0)	4.7 (0.6)	93.1 (0.6)	47.2 (0.4)	96.8 (0.5)	5.1 (0.3)
6	23.5 (1.6)	88.0 (1.5)	0.5 (0.0)	36.9 (3.5)	77.9 (4.9)	4.0 (1.5)	85.4 (4.2)	37.6 (0.9)	81.0 (2.0)	4.9 (0.5)
7	21.4 (0.8)	66.1 (4.6)	0.1 (0.0)	19.7 (6.3)	45.3 (4.9)	4.0 (1.0)	62.4 (11.8)	13.6 (0.3)	39.0 (0.4)	5.0 (2.0)
8	0.0 (2.4)	26.1 (8.5)	2.9 (1.5)	12.2 (2.9)	14.7 (6.5)	1.8 (0.3)	22.6 (1.9)	6.4 (1.5)	11.8 (0.4)	0.0 (0.3)

allowed a better observation of the spectral features of the adduct eventually formed.

In Fig. 2A, experimental FT-IR spectra of VNL in CH_2Cl_2 and singly embedded into the zeolite Y are reported, along with the harmonic vibrational spectrum calculated by the DFT level for the isolated molecule (in vacuo). In the spectrum in CH_2Cl_2, although strong solvent bands in the 3250–2750 and 1500–1400 cm^{-1} range are overlapped to those of VNL, as well as the occurrence of signals coming from water traces in the region above 3600 cm^{-1}, the most part of VNL vibrations could be observed.

The assignment of the main absorptions was done by comparing the values calculated in vacuo to the experimental ones as reported in Table 3. Here, the computed harmonic frequencies are systematically overestimated with respect to the corresponding experimental absorption but the spectral pattern was reproduced accurately enough to allow the interpretation.

Noteworthy, the structure of VNL computed in vacuo is organized through an intramolecular five-membered ring with the OH group H-bonded to the methoxyl oxygen atom (νPhO-H at 3751 cm^{-1}). The same arrangement was also hypothesized in both CH_2Cl_2 and when embedded into the zeolite (νPhO-H at 3518 and 3528 cm^{-1}, respectively) owing to the nonpolar character of the solvent and the zeolite pore wall. The similar position of the other VNL bands in both environments confirmed the solvating effect of zeolite on the guest molecule. These features indicate that the interactions between VNL and the zeolite framework are due to weak
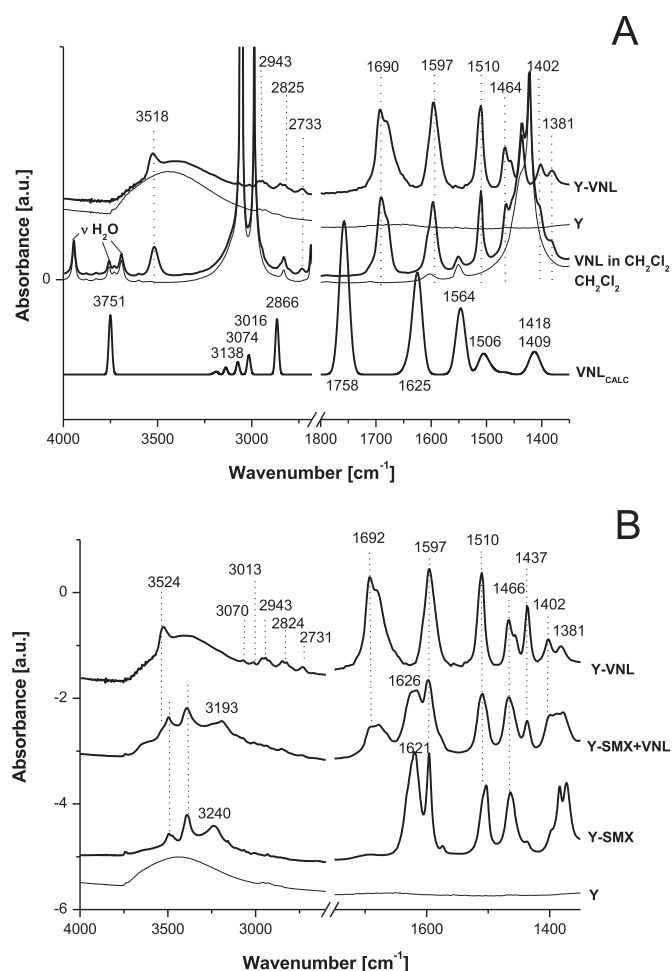
dispersive forces whose contributions are strong enough to stabilize the intramolecular H-bonded VNL into the cage.

Rietveld refinement performed on the VNL-loaded zeolite revealed the presence of about 9.5 molecules per unit cell (corresponding to 11% zeolite dw and 1.18 molecules/cage), in good agreement with the loading data (13.3% zeolite dw). These molecules are hosted in the Y cage in crystallographic sites partially statistically occupied (C1, C2, and C3 sites in Fig. 4S in the Supplementary Materials). These molecules show the aromatic ring (C1 site) in the window that joins together neighbouring cages as shown in Fig. 3A.

They can assume six different orientations which are identical and related by a rotation of 60° about **c** or by a mirror operation perpendicular to **c** (Fig. 4S in the Supplementary Materials). The C2/ C3 sites can be alternatively occupied by carbon or oxygen atoms, because the molecule symmetry is lower than *Fd-3*. The methoxylic group is given by C2 (when hosting oxygen) and C3 (when hosting CH$_3$), the carbonyl group is given by C2 (when hosting carbon) and C3 (when hosting oxygen), and finally the hydroxyl group is given by C2 (when hosting oxygen and C3 site is empty) (Fig. 4S).

The formation of more distorted wide-open apertures upon VNL adsorption is likely associated to the observed relative expansion of the framework thus explaining the increase of the unit cell parameters and the cell volume expansion (Table 1S).

Consequently, the Crystallographic Free Areas (C.F.A.) increased (42.61 Å^2) when compared with the bare material (39.07 Å^2).

acting between the VNL methoxyl/oxydryl oxygens (C2 site), as well as the methyl group or the carbonyl oxygen (C3), and the zeolite framework.

3.3. Guest-guest interactions between SMX and VNL embedded into the HS zeolite Y

To maximize the possible guest-guest interactions into the zeolite pores, a Y sample simultaneously loaded with SMX and VNL (6.9 and 20.1% zeolite dw, respectively) was investigated by infrared and Rietveld analysis. In the sample, 100% of pores contained at least one SMX molecule whereas ca. 50% embedded one VNL molecule on average.

The experimental IR spectrum of the SMX + VNL loaded mixture is reported in Fig. 2B. Here, spectra of singly loaded SMX or VNL are reported for comparison. A detailed description of the host-guest interactions developed by SMX embedded into the same zeolite in amide form has been already addressed (Blasioli et al., 2014).

In the spectrum of the loaded SMX-VNL mixture (Fig. 2B), the occurrence of bands at position similar to those of the singly embedded compounds can be resembled. As far as the VNL contributions are concerned, a clear perturbation of the carbonyl stretching region could be observed between 1700 and 1650 cm^{-1}, thus indicating this group likely involved in the stabilization of a SMX-VNL cluster. Concerning the SMX signals, the bands of singly embedded SMX (ca. 50%) are found overlapped to contributions of those clusterised with VNL (remaining 50%) and a clear perturbation of the stretching and bending NH signals was observed. In clusterised SMX, the stretching of NH at 3193 cm^{-1} is downshifted ($\Delta = -47$ cm^{-1}) with respect to its position when singly adsorbed (3240 cm^{-1}), whereas the NH bending at 1626 cm^{-1} is upshifted ($\Delta = +5$ cm^{-1}) with respect to that as a single component (1621 cm^{-1}). These findings clearly indicates an H-bonding between the VNL carbonyl and the SMX NH (VNL-C=O···HN-SMX), with the latter group which can be originated from both (i) SMX in amide form (SO_2−NH-) and (ii) the heterocycle ring NH of SMX in imide form (SO_2−N=C). Unfortunately, the computed stretching of the SMX heterocycle NH is overlapped (3563 cm^{-1}) to that of the amide SO_2−NH (3565 cm^{-1}) thus making impossible any assignment of the signal experimentally found at 3193 cm^{-1}.

The XRPD pattern collected on Y-SMX-VNL, and compared to Y-VNL and Y-SMX samples, showed differences in the intensity of the diffraction peaks, with the most significant been associated to the low 2θ angle region (Fig. 3S in the Supporting Materials), related to both the extraframework species nature and distribution.

Only small changes in the cell parameters of Y-SMX-VNL occur with respect to Y-VNL sample; in particular, a slight decrease of ***a***

Fig. 2. A) DFT calculated spectrum of VNL in vacuo (VNL_{CALC}) and experimental spectra of VNL in CH_2Cl_2 and adsorbed into zeolite Y (Y-VNL). Experimental spectra of CH_2Cl_2 and zeolite Y are reported for comparison. B) Experimental spectra of the zeolite singly loaded with VNL (13% zeolite dw) or SMX (21% zeolite dw) and with a SMX + VNL mixture (7 and 20% of zeolite dw, respectively).

Variations of ellipticity (ε) (defined as the largest/shortest oxygen-oxygen distances) of the 12MR apertures after organic molecules adsorption are also reported (ε = 1.06 and 1.02 in Y-VNL and Y, respectively).

Owing to the full reversibility of the adsorption process (Fig. 1), the refined distances can be ascribed to weak dispersive forces

Table 3
Main vibrational modes of vanillin calculated in vacuo and experimentally determined in CH_2Cl_2 and adsorbed into the zeolite Y.

Vibrational modes[a]	Vanillin		
	Computed	In CH_2Cl_2	Embedded in Y
νPhO-H	3751	3518	3524
νCH_{Ph}	3203−3186	not visible[b]	3070, 3013
νCH_3	3138−3016	not visible[b]	2943, 2824
$\nu CH_{aldehyde}$	2866	2733	2731
$\nu CO_{aldehyde}$	1758	1688	1693
νPh$_{quadrant}$ + δPhO-H	1625	1597	1595
νPh$_{sextant}$	1547	1510	1510
Def$_{out-of-phase}$ CH_3	1506	1464	1466
Def$_{in-phase}$ CH_3 + δPhO-H + $\delta CH_{aldehyde}$ + νPh$_{sextant}$	1467	not visible[b]	1437
$\delta CH_{aldehyde}$ + νPh$_{sextant}$	1418	not visible[b]	1402
δPhO-H + $\delta CH_{aldehyde}$ + νPh$_{sextant}$	1409	1381	1381

[a] For definition of ring vibrational modes see: Colthup et al., 1990.
[b] Not visible because overlapped to CH_2Cl_2 bands.
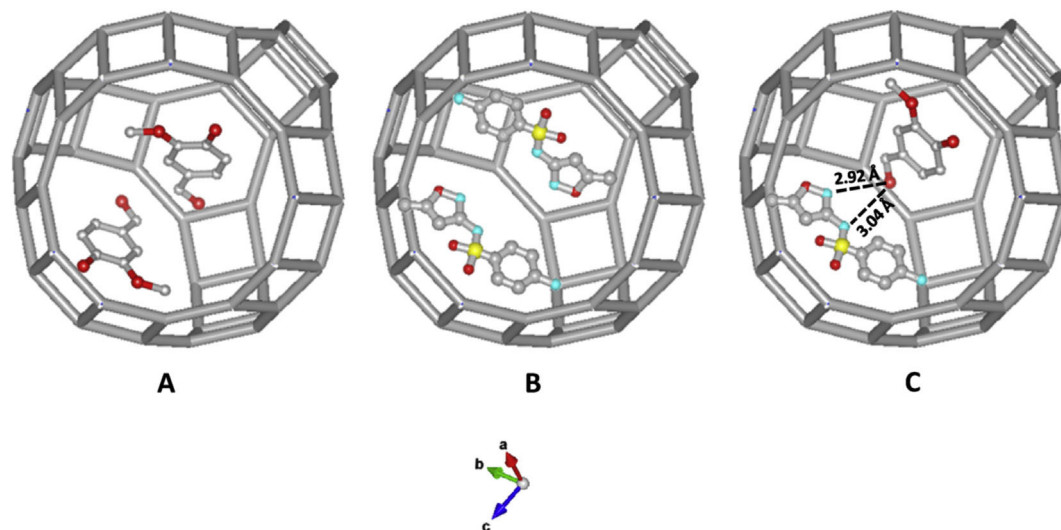
Fig. 3. Possible orientations of VNL (A), SMZ (B) and SMZ + VNL (C) in the zeolite Y cage (O: red, N: blue, S: yellow). (For interpretation of the references to colour in this figure legend, the reader is referred to the web version of this article.)

and cell volume parameters are observed (Table 1S). The Y-SMX-VNL refinement revealed the presence of 4 VNL and 10 SMX molecules per unit cell (ca. 7 and 20% zeolite dw, respectively, and ca. 0.5 and 1 molecule per cage, respectively). According to Blasioli et al. (2014), SMX molecules singly loaded are almost at the center of the supercage with its plane perpendicular to the threefold axes of the unit cell, whereas the isoxazole ring is found with six different orientations (see Fig. 3B). In the Y-SMX-VNL sample (Fig. 3C), the SMX aniline ring (C1 site) is situated in the window that joins neighboring supercages. The SMX isoxazole and aniline rings form a typical "V" configuration with the torsion angle S—N2—C7 of about 125.7°, with respect to that (126.0°) refined after adsorption of SMX as a single component (Blasioli et al., 2014).

As far as concerns coadsorbed VNL molecules, they can assume the six different orientations related by a rotation of 60° about *c* which are identical to those observed after adsorption of VNL as a single component (Fig. 3A), with the aromatic ring in C1 site, and C2/C3 sites which can be alternatively occupied by carbon or oxygen atoms, as already reported for the Y-VNL system. The 12MR apertures became more distorted ($\varepsilon = 1.08$), consequently the C.F.A. is larger (42.25 Å^2) when compared with the as-synthesized material (39.07 Å^2).

The refined bond distances between VNL and SMX in the cluster highlighted that interactions occur between these two species, in keeping with the data of FT-IR analysis. In particular, as shown in Fig. 3C, the distance between C2 site of VNL (carbonyl oxygen) and the SMX heterocycle ring N (N—C2 = 2.98(4) Å) indicates the interaction between the VNL carbonyl oxygen and the SMX heterocycle ring nitrogen as the most likely, whereas the nitrogen of the S—N—C moiety (amide form) can also interact but at higher interaction distance (3.04(4) Å, Fig. 3C). These results confirmed the occurrence of an H-bonding between the VNL carbonyl group and SMX NH, thus indicating the SMX imide form clustered to VNL.

DFT calculations could help to quantify the guest-guest interaction energy both for isolated SMX-VNL adducts and after embedding in Y zeolite. The addition energy in vacuo was computed at the B3LYP/cc-pVDZ level including Grimme's dispersion energy and the counterpoise correction to the BSSE (Boys and Bernardi, 1970), resulting −14.9 kcal/mol for the SMX imide form and −9.2 kcal/mol for the amide isomer, thus confirming the Rietveld findings. The optimized structures of the two adducts are

reported in Fig. 4.

The adduct with imide SMX was then embedded in the Y cage model and re-optimized at the same level (LANL2DZ effective core potentials were used for Si atoms): the final structure is shown in Fig. 4; besides the SMX-VNL NH—O bond already observed in vacuo, two other hydrogen bonds establish between the SMX amine group and a cage oxygen and between the cage silanol group and one sulfonamide oxygen. For the embedded cluster the interactions with the zeolite cage override the guest-guest interactions: in fact, SMX and VNL are strongly distorted inside the cage, so that the addition energy with respect to the isolated molecules is +2.9 kcal/mol, but when the interactions with the cage are added, the total energy with respect to the isolated fragments becomes −56.2 kcal/mol. Such a host-guest interaction is largely dominated by the dispersion contribution, computed through Grimme's atom-atom approach.

4. Conclusions

The effect of two model molecules of humic monomers (vanillin -VNL — and caffeic acid − CA) on the adsorption of sulfamethoxazole (SMX) by a high silica zeolite Y was assessed in batch solution within a large range of pH. The adsorption of VNL as a single component was kinetically favourable (<1 min), pH-dependent in accordance to its weak acidic character (*pKa* 7.4), and reversible at any pH. On the contrary, CA adsorption was always unfavoured owing to its higher acidity (*pKa* 4.5). The adsorption of SMX was also pH-dependent (*pKa* 5.4) but irreversible at all the pH values considered, due to its bulky "V" structure which stabilizes the embedded molecule. A SMX and VNL simultaneous adsorption was observed when the zeolite was exposed to their equimolar mixture: the formation of a bulky 1:1 SMX-VNL cluster into the zeolite pores explained their different (lower and higher, respectively) loading from what it was observed as single compounds. As defined by infrared analysis combined to Rietveld refinement, the adduct formed into the zeolite pore through an H-bonding between the heterocycle NH of SMX in amide form and the carbonyl oxygen of VNL, with a stabilization energy, computed in vacuo at DFT level, of −56.2 kcal/mol with respect to the isolated molecules. The formation of similar adducts with sulfonamide antibiotics, all bearing an heterocycle nitrogen able to stabilize other humic phenolic
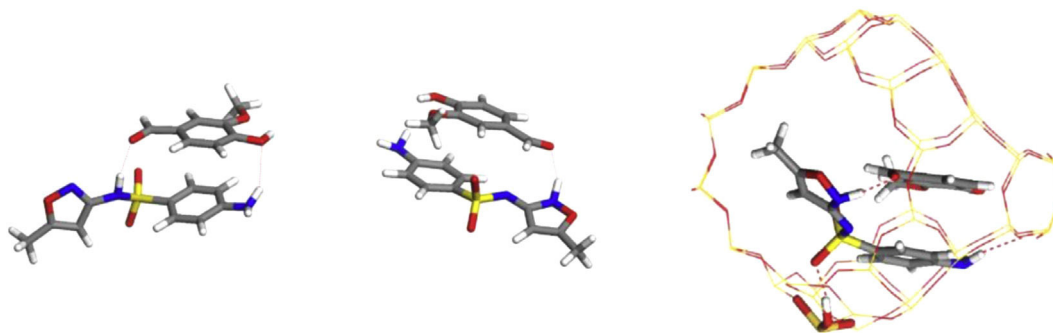
Fig. 4. DFT optimized structures of SMX + VNL complex with SMX in amide (left) and imide form (center) in vacuo and in the zeolite cage (right).

monomer into the zeolite micropores, can be hypothesized.

In addition and of more general meaning, according to our results on model molecules, humic monomers do not seem involved *per se* in the pore clogging of the zeolite, since derivatives of phenols (as vanillin) can be released by the hydrophobic porosities of the zeolite whereas the more acidic hydroxycinnamic acids (as caffeic acid) are not retained at all. These findings are of certain interest for scientists working with zeolite-based technologies to treat natural and wastewaters where a variety of humic phenolic compounds always occur.

Acknowledgements

Appendix A. Supplementary data

Supplementary data related to this article can be found at http://dx.doi.org/10.1016/j.chemosphere.2016.04.008.

References

Becke, A.D., 1988. Density-functional exchange-energy approximation with correct asymptotic behavior. Phys. Rev. A 38, 3098–3100.

Becke, A.D., 1993. Density functional thermochemistry. III. The role of exact exchange. J. Chem. Phys. 98, 5648–5652.

Blasioli, S., Martucci, A., Paul, G., Gigli, L., Cossi, M., Johnston, C.T., Marchese, L., Braschi, I., 2014. Removal of sulfamethoxazole sulfonamide antibiotic from water by high silica zeolites: a study of the involved host–guest interactions by a combined structural, spectroscopic, and computational approach. J. Coll. Interf. Sci. 419, 148–159.

Boys, S.F., Bernardi, F., 1970. The calculation of small molecular interactions by the differences of separate total energies. Some procedures with reduced errors. Mol. Phys. 19, 553–566.

Braschi, I., Blasioli, S., Gigli, L., Gessa, C.E., Alberti, A., Martucci, A., 2010. Removal of sulfonamide antibiotics from water: evidence of adsorption into an organophilic zeolite Y by its structural modifications. J. Hazard. Mat. 178, 218–225.

Braschi, I., Gatti, G., Bisio, C., Berlier, G., Sacchetto, V., Cossi, M., Marchese, L., 2012. The role of silanols in the interactions between methyl *ter*-butyl ether and high-silica faujasite Y: an infrared spectroscopy and computational model study. J. Phys. Chem. C 116, 6943–6952.

Braschi, I., Paul, G., Gatti, G., Cossi, M., Marchese, L., 2013. Embedding monomers and dimers of sulfonamide antibiotics into high silica zeolite Y: an experimental and computational study of the tautomeric forms involved. RSC Adv. 3, 7427–7437.

Brown, K.D., Kulis, J., Thomson, B., Chapman, T.H., Mawhinney, D.B., 2006. Occurrence of antibiotics in hospital, residential, and dairy effluent, municipal wastewater, and the Rio Grande in New Mexico. Sci. Total Environ. 366, 772–783.

Cilliers, J.J.L., Singleton, V.L., 1989. Nonenzymic autoxidative phenolic browning reactions in a caffeic, acid model system. J. Agric. Food Chem. 37, 890–896.

Colthup, N.B., Daly, L.H., Wiberley, S.E. (Eds.), 1990. Introduction to Infrared and Raman Spectroscopy, third ed. Academic Press, USA, pp. 261–266.

de Ridder, D.J., Verberk, J.Q.J.C., Heijman, S.G.J., Amy, G.L., van Dijk, J.C., 2012. Zeolites for nitrosamine and pharmaceutical removal from demineralised and surface water: mechanisms and efficacy. Sep. Purif. Tech. 89, 71–77.

Dibner, J.J., Richards, J.D., 2005. Antibiotic growth promoters in agriculture: history and mode of action. Poult. Sci. 84, 634–643.

Fukahori, S., Fujiwara, T., Ito, R., Funamizu, N., 2011. pH-dependent adsorption of sulfa drugs on high silica zeolite: modeling and kinetic study. Desalination 275, 237–242.

Gao, P., Munir, M., Xagoraraki, I., 2012. Correlation of tetracycline and sulfonamide antibiotics with corresponding resistance genes and resistant bacteria in a conventional municipal wastewater treatment plant. Sci. Total Environ. 421–422, 173–183.

Giles, C.H., MacEwan, T.H., Nakhwa, S.N., Smith, D., 1960. Studies in adsorption: Part XI. A system of classification of solution adsorption isotherms, and its use in diagnosis of adsorption mechanisms and in measurement of specific surface areas of solids. J. Chem. Soc. 111, 3973–3993.

Grieco, S.A., Ramarao, B.V., 2013. Removal of TCEP from aqueous solutions by adsorption with zeolites. Colloids Surfaces A Physicochem. Eng. Aspects 434, 329–338.

Grimme, S., Antony, J., Ehrlich, S., Krieg, H., 2010. A consistent and accurate *ab initio* parametrization of density functional dispersion correction (DFT-D) for the 94 elements H-Pu. J. Chem. Phys. 132, 154104–154119.

Hem, J.D., 1987. Study and Interpretation of the Chemical Characteristics of Natural Water. U. S. Geological Survey Water-Supply Paper 2254, third ed. United States Governement Printig Office.

Hay, P.J., Wadt, W.R., 1985a. *Ab initio* effective core potentials for molecular calculations. Potentials for the transition metal atoms Sc to Hg. J. Chem. Phys. 82, 270–283.

Hay, P.J., Wadt, W.R., 1985b. *Ab initio* effective core potentials for molecular calculations. Potentials for K to Au including the outermost core orbitals. J. Chem. Phys. 82, 299–310.

Kawai, T., Tsutsumi, K., 1992. Evaluation of hydrophilic-hydrophobic character of zeolites by measurements of their immersional heats in water. Colloid Polym. Sci. 270, 711–715.

Kiss, T., Nagy, G., Pécsi, M., Kozlowski, H., Micera, G., Erre, L.S., 1989. Complexes of 3,4-dihydroxyphenyl derivatives—X. Copper(II) complexes of chlorogenic acid and related compounds. Polyhedron 8, 2345–2349.

Koizumi, T., Arita, T., Kakemi, K., 1964. Absorption and excretion of drugs. XIX: some pharmacokinetic aspects of absorption and excretion of sulfonamides (1): absorption from rat stomach. Chem. Pharm. Bul. 12, 413–420.

Kordel, W., Dassenakis, M., Lintelmann, J., Padberg, S., 1997. The importance of natural organic material for environmental processes in waters and soils. Pure Appl. Chem. 69 (7), 1571–1600.

Kovacs, A., Konings, R.J.M., Gibson, J.K., Infante, I., Gagliardi, L., 2015. Quantum chemical calculations and experimental investigations of molecular actinide oxides. Chem. Rev. 115, 1725–1759.

Kummerer, K., 2001. Drugs in the environment: emission of drugs, diagnostic aids and disinfectants into wastewater by hospitals in relation to other sources: a review. Chemosphere 45, 957–969.

Leardini, L., Martucci, A., Braschi, I., Blasioli, S., Quartieri, S., 2014. Regeneration of high-silica zeolites after sulfamethoxazole antibiotic adsorption: a combined in situ high-temperature synchrotron X-ray powder diffraction and thermal degradation study. Min. Mag. 78 (5), 1141–1159.

Manaia, C.M., Macedo, G., Fatta-Kassinos, D., Nunes, O.C., 2016. Antibiotic resistance in urban aquatic environments: can it be controlled? Appl. Microbiol. Biotechnol. 100, 1543–1557.

Martucci, A., Pasti, L., Marchetti, N., Cavazzini, A., Dondi, F., Alberti, A., 2012. Adsorption of pharmaceuticals from aqueous solutions on synthetic zeolites. Micropor. Mesopor. Mat. 148, 174–183.

Martucci, A., Braschi, I., Marchese, L., Quartieri, S., 2014. Recent advances in clean-up strategies of waters polluted with sulfonamide antibiotics: a review of sorbents and related properties. Min. Mag. 78 (5), 1115–1140.

Momma, K., Izumi, F., 2011. VESTA 3 for three-dimensional visualization of crystal, volumetric and morphology data. J. Appl. Crystallogr. 44, 1272–1276.

Muscolo, A., Sidari, M., Texeira da Silva, J.A., 2013. Biological effects of water-soluble

soil phenol and soil humic extracts on plant systems. Acta Physiol. Plant 35, 309–320.

Neu, H.C., Gootz, T.D., 1996. Chapter 11 antimicrobial chemotherapy. In: Baron, S. (Ed.), Medical Microbiology, fourth ed. University of Texas Medical Branch at Galveston, Galveston (TX).

Nuzzo, A., Piccolo, A., 2013. Enhanced catechol oxidation by heterogeneous biomimetic catalysts immobilized on clay minerals. J. Mol. Cat. A Chem. 371, 8–14.

Nyanhongo, G.S., Rodriguez, S., Georg, M., 2006. Coupling of 2,4,6-trinitrotoluene (TNT) metabolites onto humic monomers by a new laccase from Trametes modesta. Chemosphere 64 (3), 359–370.

Pan, M., Chu, L.M., 2016. Adsorption and degradation of five selected antibiotics in agricultural soil. Sci. Total Environ. 545–546, 48–56.

Rocks: Igneous, Metamorphic and Sedimentary in http://geology.com/rocks.

Sweetman, S. (Ed.), 2011. The Complete Drug Reference. Pharmaceutical Press, London.

Tamtam, F., Mercier, F., Le Bot, B., Eurin, J., Tuc Dinh, Q., Clément, M., Chevreuil, M., 2008. Occurrence and fate of antibiotics in the Seine River in various hydrological conditions. Sci. Total Environ. 393, 84–95.

The Chapman and Hall Chemical Database, 1995. Chapman & Hall/CRC, UK.

Tossel, J.A., 2009. Quinone-hydroquinone complexes as model components of humic acids: theoretical studies of their structure, stability and visible-UV spectra. Geochim. Cosmochim. Acta 73 (7), 2023–2033.

Toby, B.H., 2001. EXPGUI, a graphical user interface for GSAS. J. Appl. Cryst. 34, 210–213.

Wadt, W.R., Hay, P.J., 1985. *Ab initio* effective core potentials for molecular calculations. Potentials for main group elements Na to Bi. J. Chem. Phys. 82, 284–298.

Watkinson, A.J., Murby, E.J., Kolpin, D.W., Costanzo, S.D., 2009. The occurrence of antibiotics in an urban watershed: from wastewater to drinking water. Sci. Total Environ. 407, 2711–2723.